Spatial Nature Conservation Monitoring on the Basis of Ecological Gradients using Imaging Spectroscopy

vorgelegt von
Diplom-Geoökologe
Carsten Neumann
geb. in Cottbus

Von der Fakultät VI – Planen Bauen Umwelt
der Technischen Universität Berlin
zur Erlangung des akademischen Grades
Doktor der Naturwissenschaften
Dr. rer. nat.

genehmigte Dissertation

Promotionsausschuss:
Vorsitzender: Prof. Dr. Gerd Wessolek
Gutachterin: Prof. Dr. Birgit Kleinschmit
Gutachter: Prof. Dr. Sebastian Schmidtlein
Gutachter: Prof. em. Dr. Hermann Kaufmann

Tag der wissenschaftlichen Aussprache: 09. Mai 2017

Berlin 2017

Author's Declaration

I prepared this dissertation without illegal assistance. This work is original except where indicated by special reference in the text and no part of the dissertation has been submitted for any other degree. This dissertation has not been presented to any other University for examination, neither in Germany nor in another country.

Carsten Neumann

Berlin, November 2016

Abstract

Ecosystem conservation and ecological restoration such as the preservation of species and habitat diversity have become recognized as an important ambition for an intentional anthropogenic exertion of influence worldwide. On that account, internationally acknowledged conservation targets are defined and realized over habitat management measures in designated protected area networks. By this means, it is intended to better control the worldwide loss of biodiversity and to create exclusion areas for the observation of natural processes and traits that will develop under minimal human interventions. Remote sensing thereby offers great potentials for an area wide monitoring of arising natural process dynamics, evaluating future development tendencies and mapping legally binding conservation status indicators in largely inaccessible protection zones. For this purpose, data intensive methods are required to transfer ecological interrelations from the field plot scale to the level of spatially explicit image projections.

This thesis develops a differentiated set of methodological approaches for the determination of complex ecological gradients via responses to the spectral feature space that is utilized for the mapping of plant species and habitats by means of field and imaging spectroscopy. Numerical models are generated on the basis of vegetation characteristics and spectral reflectance signatures that were collected for open heathland areas on a former military training area, the “Döberitzer Heide” west of Berlin, Germany. By applying the Non-metric Multidimensional Scaling (NMDS) ordination technique on the field samples, continuous floristic gradients are projected onto varying ordination space configurations. On that basis, functional relations can be designed for the quantification of Natura 2000 habitat type probabilities. It can be shown that occurrence probabilities are up- or downgraded according unique species turnover in specific NMDS ordination regions that can be utilized for a Natura 2000 habitat type conservation status assessment.

Owing to the relationship between floristic gradients in NMDS ordination and spectral signatures from field references that is constructed through a Partial Least Squares Regression (PLSR) framework, continuous species shifts, habitat type occurrence probabilities and their conservation states are transferable to hyperspectral imagery. For the first time, this thesis demonstrated that multidirectional NMDS ordination space rotations provide stable and significant wavelength regions for the prediction of specific plant species gradients. A novel feature selection method is provided that identifies spectrally sensitive gradients and calibrates robust PLSR models for the allocation of transferable spectral feature combinations in a statistical learning procedure.

In a final synthesis it is demonstrated that individual cover-abundances are represented in multiple dimensions of a NMDS ordination results. A genetic optimization procedure is introduced in order to evaluate the spectral predictability of individual species abundances from the overall vegetation continuum of the study area's open heathland communities. Optimal species models are selected for distinct sets of NMDS dimensionality and assigned to spectral gradient features in a multiobjective optimization assessment. The final species models thus integrate unique parameterizations of ecological and spectral traits that can be used to predict individual species abundances on hyperspectral imagery.

The resulting vegetation patterns are semantically defined over spatially explicit representations of species coexistence, diversity clusters, succession trajectories, ecotone areas and habitat conditions. In particular, continuous measures of species cover or habitat type probabilities are projected onto the image scale. As a consequence, detailed information about nature conservation and habitat management relevant structures and processes are provided in continuous units of the reflected reality. The thesis thus states to provide a contribution for a deeper understanding of ecological processes, related spatiotemporal pattern dynamics and inducible ecosystem development trends. The generated mapping algorithms are further potentially transferable to other areas and to variable aspects of ecological restoration efforts, which is particularly promising in conjunction with upcoming drone and hyperspectral spaceborne missions.

Zusammenfassung

Der Erhalt und die Entwicklung von Ökosystemen und ökosystemaren Bestandteilen, wie etwa die Vielfalt von Arten und Lebensräumen, ist ein international anerkanntes Ziel intendierter, anthropogener Einflussnahme. Es werden weltweit Zielvorgaben definiert, die über eine Vielzahl von aktiven (Lebensraumgenese) und passiven (Wildnis) Maßnahmen in Netzwerken aus Naturschutzgebieten realisiert werden. Insbesondere soll auf diese Weise dem weltweiten Verlust der Biodiversität entgegengewirkt sowie Refugien natürlicher Prozesskreisläufe, in denen anthropogene Eingriffe minimiert sind, geschaffen werden. Die Überwachung der sich einstellenden natürlichen Prozessdynamiken, die Bewertung von Entwicklungstendenzen und die Inventarisierung naturschutzrechtlich verbindlicher Zustandsindikatoren in den großflächigen, größtenteils unzugänglichen Schutzgebieten kann zu einem großen Teil von der Geofernerkundung geleistet werden. Zu diesem Zweck werden datenintensive Verfahren benötigt, die ökologische Zusammenhänge von der Feldskala auf die Bildebene möglichst verlustfrei übertragen.

In der vorliegenden Dissertation wird dargelegt wie komplexe, ökologische Gradienten über spektrale Merkmale beschrieben und in der bildgebenden Spektroskopie abgebildet werden können. Hierfür wurden Vegetationseigenschaften wie Arten und Deckungen sowie dessen spektrale Reflexionssignaturen einer offenen grundmoränengebundenen Heidelandschaft auf einem ehemaligen Truppenübungsplatz, der „Döberitzer Heide“ westlich von Berlin, intensiv beprobt und zur numerischen Modellierung floristischer Lebensraumeigenschaften herangezogen. Über das Verfahren der nichtmetrischen multidimensionalen Skalierung (NMDS) können dabei kontinuierliche, floristische Gradienten in einen Ordinationsraum projiziert und über funktionale Vorschriften zu Vorkommenswahrscheinlichkeiten von Natura 2000 Lebensraumtypen aggregiert werden. Es kann gezeigt werden, dass Übergänge zwischen Natura 2000 Lebensraumtypen durch spezifische Artgradienten gekennzeichnet sind, welche wiederum zur Bewertung eines naturschutzrechtlichen Erhaltungszustandes genutzt werden können.

Über den Zusammenhang zwischen Ordinationsraumgradienten und spektralen Feldsignaturen, der in einem Partial Least Squares Regressionsansatz (PLSR) kalibriert wird, lassen sich kontinuierliche Artgradienten, Lebensraumwahrscheinlichkeiten und Bewertungsstufen auf Bildpixel von hyperspektralen Überflugdaten übertragen. Erstmalig wird in der Dissertation gezeigt, dass sich in einer multidirektionalen Rotation von Ordinationsraumgradienten stabile und signifikante Wellenlängenbereiche für spezifische Artübergänge identifizieren lassen. Zu diesem Zweck wird ein neuartiges Selektionsverfahren eingeführt,

welches spektral sensitive Gradienten auswählt, diese in einem PLSR Ansatz kalibriert und gleichzeitig über ein statistisches Resampling auf Robustheit in der Übertragung überprüft.

In der finalen Zusammenführung wird gezeigt wie Deckungsabundanzen von Einzelarten im NMDS Ordinationsraum beschrieben sind und wie diese über zuordenbare spektrale Gradienten modelliert werden können. Dabei wird ein neuer Ansatz zur Bewertung der Vorhersagbarkeit einzelner Arten aus dem gesamten Vegetationskontinuum aus dem Bereich der genetischen Optimierung adaptiert. Darin wird ein multikriterieller Optimierungsverlauf zur Selektion eines optimalen Artmodells unter Bestimmung der geeigneten Ordinationsraum-dimension und der spektralen Gradientenmerkmale durchgeführt. Die finalen Artmodelle integrieren artspezifische Parametrisierungen zur räumlich expliziten Vorhersage von Einzelartenabundanzen auf Hyperspektralbildern unterschiedlicher phänologischer Phasen.

Die abgebildeten Vegetationsmuster eröffnen die Möglichkeit zur expliziten Darstellung von Koexistenzen, Diversitätsclustern, Sukzessionsstadien, Ökotonen und Lebensräumen. Es werden insbesondere kontinuierliche Größen wie Deckungsgrade (Arten) oder Wahrscheinlichkeiten (Lebensräume) räumlich vorhergesagt. Auf diese Weise werden gerade im Hinblick auf Anforderungen im Naturschutz detaillierte Informationen über die stetige Struktur der Realität geliefert, welche Einblicke für ein tieferes Prozessverständnis ermöglichen und somit einen Beitrag zur frühzeitigen Erkennung von ökosystemaren Entwicklungstendenzen leisten. Die generierten Abbildungsalgorithmen können potentiell auf andere Gebiete und auf neue naturschutzfachliche Herausforderungen in Verbindung mit zukünftigen, operationellen Drohnen oder hyperspektralen Satellitenmissionen übertragen werden.

Contents

List of Figures

List of Tables

List of Abbreviations

AISA .....Airborne Imaging Spectrometer for Applications
APEX .....Airborne Prism Experiment
ASD .....Analytical Spectral Devices, Inc.
ATCOR .....Atmospheric/Topographic Correction
BON .....Biodiversity Observation Network
CA .....Correspondence Analysis
CBD .....Convention on Biological Diversity
CCA .....Canonical Correspondence Analysis
CEOS .....Committee on Earth Observation Satellites
CRSNet .....Conservation Remote Sensing Network
DBU .....Deutsche Bundesstiftung Umwelt
DWD .....Deutscher Wetterdienst
EBV .....Essential Biodiversity Variables
ELI .....Empirical Line
EnMAP .....Environmental Mapping and Analysis Program
GBIF .....Global Biodiversity Information Facility
GDS .....Global Basic Data Set
GEO .....Group on Earth Observations
HSS .....Heinz Sielmann Stiftung
HyspIRI .....Hyperspectral Infrared Imager
IQR .....Interquartile Range
LOO .....Leave-One-Out
LRT .....Lebensraumtyp
LV .....Latent Variable
MTA .....Military Training Area
NeoMaps .....Neotropical Biodiversity Mapping Initiative
NEON .....National Ecological Observatory Network
NILS .....National Inventory of Landscapes
NIR .....Near Infrared
NMDS .....Non-metric Multidimensional Scaling
NSGA .....Non-dominated Sorting Genetic Algorithm
OLS .....Ordinary Least Squares
OAA .....Overall Accuracy
PCA .....Principal Component Analysis
PLSR .....Partial Least Squares Regression
PREDICTS .....Projecting Responses of Ecological Diversity In Changing Terrestrial Systems

RMSE .....Root Mean Square Error
ROME.....Reduction Of Miscalibration Effects
SAC .....Special Area of Conservation
SD .....Standard Deviation
SDM .....Species Distribution Modeling
SIFT.....Scale Invariant Feature Transform
SPECTATION.....Spectral Library for Vegetation
SSN.....Sum of Squared Null-model Residuals
SSR.....Sum of Squared Residuals
SWIR .....Shortwave Infrared
TOC .....Top of the Canopy
UAV .....Unmanned Aerial Vehicle
UFZ.....Helmholtz Centre for Environmental Research
UTC .....Coordinated Universal Time
UV .....Ultraviolet
VIS.....Visible
VM.....Variable Mean

Rationale and Motivation

Anthropogenic interferences with natural process dynamics increasingly induces ecosystem alterations that recently affects up to one half of the earth's terrestrial surface (Ellis et al., 2010; Sterling and Ducharne, 2008; Vitousek, 1997). Human-driven modifications thereby significantly impair ecosystem functioning and taxonomical complexity via the local loss of biodiversity (Hautier et al., 2015). In order to maintain habitat integrity and species diversity by minimizing human ecosystem interventions, nature conservation and ecological restoration is realized in protected area networks worldwide (Geldmann et al., 2013; Hockings, 2003; Watson et al., 2014). In particular, specifically designated military training areas (MTAs) exhibit high conservation values for various rare and endangered species and threatened habitats since they are affected by multiple disturbance regimes outside intensively used crop, pasture and urban areas (Lawrence et al., 2015; Warren et al., 2007; Zentelis and Lindenmayer, 2015). Although MTAs have the potential to increase the worldwide protected area coverage from now 15.4 % (Juffe-Bignoli et al., 2014) by at least 25 % (Zentelis and Lindenmayer, 2015), which is far more than defined in the international 2020 Aichi Biodiversity Targets (Woodley et al., 2012), their actual distribution, habitat inventories and conservation states are poorly documented due to difficult area access.

Against this background, the "Deutsche Bundesstiftung Umwelt" (DBU) launched a project in collaboration with the private nature foundation "Heinz Sielmann Stiftung" (HSS) to investigate the applicability of remotes sensing techniques for the mapping and monitoring of vegetation current states and developments on the former MTA "Döberitzer Heide" (Neumann et al., 2013). The project sets out to address two main issues of vegetation pattern analysis, simultaneously. On the one hand spatial patterns of succession, habitat conversion and gradual species shift provide intrinsic ecological knowledge that needs to be utilized to evaluate the effects of different management strategies such as big mammals grazing, mowing and tree removal that were implemented by HSS for the preservation and development of the MTA's open dryland areas. On the other hand, spatially explicit biological indicators on the habitat conservation status have to be reported regularly since these areas are protected in the European Natura 2000 network and by other legal protection frameworks.

The overall research approach was thus directed towards connecting conventional indicator mapping with continuous patterns recognition form ecological gradient analysis. The investigation thereby had to cope with the high spatiotemporal ecosystem complexity of the MTA's open drylands comprising small-scale heterogeneous floristic transition in multiple succession trajectories that are triggered by various disturbance regimes and highly variable habitat factors. Such characteristic vegetation patterns are distributed over an area of 30 km² in mostly inaccessible protection zones which facilitate a broad leverage in remote sensing related applications. A versatile procedure is needed that establish advanced numerical methods for the transfer of ecological field plot data to imagery. The intended methodological

framework ought to incorporate measures and units of three basic spatial mapping systems and related requirements for application purposes:

A) Monitoring of habitat management measures that requires patterns of habitat types, species change in time and disturbance parameters

B) Mapping ecological gradients, processes and dynamics for scientific epistemology that requires patterns of plant and animal abundances and abiotic ecosystem factors

C) Inventory legal conditions of protected areas that requires patterns of habitat types, conservation states assessment parameters and biological indicators

Since the arising challenges of multiple mapping perspectives are framed by different kinds of dense thematic and survey information, a recombination and development of methods in field and imaging spectroscopy are required. This evaluation of spectroscopic mapping potentials of different ecosystem properties for various application needs provides an important prerequisite in view of the operational use of upcoming hyperspectral spaceborne missions, such as EnMAP (Guanter et al., 2015).

The thesis takes up the challenges and requirements for a comprehensive ecosystem mapping and tries to reformulate patterns of perception between values of the ecological and the spectral continuity. There are two fundamental questions for the comprehension of the underlying logical units that will be reflected in an appropriate model design:

A) Can the ecological continuum of a MTA's open dryland areas adequately be described and broken down to various continuous ecosystem mapping units?

B) Is it possible to transfer various ecosystem variables formed by vegetation patterns from field point surveys to imagery via significant spectral relationships?

Which lead to the overall research question that determines the basic frame of the thesis:

C) How can a remote sensing based monitoring system be designed that incorporates different aspects of nature conservation and habitat management practice into a refined understanding of ecosystem processes and dynamics?

The following text will systematically approach the questions raised above from the concept of reductionism. It defines the smallest vegetation unit to capture the problem, draws connections to the spectral unit and finally integrates into the mapping unit for ecosystem characterization and conservation efforts.

Chapter I: Introduction

1 Object of Investigation - Vegetation

The term vegetation can be very generally regarded as “plant life” or “plants in general” that cover a certain area as part of the biosphere (Keddy, 2007; Küchler and Zonneveld, 1988). (Maarel, 2005) provides a stricter interpretation as he explicitly excludes non-spontaneously growing plants. This definition is taken up by the thesis and hereinafter referred to as natural vegetation where natural processes predominate (Burrows, 1991). But what are the basic units of vegetation? And what are the logical concepts behind such units that can be translated into empirical measures for inductive reasoning? Such definition provides a crucial starting point as this thesis is intended to draw predictive conclusions from distinct vegetation characteristics. The fundamental nature of vegetation is therefore disassembled into quantifiable units according to different theories in vegetation science (Section I-1.1) whereas the concept of vegetation continuum is emphasized. On that basis, vegetation as a state variable is introduced in order to explain time-space variations for pattern formation (Section I-1.2). Vegetation is then raised to the anthropocentric level where characteristic units are related to conservation and restoration efforts at a broader scale (Section I-1.3). Finally, different levels of vegetation differentiations are synthesized for a coherent characterization of species, processes and dynamics in the research area (Section I-1.4).

1.1 Vegetation as a Continuum

For an effective description of vegetation it can generally be stated that vegetation consists of plants that can be classified into different units. The two fundamental units comprise life form morphology (e.g. tree, shrub, grass) and plant species taxonomy. Both categories can further be described by additional characteristics such as biomass, cover or density (Bonham, 2013a). At the beginning of the 20th century, Frederick Clements, a plant ecologist, opened up a fundamental debate about the basic concepts behind vegetation characterization. From his research about the floristic composition of succession stages, he concluded that plant species are always organized in patterns of communities, associations or stands (Clements, 1916). A plant community is thereby assumed to be a really existing, discrete entity that consists of a certain, recurring species composition with some common peculiarity. This entity is introduced as integrated vegetation unit where species occurrences are interrelated and strictly constraint to a group in such a way that their distribution limits are compulsorily formed together (Whittaker, 1962). This is substantially contrasted with Henry Gleason’s concept of individualistic plant species behavior that makes no assumptions about compositional group memberships. Therein, each species grows in response to a set of abiotic and biotic environmental factors that individually influence site specific growth conditions (Gleason, 1926; Goodall, 1963; McIntosh, 1967). Multiple environmental responses consequently produce complex interactions where a single species may establish or not. Beyond organized

group interrelations and triggered responses in the community concept, here in particular, individual species responses to the environmental background were analyzed and synoptically extended to the concept of a vegetation continuum (Austin, 1985; Goodall, 1963; McIntosh, 1967; Whittaker, 1967). The underlying nature of vegetation can thus be understood within a continuous space of gradually changing influential factors that steadily determine the floristic composition. Besides species taxonomy, a designation of vegetation units is realized over individual growth characteristics that can be quantified by measuring e.g. species occurrences, abundances or frequencies (see Figure I-1 for a schematic overview).

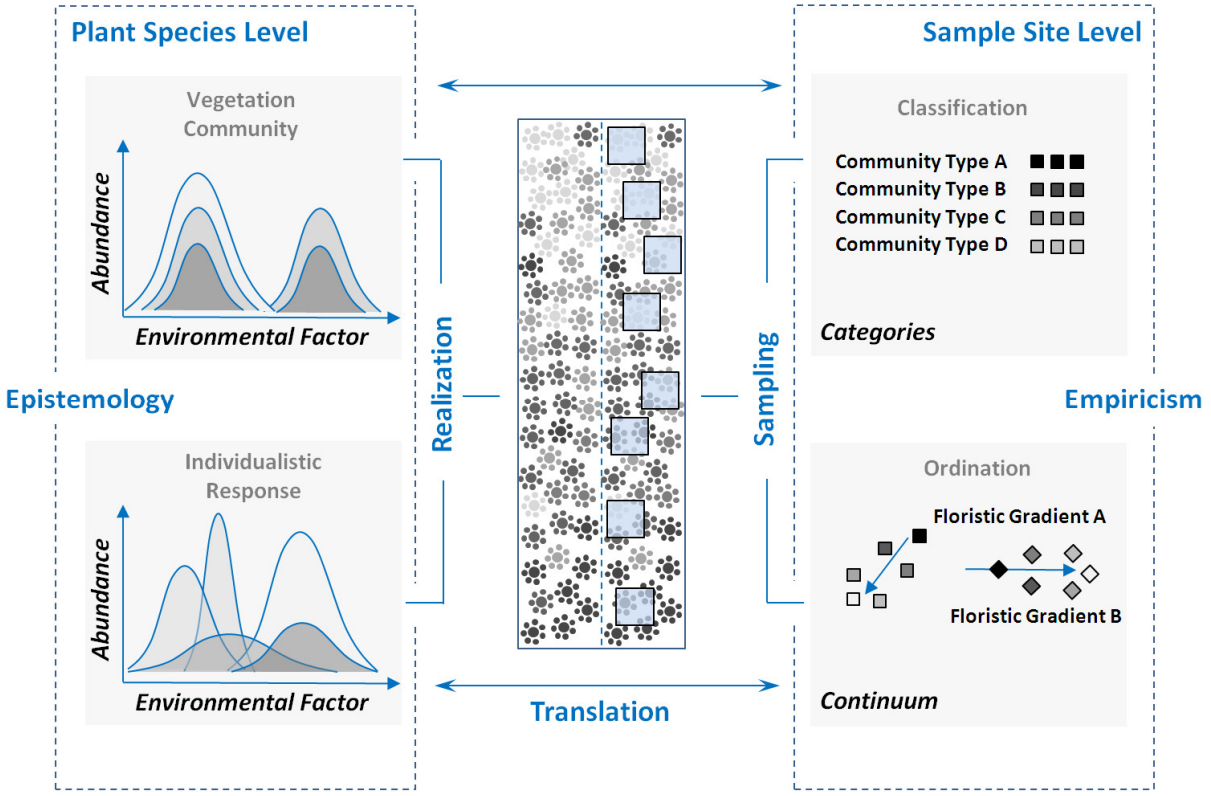

Figure I-1: *Conceptual models for vegetation characterization as comparative epistemological and empirical methods for plant species allocation and organization*

In the following, the concept of vegetation continuum is accepted as fundamental premise in this thesis. Species occurrences in conjunction with taxonomical diversity as well as distinct measures of growth conditions are used in order to describe vegetation characteristics. The rationale behind this initial premise can be found in the principles of constructivism and reductionism. The radical constructivism would argue that categories like communities are inconsistent units created by a reciprocal relationship between the human mind and the environment. As a consequence the resulting units are therefore constituted with the inherent experiences, external relations and expectations in each observer's personal mind. Supporting evidence provides the fact that until today no consistent, universal definition for a vegetation

community has been established so far. Moreover, the scientific agreement about the terms and common properties of community definitions such as homogeneity, integration, discreteness could not yet been achieved (Moravec, 1989; Palmer and White, 1994; Whittaker, 1962). Additionally, according to Occam's razor law of parsimony it is not strictly necessary to introduce an ad hoc hypothesis about vegetation's community organization. In fact, the methodological reductionism offers the possibility to clearly explain natural phenomena or systems on the basis of their smallest possible entities. This practice forms the basic framework of many fields of science and will be adopted in this thesis as well, investigating individual species behavior as a continuum for drawing further inductive conclusions.

Numerical methods for the delineation of species variations in relation to internal and external environmental factors can generally be termed as ecological gradient analysis. Thereby, an analytical way to quantify multi-species relations solely based on species occurrence and abundance without integrating external explanatory variables is specifically realized with indirect gradient analysis, commonly referred to as ordination (e.g. Austin, 1986, 1985; Ter Braak and Prentice, 2004; Whittaker, 1967). The initial unit of the continuum analysis is the sample unit that is acquired during floristic field surveys at the study site. As a result, species abundances; in this study cover values after the enhanced Braun-Blanquet method (Wilmanns, 1998); are transferred into a sites-by-species matrix. This matrix can be considered as the n-dimensional species space (where n = number of species) that determines the floristic continuum of the study side. In view of the constraints of human perception, this numerical continuum can neither be captured nor interpreted. Ordination provides a method for reducing the initial number of dimensions by ordering vegetation samples along artificial, mathematical axes in a way such as to preserve sample similarity that is determined by the floristic composition. In consequence, vegetation samples are projected along a reduced number of abstract ordination score axes that allow a quantification of sample position through axes score coordinates. In indirect gradient analysis such score axes are calculated according to different principles. While in Principal Component Analysis (PCA) (Hotelling, 1933) the floristic variance between samples is maximized along axes scores through correlation, Correspondence Analysis (CA, CCA) (Hill, 1973; Hill and Gauch, 1980) creates theoretical gradients by iteratively combining artificial gradient values with real species abundances until sample gradients reflect an inherent gradient direction. The score coordinates in the final low-dimensional ordination space represent new synthetic variables to describe the similarity between the samples. However, there are three underlying assumptions that have to be considered. In both methods vegetation samples are ordered along axes score gradients that are arranged orthogonally to each other. The final structure of the ordination space is then determined by a fixed similarity measure between the samples, representing Euclidean

distances for PCA and Chi-squared distances for CA. Both methods additionally presume linearity between species abundances on the sample points.
In order to reduce the number of a priori assumptions in numerical modeling, this thesis utilizes the Non-metric Multidimensional Scaling (NMDS) (Kruskal, 1964) approach for species ordination. In NMDS the initial sites-by-species matrix is directly projected into an n-dimensional ordination space. The criterion is thereby not to explain floristic variances along orthogonal score axes but rather to minimize the deviation of sample distances (similarities) between the original and projected matrix. The distance measure can be freely selected, whereby in this thesis the robust and frequently used Bray-Curtis-distance (Clarke, 1993; Faith et al., 1987) was chosen. The projection itself is realized by iteratively comparing the rank order (non-metric relation) of original and projected distances until an optimal monotonic, increasing relationship is established. The samples are continuously re-ordered, starting from a random configuration, and the projection is finalized for the n-score axes that exhibit the minimal average residual deviation in the rank order relation. This approach can be understood as a species composition restoration (De'ath, 1999) since the score axes solely represent abstract dimension that can be related to the floristic composition and external factors by post hoc analyses as conducted in this thesis.

1.2 Vegetation Patterns and Dynamics

Since the research object vegetation has to be defined by competitive human perspectives, it inherits components and characteristics that are embedded in the time-space domain. There are a number of different approaches to precisely assign spatial and temporal dimensions in which vegetation itself is realized as patterns. It can be shown that this propagation of vegetation characteristics into the time-space domain creates unique pattern dynamics that can be related to processes and function in ecosystems (Delcourt et al., 1982).

The spatial dimension of formed vegetation patterns can be delineated using point sample statistics (Law et al., 2009; Legendre and Fortin, 1989), abiotic factor grids for species distribution modeling (Austin, 2002; Franklin, 1995; Guisan and Zimmermann, 2000; HilleRisLambers et al., 2001) or, as conducted in this thesis, remote sensing derived vegetation maps on image pixels (Adam et al., 2010; Thenkabail et al., 2012; Xie et al., 2008). The spatial propagation of vegetation characteristics thereby crucially depends on the essential finding that vegetation patterns vary continuously over different spatial scales (Dale and MacIsaac, 1989; Palmer, 1988; Scheuring and Riedi, 1994; Wiens, 1989). In this respect, the concept of vegetation continuum supplies a descriptive method for a scale invariant representation of spatial vegetation patterns. In contrast to scale-dependent community unit definitions, it is based on gradual species shifts along continuous environmental gradients. The sequential order of species composition can be mapped as internal floristic gradients using similarity measures from ordination. External environmental variables are therein

inherently reflected as they control directional spatial changes in species composition. In this way, the fundamental spatial pattern of homogeneity - heterogeneity transition can be fully represented. Especially transition zones (ecotones) that hold information on species shifts or, more general, on habitat development can be mapped in order to connect temporal process dynamics.

The combination of time-space phenomena in vegetation pattern development results in the formulation of some basic hypotheses about ecological process dynamics. One basic and most central process, the species change over time (turnover), is thereby described in the concept of ecological succession. It enables the delineation of species assemblage variations that follow disturbance regimes on successional trajectories. Again there is no mutual agreement about the definition of succession between community ecologists and the individualistic concept; however, this thesis will espouse the commonly held view now that is derived from Gleason's perspective (see Section I-1.1). Here, the species turnover is not linearly directed and rarely reaches a culmination point that represents a stable equilibrium. In fact, successional trajectories are often redirected or reset by multiple disturbance regimes that vary in time and space (Gleason, 1926; Walker and Moral, 2003; White and Jentsch, 2004; Whittaker, 1974). Ecological succession is further an exclusively species-driven characterization of spatiotemporal vegetation pattern dynamics. External environmental factors are related a posteriori in order to describe rates of species turnover, disturbance effects or ecosystem resiliencies (Sterling et al., 1984; Vetaas, 1997; Wali, 1999).

Succession generally addresses changes in plant compositional pattern. On the plant individual level another important dynamic predominates pattern dispersal and configuration, called fluctuation (Miles et al., 1989). Within fluctuation patterns, individuals appear or disappear due to ontogenetical sequences or external factors such as predation, competition or stochastic environmental stress (Pickett et al., 1987). In particular, ontogenetical fluctuation opens up a supplementary aspect of pattern recognition as it entails structural composition changes in time and space. Thereby, phases of degeneration and regeneration alternate in plant life cycles comprising stages of e.g. juvenile growth, senescence and death that is superimposed with phenological growth variations (Crawley, 1996; Grime, 2006; Watt, 1955). However, structural pattern variations may also be associated to cyclic successional trajectories that are not necessarily triggered by disturbances (Huston and Smith, 1987).

In summary, the concept of vegetation continuum can be complemented by units of space and time. The basic terms used here are spatial transition and temporal change of composition and structure. These are the fundamental properties out of which the relevant information about ecosystem management will be derived at the next, anthropocentric level.

1.3 Nature Conservation and Ecological Restoration

As part of the living environment, humans actively shape or even completely construct their ecological niches to optimize evolutionary processes. By now, anthropogenic alterations of ecosystems are ubiquitously pervaded whereas up to one half of the earth's terrestrial surface is modified directly by human influence (Ellis et al., 2010; Vitousek, 1997). However, there are different degrees of human impacts on ecosystems that can be described by levels of hemeroby (Hill et al., 2002; Jalas, 1955; Steinhardt et al., 1999). The hemerobic index indicates the "closeness to nature" or "degree of naturalness" whereas metahemerobe and polyhemerobe systems, such as agriculture and urban areas, are heavily modified or artificial. This thesis is located in the area of oligohemerobe or ahemerobe quasi natural terrestrial ecosystems that are merely influenced by immissions through soil, water and air. Spatiotemporal vegetation patterns are here created and modified by natural process dynamics, such as succession, to a great extent. Such systems particularly benefit from two conscious anthropocentric resolutions, which vote from a moral, social, esthetic or even economic point of view (see ecosystem services: (Daily, 1997) for ecosystem preservation and rehabilitation.

The essential aspect of preservation is reflected in nature conservation that lists threatened species and habitats in order to designate protected areas. These areas of various different kinds (Juffe-Bignoli et al., 2014) are designed globally for the conservation of the world's biological diversity (CBD, 1992). They are considered as the cornerstone for implementing conservation strategies (Geldmann et al., 2013; Hockings, 2003; Watson et al., 2014). The spatial distribution of species assemblages and external abiotic drivers are therein often merged into the habitat unit that represents an extended zonal continuum of uniform living conditions for both plants and animals. Since protected areas are permanently affected by habitat conversions due to a multitude of ecological processes and dynamics, an effective habitat management needs to be realized to maintain a favorable conservation status.

The term habitat management encompasses intentional methods and means of assisted ecosystem regulation by humans (Ausden, 2007). The scientific concepts behind these practical manipulations of species, habitats and processes are delineated in the field of ecological restoration (Aronson et al., 2006; Jordan, 1996; Lake, 2001; Walker et al., 2007; Young et al., 2005). Thereby, restoration aims to recover a damaged, degraded or destroyed ecosystem by protecting natural process dynamics from anthropogenic interferences (Dietz et al., 2015; Prach and Hobbs, 2008) or by an active intervention through habitat management. An active intervention directly affects spatiotemporal vegetation pattern by influencing different types of ecological processes. Modifications of establishment dynamics, facilitation, competition and extinction thereby control patterns of species invasion, species richness and habitat states along successional trajectories (Herrick et al., 2006; Prach and Walker, 2011).

For the creation of successional tipping points, regeneration phases and species realignment, disturbance regimes can be artificially introduced by e.g. mowing, burning, grazing or targeted removals.

One of the key aspects of restoration projects is the implementation of appropriate monitoring systems (Bestelmeyer et al., 2006; Ewen and Armstrong, 2007; Lake, 2001). For the purpose of evaluating the management input, development stages and ecological responses with regard to effects on species, habitats and processes, spatiotemporal vegetation patterns can be mapped using points, point-line intercepts, transects or remote sensing grids. Spatially explicit grids are thereby advantaged as they are capable to reproduce the full complexity of species arrangement throughout a large scale spatial continuum (Bestelmeyer et al., 2006; Nagendra et al., 2013; Turner et al., 2003; Wiens et al., 2009). In particular, multiple transition zones, where species turnover is most relevant and hence management strategies are most effective (Gosz, 1991; Łuczaj and Sadowska, 1997; Risser, 1995), can only be coherently projected in grid based mapping approaches.

1.4 The Research Area: Vegetation States and Management

The research was conducted on a former military training area (MTA), Döberitzer Heide, located at 53° latitude North and 13° longitude East west of Berlin, Germany (Figure I- 2). The entire MTA encompasses 52 km² of which 27 km² are designated as a Special Area of Conservation (SAC) as part of the European Natura 2000 network. The SAC belongs to the global inventory of protected areas for nature conservation (see Section I-1.3) and consist of habitats and species that are listed in annex I and II of the European Union's habitat directive (EU, 1992). Within this thesis, research is aimed at open dryland areas on glacial ground moraine deposits on which the Natura 2000 habitat types 2330 (Inland dunes with open Corynephorus and Agrostis grasslands), 6120 (Xeric sand calcareous grasslands) and 4030 (European dry heaths) are declared. The major objective for these habitat types is legally defined as to reach or maintain a favorable conservation status. For this purpose, reference values for habitat assessments to indicate stable ranges of species and habitat extents have to be measured, controlled and reported in a 6 year cycle (Cantarello and Newton, 2008; Epstein, 2016; Louette et al., 2015; Ostermann, 2008).

The MTA's open dryland habitats were only able to rise due to exposure to long-term military use, including soil translocation, tree removal or fires from bombardments. After the withdrawal of troops in 1991, the open training fields were left undisturbed. Since then, processes of natural succession, particularly, invasion by grasses and woody species induced mosaicking and interpenetration of different habitat types. Starting from open pioneer stages with *Corynephorus canescens* and *Rumex acetosella* stands on open sandy, acidic soil substrates, succession pass over onto cryptogam stages (e.g. *Cladonia spec., Polytrichum*

piliferum) that are further emerged into stands of *Calluna vulgaris* or *Festuca ovina agg./ Agrostis capillaris* grasslands. A small scale floristic heterogeneity is additionally controlled by nitrate eutrophication (*Calamagrostis epigejos*) and local base enrichment (e.g. *Galium verum, Peucedanum oreoselinum*) whereas the overall dominating process of scrub invasion mainly occurs through *Populus tremula, Sarothamnus scoparius, Betula pendula* and *Prunus seoritna*. In consequence, a complex continuum of species turnovers, transition zones and life cycles coexists in conjunction with natural processes at different states of development. The diversity of species and processes is protected in a nature reserve that is home to an estimated 5500 species of plants and animals, whereby 980 species are classified as endangered or threatened (Beier and Fürstenow, 2001; Oehlschlaeger et al., 2004).

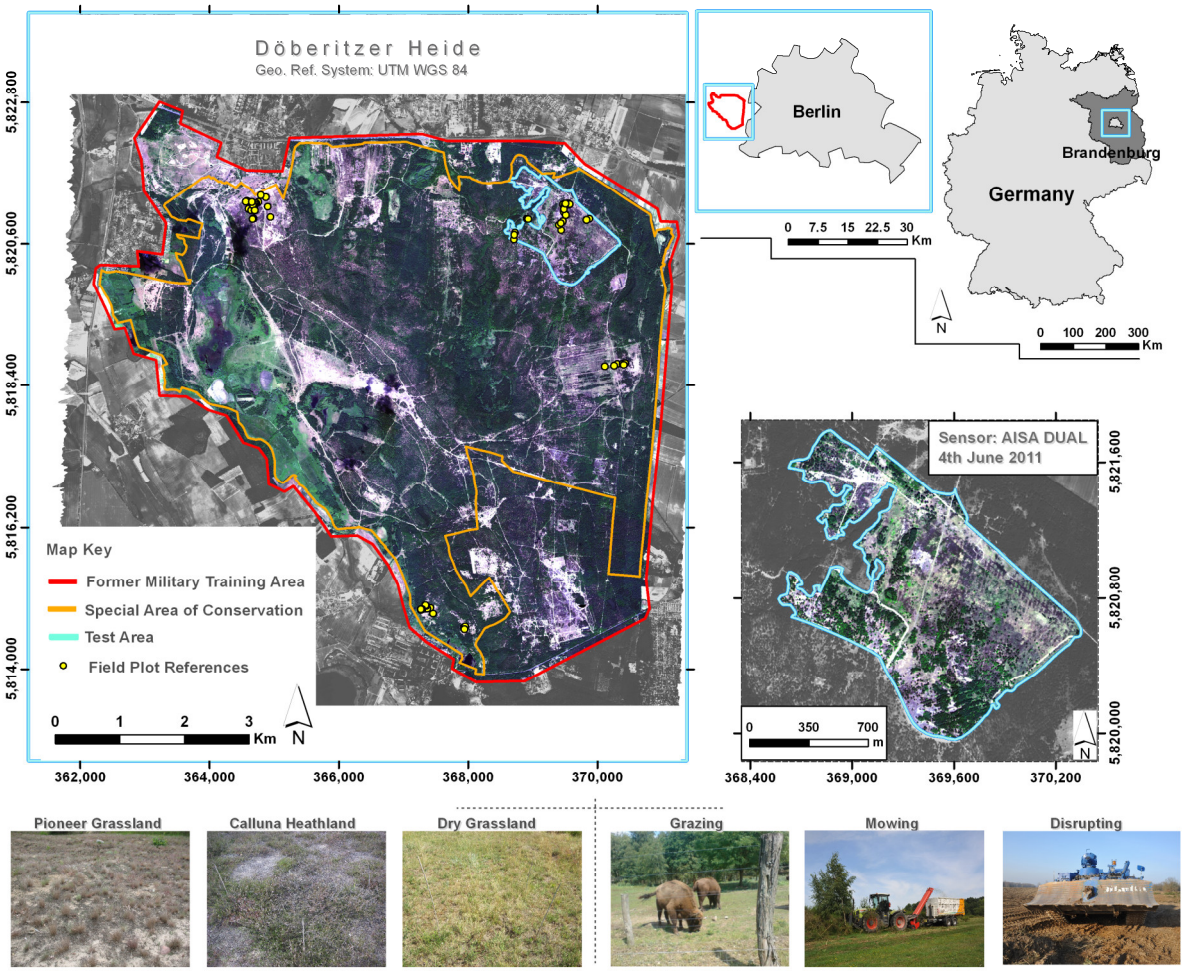

Figure I-2: *Research Area Döberitzer Heide and open dryland test side visualized on an AISA DUAL image mosaic; three main habitat types on glacial ground moraine deposits and typical management measures for habitat restoration (images by courtesy of Jörg Fürstenow, Heinz Sielmann Stiftung)*

The outstanding MTA's value for nature conservation entails efforts and activities to maintain high values of biodiversity, control habitat conversion and preserve a variety of disturbance regimes and successional trajectories that are principally set at the level of vegetation patterns (Warren et al., 2007; Zentelis and Lindenmayer, 2014). Since 2004, the nature foundation Heinz Sielmann Stiftung implements a bundle of management measures to approach these conservation objectives. Particular emphasis is placed on big mammals grazing such as European bison (*Bison bonasus*), wild horse (*Equus ferus przewalski*) and sheep flocks in conjunction with active tree removals for open dryland regeneration and establishment. Pioneer stages are artificially constructed by vegetation layer removal and soil profile disruptions using heavy military vehicles (conservation tanks). The Calluna heathlands are periodically mown, shrubs and young trees are cut and organic material is completely removed to minimize nutrient accumulation. Hence, natural succession is permanently modified at different spatial extents and varying temporal intervals.

2 Spectroscopy as a Tool for Vegetation Pattern Analysis

Ecological restoration by means of habitat management requires the monitoring of arising vegetation patterns and dynamics. One may simply ask how the habitat manager can know whether the implemented practice is successful or has achieved intended spatiotemporal effects. To answer this question, this thesis examines the potentials of imaging spectroscopy for monitoring vegetation patterns on a spatial grid basis. Initially, it will be demonstrated how hyperspectral reflectance signatures can be utilized as quantifiable proxies for the characterization of the vegetation continuum's entities such as species, gradients and states (Section I-2.1). Subsequently, a link will be drawn from spectral quantification towards image pixel transfer for spatiotemporal vegetation pattern recognition (Section I-2.2). At the end, the spectral sampling design and image acquisition is outlined as basis for further analyses in the study area (Section I-2.3).

2.1 Spectral Properties of Plants

Information about vegetation on earth, in sensu stricto plants, can be derived from sun emitted electromagnetic radiation that is reflected, absorbed and transmitted by components of plant cell compounds (Gates et al., 1965; Knipling, 1970). Optical properties of plants are therein manifested as the amount of released energy in different wavelength regions as a result of energy conversion through overtone, bend, stretch, deformation, rotation and electron transition at the chemical bonds of organic molecules (Curran, 1989; Fourty et al., 1996; Himmelsbach, 1989). It is widely accepted that wavelength specific absorption/reflection features can be linked with variations in foliar biochemistry and biophysical properties of plants and stand canopies (Kumar et al., 2002; Ollinger, 2011). There has been found empirical evidence on significant coherencies within wavelength regions for the detection of e.g. pigments (Blackburn, 2006; Gitelson et al., 2003; Sims and Gamon, 2002), nitrogen (Kokaly, 2001; Smith et al., 2002; W. C. Bausch and H. R. Duke, 1996), lignin and cellulose (Elvidge, 1990; Kokaly and Clark, 1999), water (Danson et al., 1992; Huntjr and Rock, 1989; Tucker, 1980) or physiological structure (Darvishzadeh et al., 2011; Gausman et al., 1970; Thorp et al., 2011). Hyperspectral reflectance signatures are therefore applied to extract information on the level of plant traits and interacting external abiotic factors. It has been shown that knowledge about plant stress regarding nutrient supply, pollutant contamination, disease effects or competition (e.g. Carter, 1994, 1993; Clevers et al., 2004; Jackson, 1986) and plant growth regarding senescence, phenology or biomass (Gitelson and Merzlyak, 1994; Serrano et al., 2000; Thenkabail et al., 2013) can be reliably extracted and used for spatial mapping purpose. However, empirical research on wavelength coherencies can only provide an estimate of plant states under clearly restricted conditions. Due to multiple superimpositions of chemical compounds, plant traits and measured spectral responses,

empirical evidence is mainly modeled at the species level. By this means, the state of a single individual within the vegetation continuum can be described coherently (see Figure I-3 for a broad semantic partition of plant's reflectance signature).

The differentiation between plant species on the basis of spectral reflectance signatures has to cope with above-mentioned intra-species biochemical and physiological variations. Today the total number of plant species is estimated between 300.000 and 600.00 ("The Plant List," 2013). From an epistemological point of view, a unique, physically based spectral modeling of species varieties disintegrates into suchlike complexity that favors statistical approaches. To date, there is surprisingly little research published on the discrimination of plant individuals by means of spectral reflectance analysis, especially on natural vegetation sites. The basic statistical procedure here is to apply parametric or nonparametric hypothesis testing in order to find out significant wavelength specific differences between inter- and intra-species variances. In doing so, species from grass rangeland (Schmidt and Skidmore, 2001), Mediterranean (Manevski et al., 2011), mangroves (Vaiphasa et al., 2005; Wang and Sousa, 2009), forest trees (Clark et al., 2005; Cochrane, 2000; Gong, 1997; van Aardt and Wynne, 2007) and wetlands (Adam and Mutanga, 2009; Prospere et al., 2014) could be spectrally discriminated by point spectroradiometer measurements. The results theoretically implicate spectral separability at the species level, however, an important entity of the vegetation continuum; namely transition; needs to be incorporated into the final mapping transfer.

Species transition as stated by the concept of vegetation continuum is manifested in increments of abundance values (fractional species cover per unit of area). Since remote sensing of plant species for the purpose of mapping always requires the transfer of spectral models to surface elements (pixels), species abundances are mostly represented in the projection of mixed vegetation stands. This is particularly true for small-scale heterogeneous floristic patterns that occur in managed (semi-) natural open land ecosystems. The spectral attribution for species and states is supplemented by reflectance variances from different floristic gradients. By way of illustration the spectral reflectance curves of *Calluna vulgaris* in a dominance stand and in three stands of similar abundance but with differing second species invasion is visualized (Figure I-3). Depending on variable stand compositions, the spectral reflectance crucially differs for the *Calluna* individual taxon with constant abundance values and in the same growth state. This phenomenon is well understood, however, by now only investigated by a few studies (Feilhauer et al., 2010; Irisarri et al., 2009).

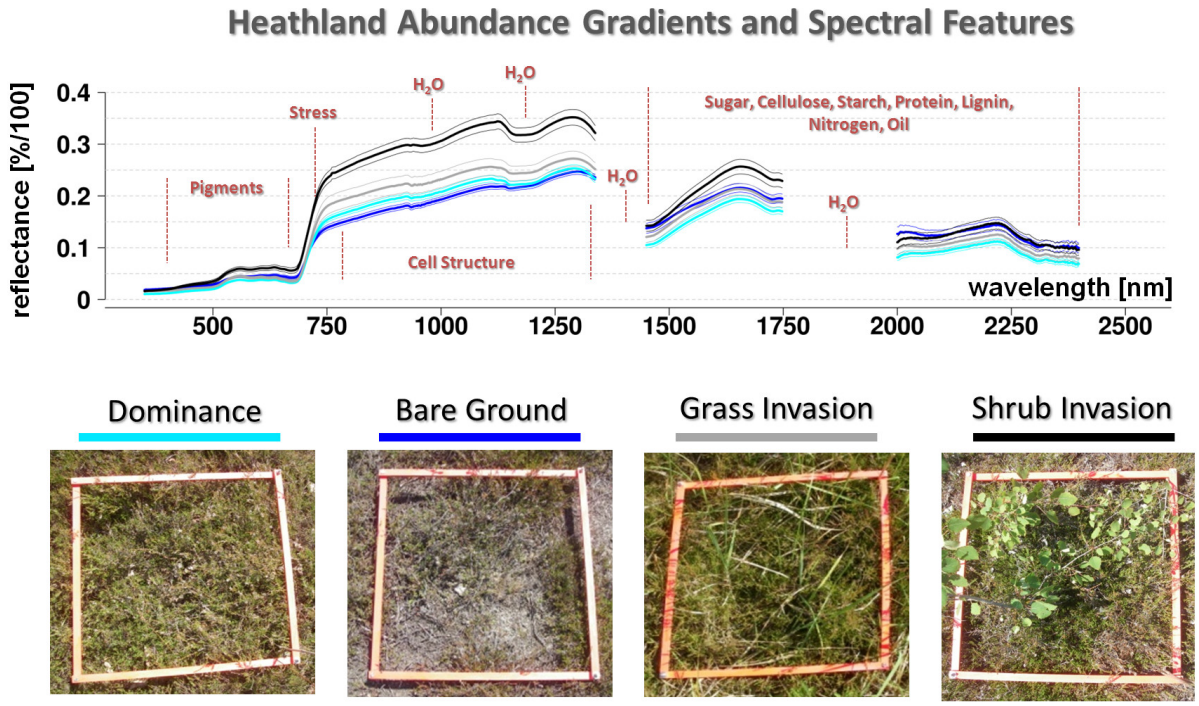

Figure I-3: *Typical semantic determination of different wavelength regions in plant's reflectance spectra visualized with Calluna vulgaris spectroradiometer measurements at field plot scale; varying gradients of invasive species for constant heath abundance pattern exhibit different spectral responses*

2.2 Imaging Spectroscopy for Vegetation Mapping

Remote sensing of ecosystem patterns and processes has become common in the field of ecology to monitor changes, aid conservation effort and model ecosystem functioning (Aplin, 2005; Kerr and Ostrovsky, 2003; Nathalie Pettorelli et al., 2014). Spatial maps are provided for vegetation patterns and dynamics that can be related to measures of biodiversity (Gould, 2000; Lausch et al., 2016; Nagendra, 2001; Turner et al., 2003), habitat conditions (Corbane et al., 2015; Nagendra et al., 2013; Weiers et al., 2004) and various other conservation units (Vanden Borre et al., 2011; Wiens et al., 2009; Willis, 2015). Imaging spectroscopy is thereby capable of resolving the high spatial and compositional complexity of observed natural landscape compartments due to the inherent dense spectral sampling interval (Schaepman et al., 2009; Ustin et al., 2004; Wang et al., 2010). It enables a direct transfer of empirical knowledge about wavelength-specific spectral responses and plant's biochemical and physiological properties to image pixels. Further relationships between vegetation traits and plant/ecosystem functions (e.g. biomass, productivity, competition) (Schweiger et al., 2016; Smith et al., 2002; Ustin and Gamon, 2010), habitat status indicators (e.g. grass, shrub, tree encroachment) (Delalieux et al., 2012; Mücher et al., 2013) and vegetation community

structures (Cole et al., 2014; Oldeland et al., 2010a) have been derived for spatially explicit mapping.

It is important to keep in mind that functions, indicators and communities still operate at the level of abstract, pre-defined vegetation units that incorporate a priori concepts about the nature of mapping units. The mapping of individual species distributions as a whole in a landscape's vegetation continuum is recently approached by single invasive species mapping in open land (Lawrence et al., 2006; Underwood, 2003; Ustin et al., 2002) or forest (Asner et al., 2008; Clark et al., 2005; Cochrane, 2000) habitats. To cope with the dense information content provided by hyperspectral reflectance signatures, new methods from statistical machine learning theory (e.g. Partial Least Squares Regression, Random Forest, Support Vector Machine) are used and adapted for spectral feature selection for species identification. It is recognized that an intense coexistence of complex environmental interactions affecting plant states and compositional gradients impede distinct spectral separation of species integrities (Andrew and Ustin, 2008). However, especially an increased side complexity indicates patterns of high biological and process diversity that are prioritized as key components in conservation management, since they are particularly prone to processes of habitat conversion (Hodgson et al., 2011).

One possible approach to delineate species occurrences along varying floristic gradients can be realized by species abundance mapping. By now, there are only a few studies that investigate spectral characteristics of vegetation abundance pattern in open land communities (Lu et al., 2009; Miao et al., 2006; Parker Williams and Hunt, 2002). Due to the complexity of possible gradient structures in multi-species environments, a coherent mapping of multidirectional species transition has not been realized so far. At this point numerical methods from ecological gradients analysis combined with machine learning algorithms on hyperspectral reflectance signatures open up new perspectives for the analysis of species responses in varying compositional patterns. Nigel (Trodd, 1996) showed that ordination score axes (see Section I-1.1) can be related to spectral reflectance values measured at vegetation survey's plot locations. For the first time he presented the general possibility to model species transition by reflectance signatures in an ordination space. Since ordination space axes represent different species gradients that respond to changes in spectral reflectance, it was then proven that multidimensional transition and compositional change can directly be projected to imagery (Armitage et al., 2004; Schmidtlein et al., 2007; Schmidtlein and Sassin, 2004; Thessler et al., 2005). Such gradient maps crucially differ from common discrete vegetation unit approaches as they coherently transfer the entire vegetation continuum to the pixel scale without ad hoc category aggregations. In consequence, the mapped continuum holds a wide range of additional information about e.g. the abiotic background (Schmidtlein, 2005), plant functions (Schmidtlein et al., 2012) and species

(Feilhauer et al., 2011) that could be integrated in habitat management and monitoring (Feilhauer et al., 2014).

2.3 The Spectral Sampling of the Research Area

The spectral data base for the description of vegetation entities, pattern and dynamics was collected at the scales of field plot locations and imagery extents. A field plot was defined as a 1 square meter area in which the fractional percent cover of all vascular plants, mosses and lichens was estimated according to the modified Braun-Blanquet method (Braun-Blanquet, 1964) using species nomenclature based on (Rothmaler, 2005). Spectral measurements were conducted with a portable ASD field spectroradiometer (ASD Inc., Boulder, CO, USA) that collects relative reflectance spectra from visible (VIS) to short wave infrared (SWIR) (350 nm – 2500 nm) in 2151 spectral bands related to a white reference panel. Every field plot was covered by 25 single reflectance signatures that were collected at 1.4 m above canopy using an 8° foreoptic. The sampling was performed in a 5 x 5 grid traverse for point measurements with a footprint of 0.2 m diameter that altogether span the entire field plot area. In total, 58 reference plots were sampled in open dryland sides over the entire MTA (Figure I-2). Field plots were systematically located in dominance stands and typical transition zones and disturbance regimes between and within known Natura 2000 habitat types. Measurements took place in spring, summer and autumn phenological phases up to 5 times per year during a period between 2007 and 2011. Vegetation surveys are thereby continuously completed and re-visited in each year. The final data infrastructure was made publicly available in a comprehensive spectral database, called (“SPECTATION,” 2015).

Hyperspectral imagery was acquired during two airborne overflight campaigns in the midsummer and midautumn phenological phase of the year 2011. On June 4th between 10:00 and 12:30 UTC (Coordinated Universal Time), the first acquisition was carried out with an Airborne Imaging Spectrometer for Application (AISA DUAL (Lausch et al., 2013; Makisara et al., 1993)) that recorded 22 flight stripes in 300 samples per scanning line. The spectra that were provided consist of 367 wavelength bands from 401 nm to 2406 nm. The second overflight was realized using an Airborne Prism Experiment (APEX (Schaepman et al., 2015)) imaging spectrometer that scanned 1000 samples per line in 288 wavelength bands between 413 nm and 2449 nm. Here, the acquisition time was set between 08:27 and 09:12 UTC on September 21st. After geometric registration the final image mosaics were resampled to 2 m (AISA) and 2.5 m (APEX) pixel sizes. Starting from at sensor radiance provided by internal radiometric calibration coefficients, spectral binning, smear correction and destriping (ROME) (Rogaß et al., 2011) was conducted followed by radiative transfer modeling (Atcor-4) (Richter and Schläpfer, 2002) for the retrieval of top-of-canopy reflectance signatures. Additionally, spectral wavebands were corrected to overflight conditions using reference targets for empirical line calibration (Eli) (Smith and Milton, 1999).

3 Research Objectives and Structure

The thesis is clearly structured along two fundamental modeling approaches that are combined for the spatial mapping of ecosystem characteristics (Figure I-4). In the ecological model, the object of investigation is contentually decomposed, quantitatively represented in numerical models and finally reassembled into assessment tools for nature conservation. The general research path is drawn from individual species occurrence over transition in a continuum towards habitat categories and gradients that are treated by means of restoration management. It will be shown that species gradients can be related to spectral reflectance signatures. The spectral model sets up the empirical relationships between species, transition and derived habitat parameters that are further used to transfer ecosystem characteristic to the image scale.

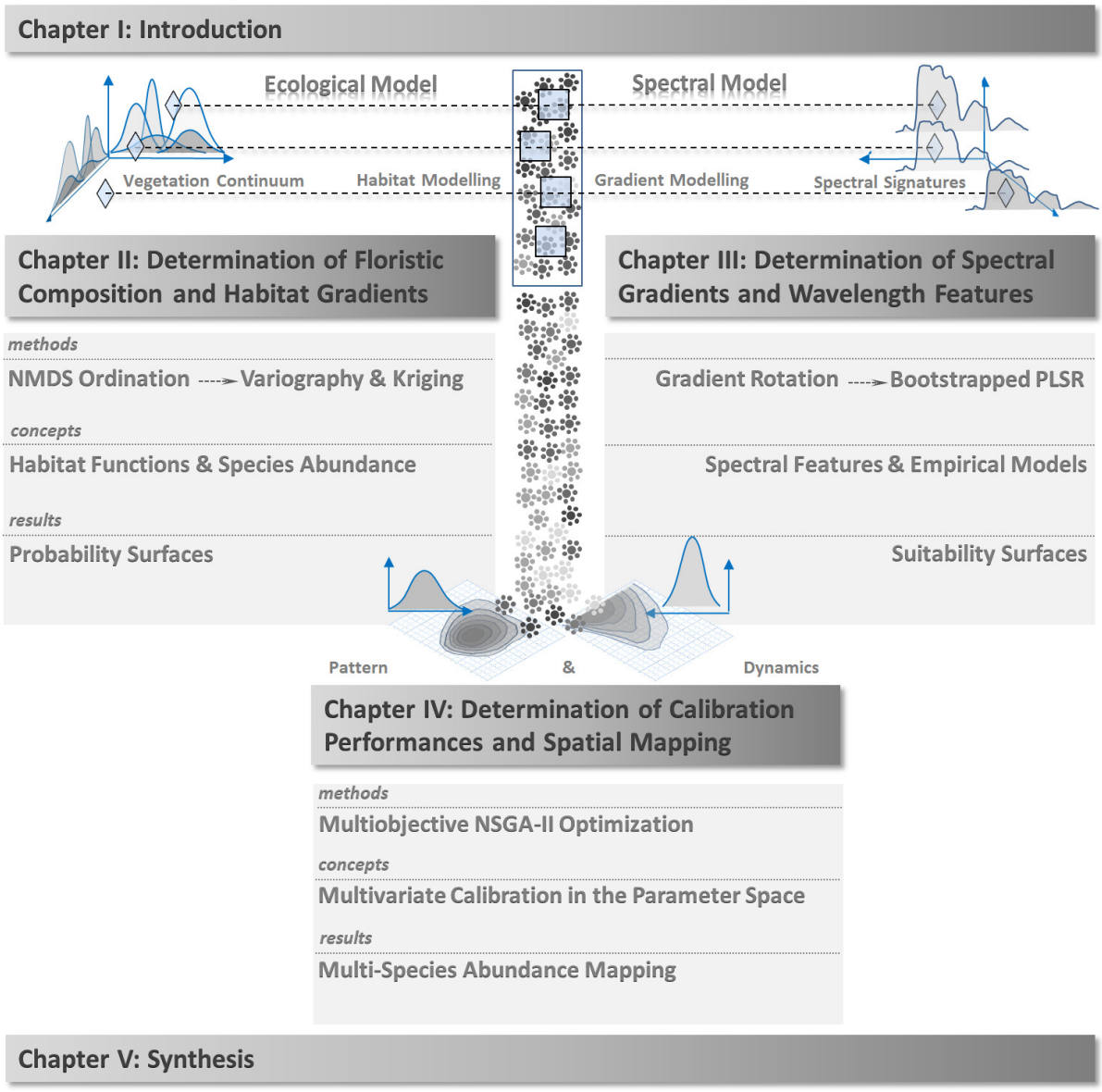

Figure I-4: *From model to mapping: conceptual framework of thesis structure with chapters arranged according to positions of method integration*

The research objectives will be explained separately with respect to three per-reviewed publications that are presented in the chapters II-IV. Each chapter is outlined by a uniform section structure containing Introduction, Material and Methods, Results, Conclusions whereby each section is individually subdivided by the inherent thematic groups. The main research questions are evolved from the chapter specific objective formulations.

Chapter II: Determination of Floristic Composition and Habitat Gradients

published as:

"Gradient-Based Assessment of Habitat Quality for Spectral Ecosystem Monitoring"

If the concept of vegetation continuum is defined as a useful approach to explain the nature of vegetation, since it makes no a priori assumptions about the inherent structures of the environment, the applicability of the numerical method used to mathematically capture the full complexity of species gradients also have to be verified. Thus, it is of utmost importance to know whether an ordination technique is capable of representing stable and significant floristic patterns of a landscape sequence. Moreover, up to now it has been rarely investigated in detail to what extent the projected complexity can be delineated and used e.g. for habitat management practice. Thereby, methods lent by the field of geostatistics could be utilized to quantify continuous patterns of species transition that can further be translated to parameters for habitat conservation status assessments.

The following research questions are asked:

I. Can the floristic variety of open drylands in the study area be described adequately by NMDS ordination?

II. Does the integration of new species change the NMDS ordination space fundamentally or are there stable and significant floristic patterns?

III. What is the particular structure of floristic pattern in an NMDS ordination? What links can be drawn to Natura 2000 habitat types and conservation status indicators?

IV. Is there a functional relationship between habitat types, transitions and habitat pressure indicators that can be projected to the specific NMDS ordination space?

V. Is it possible to integrate such functional projections into a Natura 2000 habitat conservation status assessment scheme for management purposes?

VI. Are hyperspectral image signatures significantly related to probabilities of projected Natura 2000 habitat types and conservation status parameters?

Chapter III: Determination of Spectral Gradients and Wavelength Features

published as:

"Utilizing a PLSR-Based Band-Selection Procedure for Spectral Feature Characterization of Floristic Gradients"

Since an NMDS ordinations space represents a multidimensional numerical species projection along abstract gradients, the assumption can be made that certain gradients exhibit a unique spectral signature that can be used for mapping purposes. However, in NMDS ordination the gradient direction with the greatest spectral contrast is not predefined and therefore needs to be determined in order to derive predictive models. Common statistical feature extraction algorithms thereby often fail to deliver stable and significant spectral waveband combinations for the prediction of complex species assemblages. Therefore it was proposed that a gradient delineation on a NMDS ordination result can be integrated into a statistical learning algorithm that selects spectral wavelength regions for different gradient directions. The overall objective here is to validate spectral responses for different species transitions between field spectro-radiometer measurements and image reflectance values.

The following research questions are asked:

I. Do NMDS ordination space rotations reveal different patterns of floristic transition that can be related to spectral reflectance signatures from field measurements?

II. Are there stable and significant spectral features that can be used to uniquely model different floristic gradients?

III. What is the link between spectral features and floristic gradients? Can spectral absorption/reflection be used to indicate gradient properties such as species abundance or biochemical vegetation traits?

IV. Are there spectral feature composites in predictive statistical models that are stable from field to image spectra? Can these models be transferred to hyperspectral imagery for the mapping of different gradients?

Chapter IV: Determination of Calibration Performances and Spatial Mapping

submitted as:

"Mapping Multiple Plant Species Abundance Patterns - A Multiobjective Optimization Procedure for Combining Reflectance Spectroscopy and Species Ordination"

In chapter II a method is introduced to quantify habitat parameters in an NMDS ordination. In chapter III it has additionally been proven that an NMDS ordination space can be predicted by spectral reflectance signatures of different gradients. Finally, the two approaches are brought together in order to map plant species abundances in the research area. Thereby it has to be proven whether abundance gradients can be explained by inherent patterns of ordination and

whether these gradients are uniquely determined by spectral features. These objectives were translated into a multiobjective optimization procedure for the spatially explicit characterization of multi-species environments. The aim is to provide evidence that species abundances can be mapped in various gradients with patterns of coexistence. Temporal dynamics are further investigated incorporating hyperspectral imagery acquired at different phenological phases.

The following research questions are asked:

I. Is there a functional relationship between single species abundances and gradients in an NMDS ordination? What proportion of species abundance can be explained by projected species composition?

II. Are there significant spectral features that can be related to abundance gradients in an NMDS ordination? Are these features stable and transferable from field spectra to image predictions?

III. Do mapped species abundances represent meaningful patterns of coexistence, plant associations and habitat gradients?

IV. What is the influence of plant species phenology on spectral features and predictive model calibration? Is there a phenological phase that gives an advantage to the mapping success of individual species?

Chapter II: Determination of Floristic Composition and Habitat Gradients

This is the accepted version after peer review (Postprint) of the following article:

Neumann, C., Weiss, G., Schmidtlein, S., Itzerott, S., Lausch, A., Doktor, D., & Brell, M. (2015). Gradient-based assessment of habitat quality for spectral ecosystem monitoring. Remote Sensing, 7(3), pp. 2871-2898.

DOI:10.3390/rs70302871
Received: 30 November 2014 / Accepted: 4 March 2015 / Published: 10 March 2015

Abstract

The monitoring of ecosystems alterations has become a crucial task in order to develop valuable habitats for rare and threatened species. The information extracted from hyperspectral remote sensing data enables the generation of highly spatially resolved analyses of such species' habitats. In our study we combine information from a species ordination with hyperspectral reflectance signatures to predict occurrence probabilities for Natura 2000 habitat types and their conservation status. We examine how accurate habitat types and habitat threat, expressed by pressure indicators, can be described in an ordination space using spatial correlation functions from the geostatistic approach. We modeled habitat quality assessment parameters using floristic gradients derived by non-metric multidimensional scaling on the basis of 58 field plots. In the resulting ordination space, the variance structure of habitat types and pressure indicators could be explained by 69% up to 95% with fitted variogram models with a correlation to terrestrial mapping of >0.8. Models could be used to predict habitat type probability, habitat transition, and pressure indicators continuously over the whole ordination space. Finally, partial least squares regression (PLSR) was used to relate spectral information from AISA DUAL imagery to floristic pattern and related habitat quality. In general, spectral transferability is supported by strong correlation to ordination axes scores (R^2 = 0.79–0.85), whereas second axis of dry heaths (R^2 = 0.13) and first axis for pioneer grasslands (R^2 = 0.49) are more difficult to describe.

1 Introduction

In response to the Convention on Biological Diversity (Rio de Janeiro, 1992), the European Union adopted the Habitats Directive for the establishment of a coherent network of protected sites for rare, threatened, or endemic species and habitat types. This network, called Natura 2000, is aimed at preserving and restoring ecological interdependencies, dispersal, and establishment processes. European Union members need to report on their conservation status every six years. It has become clear that extensive efforts are required to obtain regulatory, technical, and scientific information as well as comprehensive ecosystem management (Apitz et al., 2006). In particular, there is a need for ecological research to be carried out beyond the local scale to implement controllable management systems. To obtain relevant knowledge about the spatial dynamic of ecological processes that influence the conservation status of habitats, spatially explicit data on the location and distribution of species are required (Aplin, 2005).

Recent developments in remote-sensing techniques have increasingly allowed for a detailed description of spatial organization of habitat characteristics and driving environmental factors (Aplin, 2005; Kerr and Ostrovsky, 2003; Turner et al., 2003). However, currently, only a few studies have implemented ecological knowledge in remote-sensing-based assessment systems

for Natura 2000 monitoring (Spanhove et al., 2012; Stenzel et al., 2014; Vanden Borre et al., 2011). There is still a considerable gap in knowledge transfer between remote-sensing specialists and ecologists in conjunction with the application demands of legal authorities (Asner et al., 1998; Vanden Borre et al., 2011; Wang et al., 2010). The first steps in combining ecological knowledge with Natura 2000 habitat management are usually carried out using indicator species mapping (M. Bock et al., 2005; Cantarello and Newton, 2008; Förster et al., 2008), whereby habitat types and indicator species for habitat-status assessment are modeled separately or on the basis of object classes describing habitat quality and quantity in aggregate forms as habitat units (Feilhauer et al., 2014; Haest et al., 2010; Mücher et al., 2009, 2013). Such approaches start from the premise that vegetation and habitat structures exist in a discrete pattern that can be classified a priori into categories (Xie et al., 2008). It is assumed indirectly that habitat types and conservation status can be described by co-occurring species assemblages, as stated in the concept of ecological community assembly. The basic problem of these models is that the categories depend on ad hoc hypotheses on the observed and expected ecological relevance and cannot be adapted to new findings or changes without changing the whole model. Moreover, multiple species gradients are aggregated within a limited number of categories in which derived biotope/habitat types become difficult to interpret in terms of both class membership and spectral representation (Rocchini et al., 2013).

There are different approaches regarding the spatial analysis of species assemblages. A number of basic concepts, e.g., distance decay and fractal scale, as summarized in Palmer and White (Palmer and White, 1994), suggest the concept of vegetation continuum (Gleason, 1926; Goodall, 1963; McIntosh, 1967) as a more universal description of vegetation structures. It is generally stated that vegetation compositions vary continuously along environmental gradients. Fractal self-similarity of spatial vegetation pattern is solved by setting the observation scale to individual species abundances. Species assemblages are used to describe vegetation as a whole. Therein, plant species variations are capable of representing the negative relation of distance and similarity in ecological phenomena as evidence of species turnover along an environmental gradient. Transitions are no longer unexplained sources of variance. In fact, they are thought of as fundamental properties of vegetation. In particular, management strategies need to focus on these transitional ecotones, where species richness is occasionally maximized, and competition increases sensitivity on external factors (Gosz, 1991; Risser, 1995). Gradients between or at the edge of community clusters are likely to represent patterns of processes that determine habitat structure. Such multidimensional transition areas are of utmost importance in ecosystem management as required in the Natura 2000 network, where gradual differences in habitat conditions determine the required management actions (Velázquez et al., 2010). In contrast to a pre-definition of discrete habitat

units, n-dimensional representation of species–environmental interrelations can be described quantitatively using ordination techniques (Austin, 1985).

Floristic ordination spaces have been proven to be statistically coherent with spectral signatures extracted from remote-sensing images. There are several studies relating ordination-space arrangement, e.g., of heathlands (Feilhauer et al., 2011, 2013; Trodd, 1996), bogs and wet meadows (Armitage et al., 2004; Schmidtlein et al., 2007; Schmidtlein and Sassin, 2004), tree species (Thessler et al., 2005), plant strategy types (Schmidtlein et al., 2012), and plant functional responses (Schmidtlein, 2005) to spectral gradients, whereby evidence for spatial prediction capabilities is provided. However, to date, no detailed analyses of the Natura 2000 habitat-type-specific ordination arrangement for management purposes have been published. This study was designed on an interdisciplinary basis to describe ecologically and predict spectrally the Natura 2000 habitat types and their conservation status on the basis of floristic gradients in an ordination space. We want to find out which habitat types and pressure indicators are adequately represented in ordinated structures. It is intended to reveal habitat transition as well as habitat threat owing to species shift induced by e.g., habitat management, as reflected by species gradients in a vegetation continuum. Such habitat quality parameters are required for reporting Natura 2000 conservation status in a six-year cycle. We are, furthermore, interested in determining whether habitat types and related pressure indicators can be modeled using hyperspectral reflectance signatures. Spatially explicit transfer of habitat characteristics can help to establish area-wide remote-sensing-based monitoring systems for the conservation of valuable natural habitats. Thereby, the mapping of gradual changes in plant species and habitats shall give a detailed representation of ecological interdependencies for selecting optimal management strategies. This paper introduces a methodological framework for integrating ecological knowledge into habitat conversion monitoring. It demonstrates a combined procedure of habitat conservation status assessment from a species ordination and hyperspectral image predictions. For this purpose this study is directed by three key hypotheses:

(a) The floristic variety can be described by ordination; integration of new species does not change the ordination space fundamentally;
(b) Habitat types, transitions, or pressure indicators can be described continuously within the specific ordination space via spatial correlation functions; on that basis a Natura 2000 habitat conservation status assessment can be derived for management purposes;
(c) Distinct habitat type areas in the ordination space can be related to patterns of reflectance.

In this study, an approach is presented that reveals the transition between habitat types as well as modulations in pressure affecting the conservation status of habitats. For the first time, an evaluation of management efforts is derived directly from an ordination space, as reflected in hyperspectral imagery.

2 Material and Methods

2.1 Study Area

The study was implemented on a former military training area, Döberitzer Heide, located at 53° latitude North and 13° longitude East in the west of Berlin, Germany (Figure II-1). As a result of long-term military use, open dryland assemblages established on glacial ground moraine deposits that are mainly characterized by sandy, acidic substrate in Regosol, Cambisol, and Podzol soil types (World Reference Base) (Nachtergaele et al., 2000). Translocation of soil substrate during military actions is reflected in a small-scale floristic variability with mosaics and interpenetration of xeric sand grasslands, herb-rich grasslands, dry heath, and pioneer woods. The main area of 3946 ha is protected as a Special Area of Conservation (SAC) within the European Natura 2000 network. The SAC includes habitat types (Lebensraumtyp (LRT)) such as Inland dunes with open Corynephorus and Agrostis grasslands (LRT 2330), European dry heaths (LRT 4030), and Xeric sand calcareous grasslands (LRT 6120). Within the study area, these Natura 2000 habitat types can be characterized by major indicator species according to Zimmermann (Zimmermann, 2015). The most prevalent indicator species are Corynephorus canescens for LRT 2330, Calluna vulgaris for LRT 4030, and Festuca brevipila grouped into Festuca ovina agg. for LRT 6120. Natural succession takes place in various patterns and different phases, just as a bundle of management activities is realized in order to preserve habitat quality. Especially open pioneer stages are threatened owing to degeneration phases where cryptogams (e.g., Cladonia sp., Polytrichum piliferum) and different grass species cover increase. Within the entire area, open drylands are generally affected by scrub encroachment (e.g., Populus tremula, Sarothamnus scoparius) and the invasion of highly competitive grasses (e.g., Calamagrostis epigejos). Heathland conversion is additionally characterized by grass encroachment (e.g., Deschampsia flexuosa) and degeneration phases where mosses and lichens cover increase as the canopy of Calluna decreases (Barclay-Estrup and Gimingham, 1969). Calluna heathlands are widespread over the whole study area with varying habitat quality conditions. The conservation of open pioneer stages is mostly realized in coherent areas where heathlands and different grasslands types are adjoined. The distribution of typical xeric and sand calcareous grasslands is patchier, with only rare sites reaching a good conservation status. Soil substrate variations particularly influence the quality of calcareous grassland habitats by inducing species shift along acidity gradients (e.g., Luzula campestris). Since 2004, different strategies of habitat management have been implemented by the nature foundation Sielmanns Naturlandschaften. These include the repressing of tree species or highly competitive grasses growth through big mammal grazing (e.g., Bison bonasus and Equus ferus przewalski), tree removal, and mulching of Calluna heath to support regeneration.

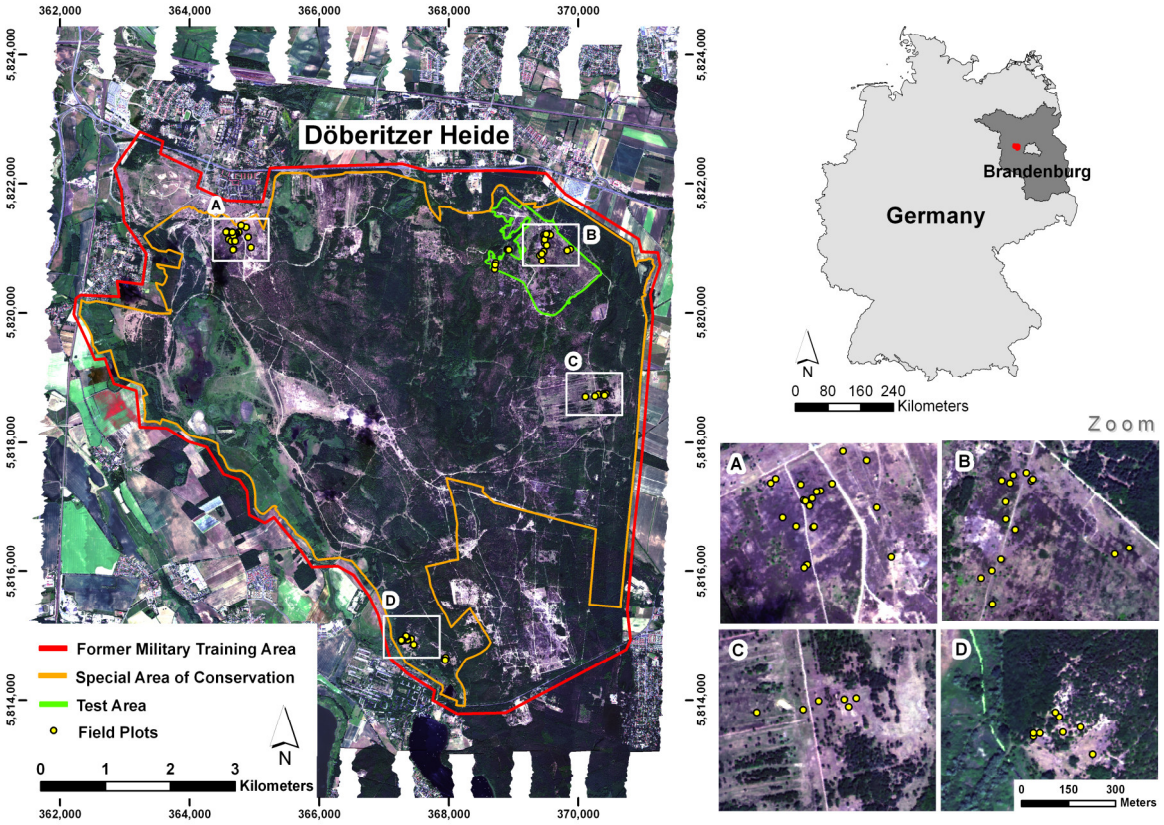

Figure II-1: *The former military training area Döberitzer Heide, visualized on flight stripes of the hyperspectral airplane campaign; field plots for plant species sampling are distributed in four open dryland areas; the test area for spatially explicit model transfer is marked in green.*

2.2 Floristic Data

In order to determine the vegetation continuum for open dryland habitats (including LRT 2330, LRT 4030, and LRT 6120) of the research area, vegetation samples were collected on 58 plots. Species abundances were estimated using the enhanced Braun–Blanquet method (Wilmanns, 1998), whereby species nomenclature is based on Rothmaler et al. (Rothmaler, 2005). Additionally, for every plot the Natura 2000 habitat type as well as the habitat conservation status was mapped. Terrestrial mapping of conservation status was conducted using the national assessment scheme framework proposed by "Bund/Länder Arbeitsgemeinschaft Naturschutz, Landschaftspflege und Erholung" (LANA, 2015) and adapted for the federal state of Brandenburg by Zimmermann (Zimmermann, 2015). It incorporates the core assessment criteria; habitat structure, species inventory, and habitat disturbance; towards three assessment categories for a favorable (A: excellent, B: good) or an unfavorable (C: adverse) conservation status. All criteria are defined by thresholds of plant species abundances and expert evaluations (e.g., present, low, extensive) (Zimmermann, 2015) integrating characteristic communities of habitat conversions that are typical for our

study area (see Section II-2.1). Consequently, habitat pressure, represented in B/C assessment categories, can be described by structural parameter (e.g., senescence, vitality) and listed plant species assemblages (Zimmermann, 2015). Pressure strength is maximized when (a) structural and species diversity is low or (b) the influence of disturbance species is high. On the basis of expert knowledge, the spatial distribution of the sample plots was chosen so as to cover all relevant vascular plant species, mosses, and lichens, thus including all important habitats with typical transitions, succession states, and pressure indicators. In total, the fractional cover of 98 species was estimated in 1-m² plots. To ensure that the vegetation properties can be adequately mapped with hyperspectral imagery, the plots were located within homogeneous structures according to species composition, bare soil, and litter cover within a minimum radius of 5 m.

2.3 Species Ordination and Floristic Pattern Significance

In our first hypothesis, we argue that only a stable and significant floristic pattern, reflected in an ordination space-derived vegetation continuum, can be used to describe habitat characteristics for management purposes. We applied a nonmetric multidimensional scaling (NMS) procedure (Kruskal, 1964) on a site-by-species matrix to project rank-ordered species similarities into two-dimensional ordination space (Figure II-2A). The original number of plant species was reduced to omit species that rarely appear with low abundances over all field plots. These are known to produce strong distortion effects on the final ordination topology without increasing floristic pattern significance (Gauch, 1982). Furthermore, owing to a weak spatial representation, their introduced variance cannot be assumed to be causally related to image spectra. Similarities were then calculated using the Bray–Curtis distance measure (Clarke, 1993) on the final matrix of 58 sites by 38 species. We used Kruskal's stress value (Kruskal, 1964) to interpret the goodness of fit for the resulting ordination space topology. To avoid local minima for stress values, the procedure searches within 1000 random start configurations until a stable solution is reached.

Since an ordination space for species assemblages is a generalized representation of the ecological environment, projected floristic patterns need to be assessed on their ability to represent ecological relevant structures. Furthermore, the stability of the projected patterns reveals whether an appropriate sample size was chosen to describe floristic heterogeneity adequately. Hence, we define two null hypotheses stating that there is no stable ordination plot configuration, and the ordinated pattern is not significantly different from random configurations. We used a combined statistical algorithm, testing sample stability and structural strength on ordination axes scores introduced by Pillar (ManjarréS-MartíNez et al., 2012; Pillar, 1999).

Stability was tested by generating 1000 bootstrapped samples (Efron and Tibshirani, 1993; Knox and Peet, 1989) from the final site-by-species matrix. The bootstrapped matrices were then projected into ordination space with NDMS transformation and axes scores were compared to reference ordination after score matrix matching by Procrustes adjustment (Schönemann and Carroll, 1970). Subsequently, stability (C) was evaluated using the average Pearson product moment correlation (r) between reference scores (S) and test scores (S*) in each ordination dimension (i) over all bootstrapped samples (n): $C = \sum_{i=1}^{n}[r(S_i, S_i^*)]/n$.

Pattern Significance was tested, generating 1000 random permutations from the final site-by-species matrix. Permuted scores were calculated using NMS transformation and compared with test scores taken from a second NMS on the permutation matrix using the same bootstrap samples as derived in the stability test. Permutation scores (S^p) were then correlated (r) to the bootstrapped permutation scores (S**) and results were compared to the bootstrapped correlation from the stability test. We then calculated the probability (P) of permutation correlation being greater or equal to our reference correlation over all bootstrapped sample (n): $P = [r(S_i^p S_i^{**}) \geq r(S_i S_i^*)]_n$.

We can now reject our null hypotheses for $1 - C < \alpha$ and $P < \alpha$, respectively, whereby α probability threshold was defined with 0.10.

2.4 Habitat Type and Habitat Pressure Aggregation

Aggregation techniques are needed in order to translate species composition of ordination plots into Natura 2000 habitat categories (Figure II-2B). On the basis of expert knowledge, site-specific vegetation characteristics (see Section II-2.1), and listed Natura 2000 habitat indicator species (Zimmermann, 2015), a functional plant species relation was developed for habitat type and habitat pressure evaluation. Specific habitat functions consist of a weighted sum of cover values for indicator species (Table II-1). Again, weights are defined by expert knowledge incorporating site-specific habitat characteristics and legal requirements for the conservation status assessment. The weighted aggregate of habitat function components was standardized between 0 and 1 over all plots to represent a probability scale in case of habitat-type aggregates or a relative strength of influence for pressure aggregates. Standardization was performed by dividing the weighted sum of a plot by the maximum that can be reached considering probabilities in all plots. Every plot can be uniquely defined by score coordinate pairs at positions u in the ordination space. Thus, we can describe information related to plots as a realization z(u) of a spatial random variable Z that holds the distribution function for all possible realizations (Matheron, 1971). A realization of a habitat/pressure function can consequently be written as $z(u)[0,1] = (\sum_{i=1}^{n}\beta_i N_i)/\max(\sum_{i=1}^{n}\beta_i N_i)$, where β denotes the weights of the components (e.g., plant species) N for the plots i–n. Single components and related weights were selected as indicators for defining the habitat types (typical habitat

indicators) as well as pressure parameters (negative pressure indicators) to assess the conservation status (Table II-1). We thus assumed that the habitat indicator species would be positively linked to the occurrence probabilities of habitat types when they are known as typical character species. A negative link can be discerned when they are considered to be pressure indicators for habitat conversion. Finally, probability/strength values can be assigned to plots in the ordination space as discrete translation of the allocated species composition.

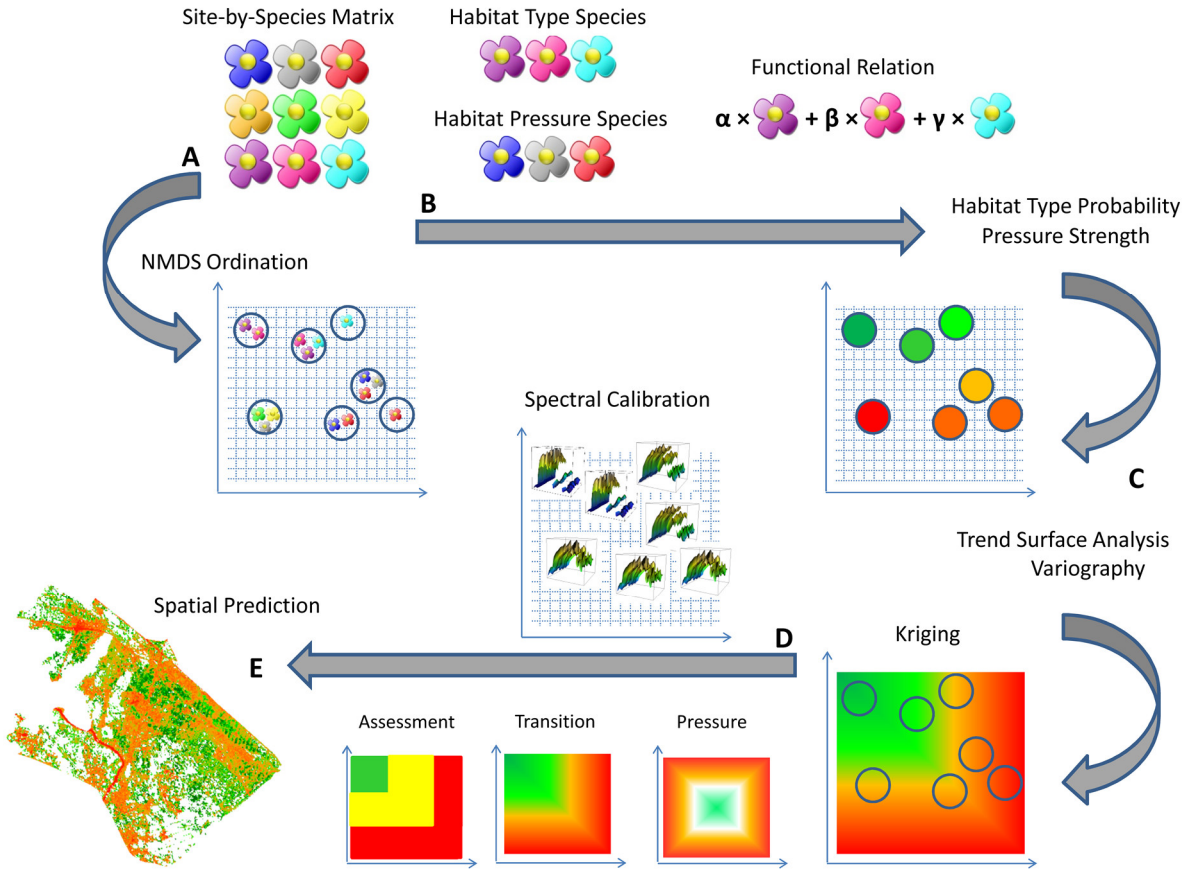

Figure II-2: *Methodological framework presented as a conceptual workflow: (A) plant species ordination; (B) functional habitat type and pressure aggregation; (C) continuous pattern prediction; (D) pattern recognition and spectral calibration; and (E) spatially explicit predictions on the basis of image spectra.*

2.5 Surface Analysis and Interpolation in the Ordination Space

Our hypothesis states now that z(u) is spatially determined and therefore can be described by spatial correlation functions to predict habitat-type probabilities and pressure strength on unknown grid cells for the entire ordination space (Figure II-2C). However, as a nature of ordination, similar information is grouped in clusters with gradual changes to adjacent regions with different floristic compositions (Borg and Groenen, 2005). This trend violates the intrinsic hypothesis as an assumption for geostatistical prediction (Matheron, 1970) and

superimposes inner group variability that should be detected in order to assess habitat quality. To overcome this, we first separated the spatial trend. This was done by fitting first-, second- and third-order polynomial regression models for score axes with ordinary least squares (OLS). The best model according goodness of fit was selected to predict the broad scale trend of habitat type characteristics within the ordination space. Subsequently, a variogram analysis was carried out on the model residuals. We used the geostatistical approach, which combined spatial correlation modeling (variography) with subsequent spatial predictions (kriging) (Matheron, 1963).

Table II-1: *Species list for habitat-type-specific habitat functions. Species are aggregated according to weighted composites of habitat indicator species (indicating a Natura 2000 habitat type) and pressure indicator species (indicating habitat conversion/threat) in order to represent typical habitat realizations within the ordination space of the study area.*

	Habitat Type Probability z(u)		**Pressure Strength z(u)**	
Habitat type	**Weight [β]**	**Component [N]**	**Weight [β]**	**Component [N]**
LRT 2330	1	*Corynephorus canescens*	1	*Calamagrostis epigejos*
	0.5	*Bare ground cover*	1	*Agrostis capillaris*
	0.2	*Cladonia sp.*	1	*Rubus caesius*
			0.5	*Rumex acetosella*
			0.5	*Polytrichum piliferum*
			0.5	*Hieracium pilosella*
			0.2	*Cladonia sp.*
LRT 4030	1	*Calluna vulgaris*	1	*Populus tremula juv.*
	0.5	*Cladonia sp.*	1	*Sarothamnus scoparius*
			1	*Deschampsia flexuosa*
			1	*Festuca ovina agg.*
			1	*Nardus stricta*
			1	*Calamagrostis epigejos*
			1	*Agrostis capillaris*
			0.5	*Polytrichum piliferum*
			0.2	*Cladonia sp.*
LRT 6120	1	*Festuca ovina agg.*	1	*Populus tremula juv.*
	0.5	*Agrimonia eupatoria*	1	*Sarothamnus scoparius*
	0.5	*Galium verum*	1	*Rubus caesius*
	0.5	*Koeleria macrantha*	1	*Luzula campestris agg.*
	0.5	*Ononis repens*	1	*Calamagrostis epigejos*
	0.5	*Peucedanum oreoselinum*	1	*Plantago lanceolata*
	0.2	*Agrostis capillaris*	1	*Arrhenatherum elatius*
			1	*Tanacetum vulgare*
			0.5	*Deschampsia flexuosa*
			0.5	*Holcus lanatus*
			0.5	*Rumex acetosella*
			0.5	*Artemisia campestris*
			0.2	*Festuca ovina agg.*
			0.2	*Agrostis capillaris*

Herein, spatial correlation functions can be modeled by fitting an experimental variogram that describes spatial variance $\gamma = [z(u_i) - (z(u_i + h)]^2$ for plots i in relation to distance classes h. Every habitat function is assumed to have a typical correlation length (range) at which the maximum variance (sill) between point pairs is achieved. From that range distance, the variance decreases towards zero distance where an inexplicable minimum variance (nugget) remains. From this, one can then describe spatial correlation structures using variogram models fitting nugget, sill, and range parameters within the codomain of the spatial boundary condition of the ordination space (Dowd, 1984). We used an effective range in which 95% of the maximum variance was achieved to interpret the correlation lengths. Furthermore, we introduced a modified coefficient of determination, R^2_{var}, to describe the amount of explained variance for variogram models in comparison with a null model. As an appropriate null model where no spatial correlation could be identified, we selected the nugget effect model with no range parameter owing to maximum variance levels over all distances. The nugget level was defined as the median variance for all possible pairwise distances (sample variogram). We then built the ratio between the sum of squares for variogram model residuals (SSR) and the sum of squares for null-model residuals (SSN). According to $R^2_{var} = 1 - SSR/SSN$, spatially determined habitat functions can be identified when their variogram models contribute significantly to the explanation of spatial variance.

A list of 19 different variogram models was fitted to residuals using generalized least squares (Pebesma, 2004). The model with the best fit regarding the minimal sum of squared error (Hiemstra et al., 2009) for variances at all pairwise sample distances was selected to describe the spatial autocorrelation and calculate the kriging weights. Kriging was applied on a regular grid with 0.01 intervals that was expanded inside the score axes. This procedure was applied to (a) field-based habitat types and conservation status assessment and (b) habitat-function-based habitat types and pressure strength. For terrestrial habitat types, we used regression kriging of indicators (Hengl et al., 2007b), adding Krige interpolation and predictions from a logistic regression. A logit link function was used to transform the final results to occurrence probabilities. Simple regression kriging with a polynomial regression was applied to terrestrial habitat assessment categories and habitat-function-based habitat type probabilities and pressure strengths. In order to identify significant trend axes for regression models, we applied a backward variable selection until the Akaike Information Criterion (Akaike, 1973) was minimized. To compare the goodness of fit for coordinate regression approaches, we used adjusted R^2 and, for a better comparison, the Nagelkerke R^2 (Nagelkerke, 1991) in the logistic regression models.

For external validation purposes, we compared the final variogram models and resulting kriging interpolations for both field-based and habitat-function-based derivations of habitat type and habitat pressure. To show how terrestrial mapping as reflected in ordination

structures can be reproduced on the basis of functional relations that regularly connect plant species occurrences, the resulting kriging grids of both mapping methods were correlated. The average deviation between all kriging pixels was evaluated using the Pearson Product Moment correlation as well as the R^2 in a linear regression. Additionally, the variogram model parameters were compared in order to estimate the spatial correlation strength of habitat type and assessment/pressure within the ordination space.

2.6 Habitat Transition and Habitat Pressure Analysis

Isosurfaces derived from the combination of trend surface modeling and kriging predictions can be used to identify habitat type transitions and habitat pressures by means of isosurface recombination and reallocation of information stored in ordinated plots (Figure II-2D). Habitat-type probabilities are generally constructed to reveal the potential of habitat type establishment on the basis of typical habitat indicator species. To clearly demonstrate transition zones, we combined the occurrence probability grids by multiplying probabilities less than 50% for specific habitat type pairs. We assumed that below this individually replaceable threshold, ordination space can be used to reveal inter-habitat-type transition as typical habitat conversion. Above this threshold, we assumed that more distinct species-dependent pressures to habitat quality can be revealed. The strength of inter-transition is derived by a min/max normalization of the arithmetic product of probability surfaces for habitat type pairs.

Intrahabitat pressures that are responsible for the threat of habitat quality can be revealed by defining a habitat function on the basis of weighted indicator species (Table II-1). Here, the relative strength of pressures allocated to a habitat type with an occurrence probability above 30% is calculated as a realization of z(u). Consequently, the strength of influence is positively correlated to the number of pressure species and their fractional cover. More specifically, areas of strong pressure influence were categorized on the basis of species compositions reallocated to distinct ordination regions. The strength of individual species influence was calculated with a min/max weighting according to specific species cover of related plot position in the ordination space.

For the purpose of conservation status assessment, we combined habitat type probability functions with pressure strength functions. We assumed that the probability of a certain habitat type is reduced when pressure factors increase. In conclusion, predicted ordination space grids for habitat type occurrence probabilities were subtracted by pressure-strength grids. The result was equally scaled to three different color intensities with gradual transitions. Finally, we categorized three assessment levels (A: excellent, B: good, C: adverse; see Section II-2.2) in the center of each color class, whereas habitat probabilities ≤0% were excluded from the visualization.

2.7 Spectral Data

Hyperspectral images were acquired during a flight campaign on 4 June 2011 between 10:00 and 12:30 (Universal Time). The imaging spectrometer used was the Airborne Imaging Spectrometer for Application (AISA DUAL (UFZ, Leipzig, Germany)) ranging from visible (400 nm) to shortwave infrared (2500 nm) in 367 spectral bands. The pushbroom scanning system operated in a 24° field of view with an instantaneous field of view of 0.075° for the coverage of single ground elements. In total, 22 flight stripes with 300 samples per scanning line were recorded. The mean flight altitude was 1500 m above sea level, and the mean aircraft speed was 180 km/h. Images were geometrically corrected using an inertial measurement unit and ground control points. Overlapping flight stripes were merged into a single mosaic using an adjusted algorithm for automated control point allocation (Scale Invariant Feature Transform) (Lowe, 2004). The final product pixel size was resampled to 2 m × 2 m. Internal radiometric calibration was supplemented with spectral binning, smear correction, and destriping (Reduction of Miscalibration Effects) (Rogaß et al., 2011) to generate reliable at-sensor radiance. In order to obtain top-of-the-canopy reflectance (TOC), a radiative transfer model (ATCOR-4,) was implemented, followed by an empirical line correction (ELI) (Smith and Milton, 1999). As a reference for ELI post-calibration, we used field spectra that were collected around the acquisition time with a field spectroradiometer (ASD Inc., Boulder, CO, USA). To account for observed nonlinearity within a range of 400–600 nm, we adjusted the usual ELI procedure with polynomial regression equations until the best polynomial fit between the image and the reference spectra was found. Reflectance signatures of the field plots were finally extracted from the image mosaic. A transformation to 1035 spectral variables including continuum removal (Clark et al., 1987), first Savitzky–Golay derivative (Savitzky and Golay, 1964), and spectral indices for water, pigment, nitrogen, cellulose, lignin absorption, and band-depth-normalized absorption features (Kokaly and Clark, 1999) provided spectral predictors for a coherence analysis with ordination space arrangement. The continuum was derived by fitting a convex hull over the top of a reflectance spectrum. Subsequently, absorption features are generated by dividing the original spectrum by the continuum curve. Savitzky–Golay derivatives are produced on the basis of a second-order polynomial filter of the original spectrum. The first derivative was calculated stepwise for a five-point filter length in order to render the slope for the entire spectrum. The derived spectral variables are listed in Table S2 in the Supplementary Materials (Supplementary B). Narrow spectral bands as well as overlapping physical plant properties lead to redundant spectral information. Redundancy in statistical models causes problems of multicollinearity with unreliable estimates of regression coefficients (Farrar and Glauber, 1967; Graham, 2003). We therefore used partial least-squares regression (PLSR) (Wold, 1966), which calculates the orthogonal linear combination of original predictor dimensions (latent variables). A variable pre-selection can increase the predictive power of regression models

(Hughes, 1968; Kubinyi, 1996). Hence, dimension reduction in latent variables was incorporated with backward variable selection using a wrapper approach maximizing the model's goodness of fit based on predictor significance and variable importance implemented in the R package autopls (Schmidtlein et al., 2012). Separate models were generated for axis scores as dependent variables. Within an internal leave-one-out (LOO) cross-validation, the number of latent variables for the best model was estimated, minimizing the error of prediction. LOO statistics were used to evaluate the predictive accuracy [root-mean-square error (RMSE)] and goodness of fit R^2 for individual axis models. Furthermore, the number of selected latent and predictor variables was used to evaluate PLSR model stability. Thereby, an increase in model complexity is incident to the consequences of model overfitting (variance-bias trade-off).

3 Results

3.1 Ordination Space Stability and Pattern Significance

The final two-dimensional ordination space that showed the floristic variance distribution within our study area yielded a stress value a = 0.0016. This can be interpreted as an excellent representation of initial species composition (Borg and Groenen, 2005; Kruskal, 1964). The cover values of the major indicator species (see Section II-2.1) are well separated into different ordination plot regions with their transitions (Figure II-3a). Although a third of all samples per bootstrap iteration were excluded from the NMS ordination in each bootstrap iteration (Cutler et al., 2007), the average correlation over all iterations with n = 1000 samples was high at C = 0.969 for the first axis and C = 0.956 for the second axis (Figure II-3b). The interquartile range (IQR) is higher for the second axis, with more outliers to lower correlation. Nevertheless, the difference 1 − C for averaged correlations was lower than the α threshold 0.10 for both axes. Hence, we can reject the null hypothesis and state that the reference ordination space is stable in terms of plot selection. Comparing bootstrapped samples from randomly permuted data with the same bootstrap sampling units, we can see an increasing IQR with correlations ranging from 0 to 0.93 (Figure II-3b). Thereby, the averaged correlation of the first ordination axis amounts to C = 0.714, and for the second axis C = 0.629. With a probability of P = 0.033 for the first axis and P = 0.021 for the second axis, the permuted correlation is higher over all iterations. Again, the α threshold was undershot, and it could be alternatively assumed that reference ordination space represents significant floristic structures.

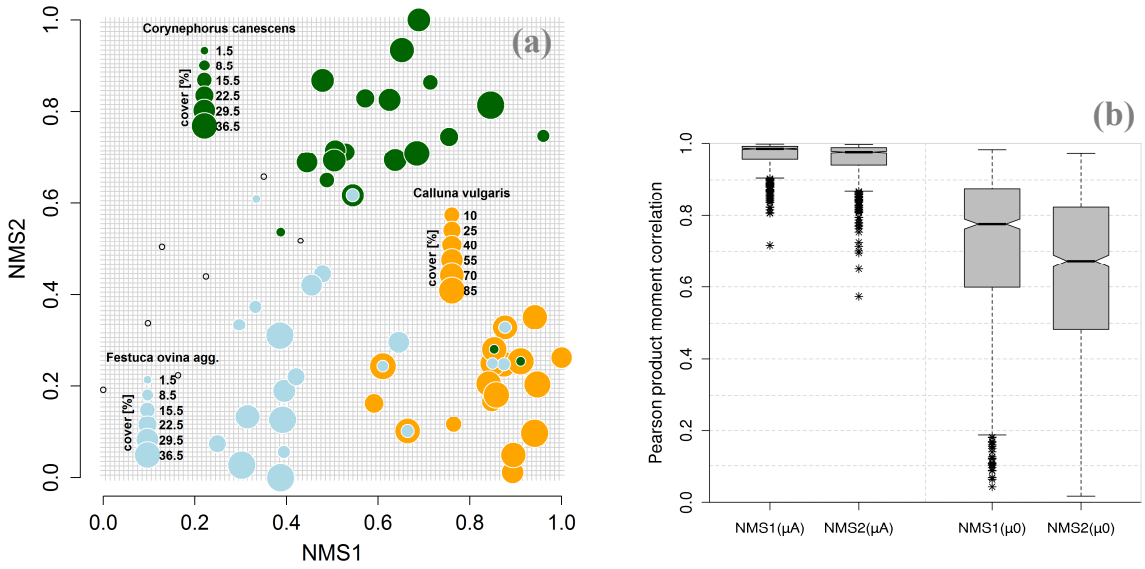

Figure II-3: *(a) Reference ordination space for open dryland habitats within the study area. Ordination scores were standardized between 0 and 1; point size is positively correlated to species cover of major indicator species. Green = Corynephorus canescens; blue = Festuca ovina agg.; orange = Calluna vulgaris. (b) Boxplot for 1000 bootstrapped correlations (μA) and for 1000 randomly permuted correlations (μ0) for ordination axes scores NMS1 and NMS2.*

3.2 Variography

For the three main habitat types in the open drylands of the Döberitzer Heide, we fitted variogram models to predict the occurrence probability of habitat types and the relative strength of pressure factors to assess conservation status on the basis of the habitat functions on the ordination plots. The results were compared with plot-specific field-survey data, including habitat-type delimitation and habitat conservation status assessment (Table II-2). As expected for all habitat types, a significant spatial coherence can be observed for both ordination axes, except for LRT 2330, where only the NMS2 direction features a significant trend. Comparing R^2_{reg}, it can be clearly seen that a spatial trend is more influential on habitat-type transition (R^2_{reg} Habitat type probability $\gg$ R^2_{reg} Pressure strength) for both habitat functions and terrestrial datasets, whereas change owing to pressure indicator species is more dependent on the floristic composition for LRT 2330 and LRT 6120, as reflected in higher values of R2vario that explain the residual variance. It can generally be revealed that species-rich plot compositions show a lower spatial dependency, which is particularly evident for LRT 6120 where $R^2_{reg} \ll R^2_{vario}$. Generally, variogram models are able to explain plot variances of experimental variograms from 69% to 95% in eight of 10 cases, considering R2vario. Only variogram models for pressure factors and the assessment parameter for LRT

4030 are less than 50% better than a null model. In the case of LRT 2330, variogram models can explain spatial variances even better than terrestrial data. In all cases, an effective range up to a maximum variance, that is, at least 68% higher than the nugget variance, can be derived.

Table II-2: *Variogram models for field-survey-based habitat types and habitat conservation status assessment (ter.), and for habitat-functions-based habitat types and pressure strength (fun.). Mat = Matern with kappa = 5; Cir = circular; Sph = spherical; Ste = Matern with M. Stein's parameterization; cn = nugget; c0 = sill; a0 = effective range; R2vario = coefficient of determination for variogram models; R2reg = coefficient of determination for coordinate regression; dim reg = significant dimensions (v1, v2) in spatial regression.*

		Spatial Regression		Variography				
	LRT 2330	R^2_{reg}	dim reg	R^2_{vario}	model	c_n	c_0	a_0
Habitat Type Probability	ter. habitat type	0.893	v2	0.704	Mat	0,000	0.059	0.214
	fun. habitat type	0.729	v1,v2	0.893	Cir	0.009	0.028	0.221
Pressure Strength	ter. assessment	0.809	v2	0.752	Mat	0.000	0.026	0.196
	fun. pressure	0.365	v2	0.839	Sph	0.000	0.086	0.306
	LRT 4030							
Habitat Type Probability	ter. habitat type	0.783	v1,v2	0.933	Mat	0.000	0.094	0.588
	fun. habitat type	0.871	v1,v2	0.932	Cir	0.002	0.022	0.366
Pressure Strength	ter. assessment	0.65	v1,v2	0.424	Mat	0.000	0.047	0.131
	fun. pressure	0.693	v1,v2	0.362	Sph	0.000	0.033	0.176
	LRT 6120							
Habitat Type Probability	ter. habitat type	0.609	v1,v2	0.954	Mat	0.000	0.193	0.555
	fun. habitat type	0.491	v1,v2	0.835	Ste	0.000	0.052	0.330
Pressure Strength	ter. assessment	0.449	v1,v2	0.875	Cir	0.000	0.076	0.412
	fun. pressure	0.418	v1,v2	0.698	Sph	0.005	0.035	0.579

3.3 Habitat Type Functions and Assessment of Pressures

Using relevant habitat type functions with specific variogram models, the occurrence probability for three different habitat types was spatially predicted within the ordination space on the basis of kriging weights (Figure II-4). Thereby, isolines represent locations with equal probabilities, whereby the 30% threshold of being a specific habitat type is highlighted with a dashed line in bold black. For all three habitat types, clear separations into different ordination space areas with typical inter-habitat transitions could be identified. Whereas LRT 4030 shows an omnidirectional decrease in occurrence probability, it can be shown that the distribution of habitat function components, bare soil cover for LRT 2330, and *Agrostis capillaris* and *Festuca ovina agg.* for LRT 6120, is more variable. These components overlap with adjacent habitat type distributions, whereby habitat conversion through transition is

made visible. Furthermore, variations of occurrence probabilities above 50% occur as a result of varying indicator species abundances owing to the presence of pressure species.

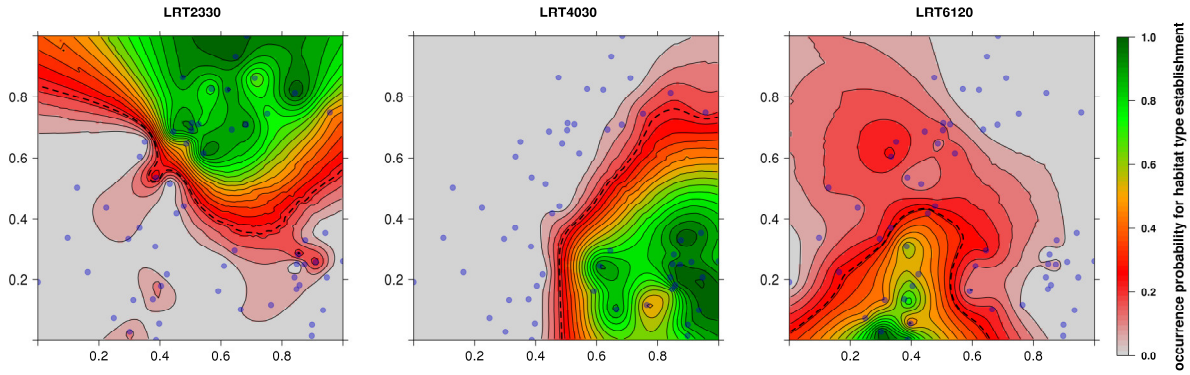

Figure II-4: *Kriging predictions for habitat type probability on the ordination plane. Isolines and allocated color transitions represent regions of similar floristic composition on the basis of realized habitat type probability functions. The 30% probability threshold is visualized with a dashed line.*

Habitat type transition within the ordination space is visualized in Figure II-5. The first transition is located between pioneer stages of inland dunes and dry heath. This gradient of overlapping probabilities is mainly characterized by a change in lichen cover. The second transition between European dry heaths and Xeric sand calcareous grasslands is realized in two situations. Changing cover of different grass species on ordination plots is overlain with decreased *Calluna vulgaris* proportions in the upper part. A direct transition to LRT 6120 in the lower part is based on a change in characterizing herb cover. This transition is weaker because a typical herbal diversity for LRT 6120 may not be directly linked to heathland transition. The typical transition is weakened by intermediate grass stages such as *Festuca ovina agg.* or *Nardus stricta*. Within the ordination space, no direct conversion between LRT 6120 and LRT 2330 can be identified.

Figure II-6 shows the kriging-predicted pressure strengths for chosen habitat types. For all habitat types, locations with strong pressure influence can be detected. In contrast, there are stable locations where there appears to be no influence of any pressure species. The plot-specific informational content within the reference ordination space can be subsequently used to assign pressure factor complexes for interpretation of habitat structures (Table II-3). Regarding the habitat-quality status of LRT 2330, an important threat can be seen in a loss of bare soil cover with increased lichens and moss cover (Aa in Figure II-6). This status changes into strong pressure complexes of establishing *Rubus* shrubs interspersed with *Rumex acetosella* and moss species (Ab in Figure II-6). An increasing *Rumex acetosella* cover is also linked to an increased pressure of grass invasion (Ac in Figure II-4).

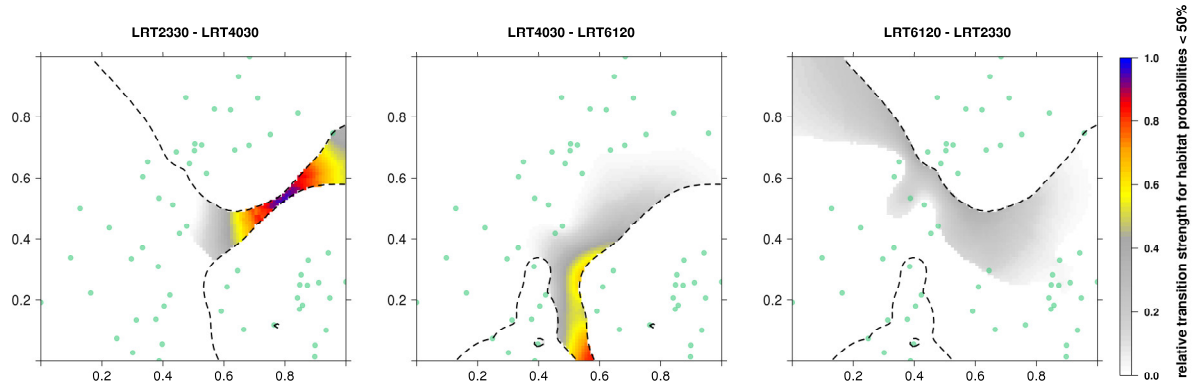

Figure II-5: *Relative strength of inter-habitat transition, as visualized by the arithmetic product of habitat-type probabilities below 50%. The color scale is min/max normalized over all transition pairs.*

In particular, *Agrostis capillaris* cover can be identified as an important parameter for grass invasion, while its presence is often connected with xeric grassland herbs (Ad in Figure II-6).

The composition of intra-habitat pressures is more complex within LRT 4030. We can discriminate between different grass invasion categories. While Ba–c in Figure II-6 is dominated by a transition between *Festuca ovina agg.* and *Calamagrostis epigejos* communities, the Bd–Bf gradient in Figure II-6 is characterized by *Nardus stricta* and *Deschampsia flexuosa* mixtures. These gradients are well defined at the transition to LRT 6120 and can be transferred to a better differentiation of grass invasion categories. In addition, ordination space arrangements enable the identification of shrub invasion with *Sarothamnus scoparius* (Bc–Bd in Figure II-6) as well as tree establishment (Bg in Figure II-6), which is superimposed with increased lichen cover.

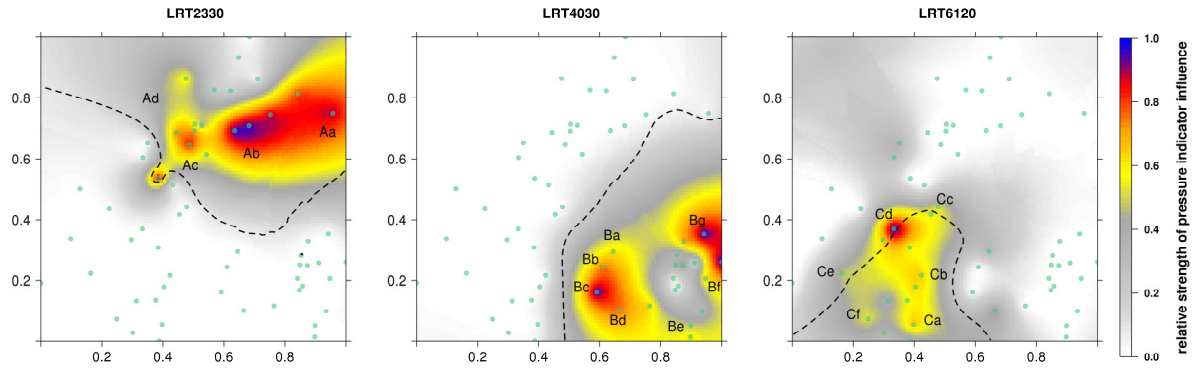

Figure II-6: *Kriging predictions for pressure strength on the basis of realized pressure functions. Letters correspond to pressure-factor complexes in Table II-3, and dashed lines denote a habitat type probability of 30%.*

Base-rich and herb-diverse LRT 6120 habitats occupy only small areas of the ordination space. These are often adjacent to grassland species that can also become established under acidic conditions. The predicted pressure strength reveals different gradients for grass species (Cc–Cf in Figure II-6) that are not characteristic for a favorable status of LRT 6120. Thereby, the ordination space arrangement can be used to separate typical habitats from various different grassland types. Furthermore, pressures through tree growth in Ca–Cb will have a strong influence on habitat quality.

Table II-3: *Pressure-complex definition on the basis of plot localization within a region of maximum pressure strengths on the ordination plane. Species cover is aggregated over a certain number of plots by min/max-normalized fractional cover values in order to assess the direction of species influence on habitat pressures.*

Pressure	LRT 2330		LRT 4030		LRT 6120	
	Fraction	Plant Species	Fraction	Plant Species	Fraction	Plant Species
a	1.00	*Cladonia sp.*	1.00	*Festuca ovina agg.*	1.00	*Populus tremula juv.*
	0.66	*Polytrichum piliferum*	0.72	*Rumex acetosella*	0.75	*Calamagrostis epigejos*
			0.60	*Agrostis capillaris*	0.47	*Luzula campestris*
b	1.00	*Polytrichum piliferum*	1.00	*Calamagrostis epigejos*	1.00	*Populus tremula juv.*
	0.99	*Rubus caesisus*	0.62	*Agrostis capillaris*	0.70	*Festuca ovina agg.*
	0.69	*Rumex acetosella*	0.55	*Rumex acetosella*	0.60	*Agrostis capillaris*
c	1.00	*Rumex acetosella*	1.00	*Calamagrostis epigejos*	1.00	*Festuca ovina agg.*
	0.92	*Agrostis capillaris*	0.52	*Sarothamnus scoparius*	0.84	*Agrostis capillaris*
	0.44	*Calamagrostis epigejos*	0.42	*Agrostis capillas*	0.80	*Rumex acetosella*
d	1.00	*Agrostis capillaris*	1.00	*Luzula campestris*	1.00	*Agrostis capillaris*
	0.90	*Hieracium pilosella*	0.83	*Sarothmanus scoparius*	1.00	*Plantago lanceolata*
	0.48	*Ornithopus perpusillus*	0.83	*Nardus stricta*	0.75	*Trifolium arvense*
e			1.00	*Nardus stricta*	1.00	*Calamagrostis epigejos*
			0.84	*Deschampsia flexuosa*	0.44	*Poa angustifolia*
			0.56	*Danthonia decumbens*	0.38	*Tanacetum vulgare*
f			1.00	*Deschampsia flexuosa*	1.00	*Calamagrostis epigejos*
			0.91	*Nardus stricta*	0.34	*Arrhenatherum elatius*
			0.57	*Cladonia sp.*	0.34	*Poa angustifolia*
g			1.00	*Populus tremula juv.*		
			0.33	*Cladonia spec.*		
			0.33	*Polytrichum piliferum*		

On the basis of derived inter-habitat transition and intraspecific pressure complexes, a Natura 2000 habitat type assessment of conservation status was realized. This results in a grid-based continuous assessment for ordination space locations dependent on habitat type positions (Figure II-7). Thereby, the conservation status can be described by three color intensities with gradual transitions. The center of each habitat type represents a favorable conservation status, whereby internal fluctuations and inter-habitat transitions are characterized by decreasing

habitat qualities. We validated the distribution of conservation status assessment within the ordination space, calculating the Pearson product moment correlation and RMSE for assessment grids derived for field-survey-based assessment functions (Table II-4a). Over all habitat types, a strong correlation with field surveys can be observed. The generated ordination space assessment approach differs at most by 15% from terrestrial assessment, which is within the range that can be achieved by subjective human differences. The lowest Pearson correlation with field surveys occurs for LRT 6120 (<0.859), which is also evident in habitat type prediction. In general, habitat type and assessment functions, generated by floristic composition on ordinated plot location, can adequately reproduce results obtained from terrestrial mapping in the study area.

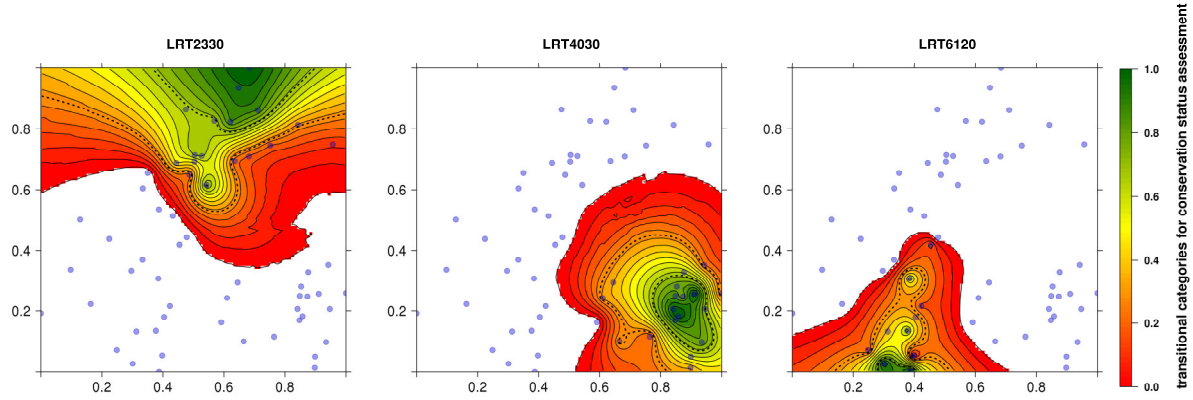

Figure II-7: *Probability for a Natura 2000 assessment of conservation status of three habitat types on an ordination plane. Equally spaced thresholds for assessment categories are shown by dotted lines.*

3.4 Spectral Predictability

Table II-4b provides a summary of the habitat-type-specific spectral PLSR model parameter and LOO accuracy assessment. Regression models that relate reflectance to scores on the first ordination axis can explain habitat-type-specific variances of up to 82% in internal validation. The lowest fit was generated at LRT 2330, where 49.1% of score variability could be explained by spectral variables. This resulted in a maximum RMSE of 21%. In second-axis models, the RMSE is maximized for LRT 4030 (RMSE = 20%). The related model provides a poor explanation for the variance in the second ordination dimension ($R^2 = 0.13$). In contrast, the explanatory power of second-axis models is high ($R^2 > 0.80$) for LRT 2330 and LRT 6120. The number of latent variables selected is small: n_C = 2 for all models. This small number of latent variables indicates model stability, owing to a high score variance, which can be explained by a minimal number of orthogonal components in PLSR. The original 1035 spectral variables were drastically reduced between 147 and 9. In particular, species-rich LRT

6120 can be explained spectrally by only a small number of significant spectral variables on the ordination plane. In order to prove model transferability and demonstrate spatially explicit habitat type monitoring, we applied PLSR models on an open dryland area of the Döberitzer Heide. There, habitat type occurrences as well as related conservation status assessment for >30% occurrence probabilities were predicted after masking any tree and shadow pixels (Figure II-8). Generally, a clear distribution pattern of specific habitat types can be mapped. Results indicate that the typical floristic composition for habitat type LRT 6120 characterization is present in only a few regions (probability >40%). This is also reflected in predicted assessment categories where conservation status is mainly assigned between C and B (unfavorable).

Table II-4: *(a) External validation between kriging grids on the ordination plane for terrestrial mapping and habitat functions. (b) Internal LOO validation between spectral variables and axis scores. cor = Pearson product-moment correlation; RMSE = root mean squared error; R2 = coefficient of determination; n_C = number of latent components in final PLSR-model; n_pred = number of significant predictors/spectral variables.*

(a)	Occurrence Probability		Assessment Categories	
	cor	RMSE [%]	cor	RMSE [%]
LRT 2330	0.937	15	0.918	12
LRT 4030	0.971	10	0.925	8
LRT 6120	0.811	20	0.859	15

(b)	Spectral Model NMS1				Spectral Model NMS2			
	R^2	RMSE [%]	n_C	n_pred	R^2	RMSE [%]	n_C	n_pred
LRT 2330	0.491	21	2	147	0.827	10	2	142
LRT 4030	0.820	12	2	68	0.130	20	2	61
LRT 6120	0.789	12	2	9	0.854	10	2	14

In fact, habitat type LRT 6120 occurs in various transitions to pioneer grasslands and dry heaths as shown in red (10–40% probability). Open pioneer grasslands and dry heaths are more common in the study area. Their conservation status mainly ranges between A and B, whereas spatial patterns indicate an expected decrease in habitat quality from core areas to edge regions (Figure 8 zoomed subplots). External validation was performed on the 58 field plots by extracting habitat types for a probability threshold of >30% and for equally spaced assessment categories. Habitat types LRT 2330 and LRT 4030 can be mapped with an overall accuracy (OAA) of 100%, whereas species diversity in LRT 6120 is more difficult to detect (OAA = 73.3%). However, degenerated stages of LRT 6120 with probabilities <30% were not included in the validation. Terrestrial assessment categories show good conformity with LRT 2330 (OAA = 84.2%) and with LRT 4030 (OAA = 89.5%). Conservation status variations are more complex in LRT 6120, which results in an OAA of 66.6%.

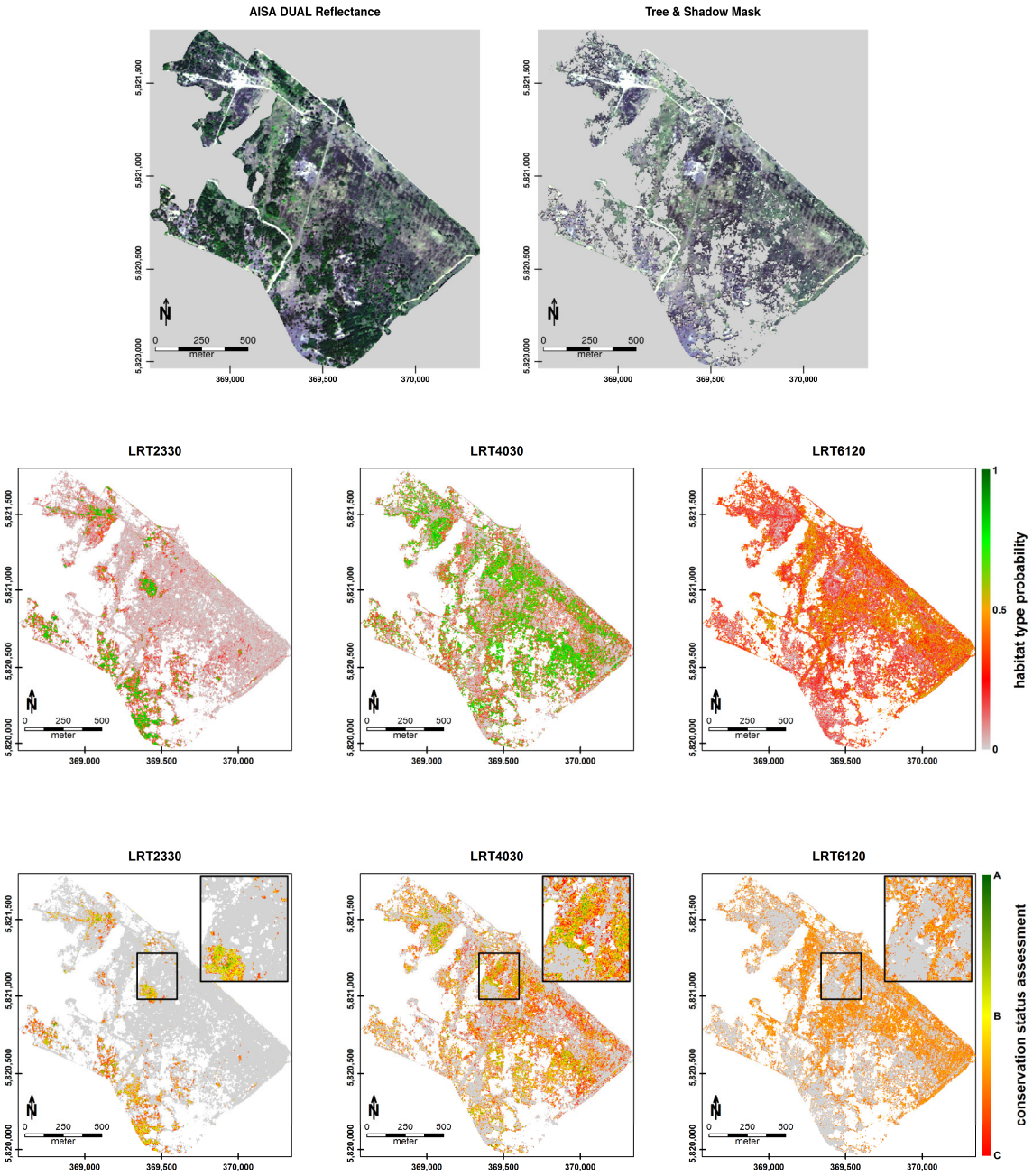

Figure II-8: *Top panel: AISA DUAL true-color composite image of the test area (left); open dryland extraction after masking trees and shadows (right). Middle panel: spatial occurrence probability predictions of three habitat types. Bottom panel: continuous habitat type conservation status predictions with color centroids representing status (A: excellent; B: good; C: adverse); a typical transitional area between the three habitat types was exposed in the subplot zoom.*

4 Discussion

4.1 Spatial Correlation

Our study demonstrates the use of spatial correlation functions to determine habitat types, pressures, and conservation status in a site-specific ordination space. As an initial step, we introduced habitat functions as representations of habitat occurrence and pressure/threat strength. It should be noted that predicted habitat patterns are strongly dependent on selected species and chosen species weights. In this respect, our study presents a straightforward procedure to determine how expert knowledge on habitats and habitat pressures can be transferred to ordination space projections. The modeled type and status therein are seen as possible representations of ecological interdependencies in a vegetation continuum. There is no general allocation of floristic composition to a certain habitat type or pressure complex. Every ordination space can be quantified individually according to the study area, assessment demands, or management purposes. Our approach provides a reproducible aggregation technique on the basis of species lists and is therefore distinct from a priori habitat classification or obviously subject-dependent terrestrial assessment.

The species composition used in this study to describe the conservation status categories for dry heath is based on the legal standards defined in Annex I of the European Habitat Directive (EU, 1992), as well as expert knowledge (Evans and Arvela, 2011; Zimmermann, 2015). However, the proposed methodology is not restricted to Natura 2000 habitat types. With an appropriate sampling of indicator species and pressure factors, every monitoring or assessment approach can be analyzed on its ability to reflect clear patterns in an ecological gradient space. Thereby, habitat type probabilities as well as pressure strength are spatially predicted on the basis of variogram models. In geostatistics, there is no standard methodology to select an appropriate model. In our study, the best model was selected by minimizing the prediction error for a choice of 19 known models. Nevertheless, it is important to keep in mind that the final results for a grid-based probability pattern are dependent on the choice of spatial correlation function (variogram model) and its overall predictive capacity. Spatial probability patterns are therefore not deterministic and can only be approximated, taking into account adapted selection algorithms (Christakos, 1984; Gorsich and Genton, 2000). Another source of spatial uncertainty is in the ordinary kriging procedure itself. The number of points used to calculate weights for an unknown grid cell can have an influence on spatial heterogeneity. We constantly used half the number of total plots per grid cell to derive reliable kriging weights.

4.2 Species Composition

Probability aggregation in ordination space dimensions is usually applied on external variables to interpret abstract gradients. Vegetation ecologists are well aware of spatial statistic methodology (Hauser and Mucina, 1991), which is used to produce isolines representing external correlation structures by means of classification approaches (EjrnÆs et al., 2002) or trend-surface analyses (Dargie, 1984). To our knowledge, this is the first time that multi-species probability estimation, on the basis of habitat/pressure functions, has been examined. In addition to habitat type and threat, the conservation status can consequently be described by ordination space structures that reveal species gradients on the basis of pressure definition. However, even though separation of general gradient patterns with axis models reveals fine-scale floristic heterogeneity that can be described by means of variography, the identification of unique species complexes may become complicated in species-rich continua. Therein, differential species contribute at different gradient positions to habitat quality and distribution. Species complexes are not generally separated in single positions in ordination owing to overlay and indifferences as part of the unexplained variance. Even if habitat types can be directly allocated using probability thresholds, a distinct separation of near-ordinated but floristic variable plot locations should be reviewed critically. Besides gradually changing species cover in adjacent plots, abrupt changes in species representation as revealed by pressure complexes (Table II-3) are evident in ordinated species composition. In addition to axis stability and pattern significance estimation, a good floristic representation can be further increased by optimizing preserved sample variance. In our study we used a two-dimensional NMS with an excellent representation of the floristic variation (stress = 0.0016) in order to demonstrate a two-dimensional Kriging procedure. The decision was based on evaluating the strength of spectral correlation to single score axes. The averaged R^2 of the first NMS axis over all habitat types was maximized in a 2D solution. However, additional variance patterns may be related to spectral signatures. For this purpose, a case-specific choice of number of ordination axes, distance metric, original dimensions (surface and vegetation structure parameters besides plant species), and a detailed analysis on recent algorithmic developments such as Isomap (Feilhauer et al., 2011; Tenenbaum, 2000) still ought to be considered.

4.3 Spectral Application

The spectral discrimination of axis gradients varies for specific habitat types and selected axes. It should be noted that as part of the applied NMS ordination, axes are principal component rotated in order to explain the maximum variances in the plot configuration. The resulting directions are not automatically related to spectral diversity, and it can be assumed that linking the spectral discriminability to axis-specific rotation angles will increase the predictive accuracy. Further research is needed to find supporting evidence for this. Another source of unexplained regression variance can be seen in the representation of the spectral

sample itself. Spatial heterogeneity on 2 m pixel size can introduce an increased signal variance owing to adjacent effects. Furthermore, spatial non-stationarity due to phenology shift or varying litter cover can influence model representation on image pixels (Feilhauer et al., 2014). In addition, image-spectra calibration always delivers spectral response models under the boundary conditions of acquisition time. Spectral library information on the basis of TOC reflectance can be considered to be an improvement for true variance estimation and transferability when phenological phases are covered adequately. Nevertheless, the transferability of regression models for floristic patterns still remains complicated owing to vegetation status, irrespective of the species (Price, 1994). Additional parameters such as the chemical constituents under the influence of plant stress and growth (Carter and Knapp, 2001), and spatial heterogeneity such as litter content and canopy height (Feilhauer and Schmidtlein, 2011), should be described in order to obtain reliable models for monitoring purposes. However, the approach presented here can enhance a Natura 2000 habitat assessment with spatially explicit predictions of conservation status incorporating floristic compositions along ecological gradients.

4.4 Conservation Status Assessment

The presented approach demonstrates a pixel-wise conservation status assessment on the basis of Natura 2000 habitat type transition and pressure indicators that are directly derived from ordination space structures. An important advantage can be seen in the decoupling of the spectral and the ecological models. We can spectrally predict the vegetation continuum and a posteriori derive information from that. It crucially differs from common remote sensing based methods, where image pixels are classified according to different habitat types (Michael Bock et al., 2005; Förster et al., 2008) or habitat quality parameters (Förster et al., 2008; Haest et al., 2010). Therein, an image pixel is determined by one attribute that was a priori defined as a relevant ecological entity for the evaluation of habitat quality. Various habitat quality indicators are developed (M. Bock et al., 2005) that allow a fine-scale prioritization of management strategies. Although remote-sensing-derived habitat quality maps show a good correlation to terrestrial mapping approaches, they can only explain variations in fine-scale conservation status indicators up to 39% (Spanhove et al., 2012). In the proposed approach, the information mapped at the pixel scale is variable. Fine-scale variations are directly transferred from ordination space via spectral coherences. Both habitat transition and pressure species complexes are transferable to images using the informational content of the ordination space that projects the floristic variation in an environmental space. This enables additional conclusions about the mapped conservation status. Thereby, an image pixel is linked to the structure of the site-specific ordination space that holds information such as the direction of habitat succession, the distribution of plant species, or, indirectly, about the abiotic gradients. Commonly, this information has to be defined before mapping and the conservation status

assessment is based exactly on these defined categories (Förster et al., 2008; Mücher et al., 2013). The functional aggregation technique coupled with probability, pressure strength, and assessment predictions also allow a continuous interpolation of ordinated plot information. Hence, habitat conversion can be made visible in continuous gradients when ordination dimensions are transferred to image data. Development tendencies with regard to species shifts can be revealed in these transitional areas. However, the aim of the study was not to give a complete conservation status assessment. It is rather aimed at providing a methodological framework for the evaluation of plant species shift that is assumed to be responsive to management in our study area (grazing, mulching, species removal). We do not include additional, structural vegetation parameters (e.g., vitality, senescence) or anthropogenic influences (e.g., burning, nutrient transfer) in the ordination that can increase the accuracy of habitat quality assessment. It has further to be mentioned that this study is based on a site-specific ordination space for open dryland habitats on former military training areas in Brandenburg. In order to reveal fine-scale variations in transition and species composition, such ordination results are restricted to certain biogeographical regions. Integration of different habitat types always depends on the availability of species data whereby comprehensive data archives such as spectral libraries can be used to transfer the proposed methodology. Plant species data as well as related spectroradiometer measurements used in this study were therefore stored in a freely accessible database called SPECTATION ("SPECTATION," 2015). Therein, field plot-specific plant species lists, vegetation class and conservation status units, and surrounding soil properties are stored for open dryland and wetland habitats in conjunction with spectral reflectance signatures for the years 2008 to 2011. This enables reproducible research on similar habitats or methodological extensions to different habitat types, which could be a subject for analysis in future studies. Species ordination and subsequent spectral variance estimation in a broader scale (e.g., country- or Europe-wide) has still to be investigated by means of new multidimensional interpolation methods. With regard to this, the crucial question for further research is: how many habitat types can we integrate in one ordination in such a way that fine-scale variations are still visible in ordination as well as in the spectral response? New statistical approaches from big data analysis in conjunction with spectral library information open future perspectives on detailed Natura 2000 habitat mapping.

5 Conclusions

The probability of a habitat being of a specific type depends on the habitat status incorporating inter-habitat transitions and pressure factors. The information content of ordination spaces can be used to continuously determine such habitat structure parameters. It can be shown that floristic patterns projected in the ordination space are significant and stable. There is strong evidence that functionally aggregated habitat characteristics on the basis of

plant species data are spatially determined over distinct regions of the ordination space. Empirical score axes models as well as residual variogram models can be used to describe the ordination space variability of habitat characteristics such as habitat type and habitat pressure. A subsequent model combination further allows a spatially continuous interpolation of habitats and related pressure strength over the entire ordination space. Habitat transition as well as pressure indicators can be made visible in distinct ordination space regions for conservation status assessment. Results correspond well to terrestrial Natura 2000 conservation status assessment. Using evidence on spectral coherence, habitat status probabilities can be used directly to produce spatially explicit maps. This approach differs crucially from conventional remote-sensing-based habitat assessment methods that assume discrete management units as predefined natural components. Spatial monitoring is no longer dependent on threshold-based changes in habitat categories. The potential of change can be directly projected over probabilities in ordination spaces, and assessment tendencies are directly transferable to spatial information. This enables the Natura 2000 monitoring to assess habitat type vulnerability more rapidly and allows a more effective prioritization of management activities to preserve a certain conservation status. This is especially true in open land habitats on former military training areas, where habitat conversion is driven along successional gradients and terrestrial mapping is complicated by undiscovered military munition.

Acknowledgments

We would like to thank the nature conservation foundation Sielmanns Naturlandschaften for enabling secure access to field plots, which involved exploration of military ordnance debris, and for sharing knowledge about area-specific details of vegetation structures and abiotic characteristics. We specifically thank Peter Nitschke, Angela Kühl, and Jörg Fürstenow. We also thank the student field workers for supporting floristic and spectral field sampling, namely Randolf Klinke and Josefine Wenzel. This work was funded by the Deutsche Bundesstiftung Umwelt (DBU) and the Environmental Mapping and Analysis Program (EnMAP).

Author Contributions

Carsten Neumann developed the methodological framework, performed programming, and conducted the analysis. Gabriele Weiss planned and conducted floristic field surveys and implemented the assessment scheme on habitat conservation status. Angela Lausch and Daniel Doktor provided the AISA DUAL Sensor data and organized the overflight campaign. Maximilian Brell was responsible for the pre-processing of hyperspectral imagery. Sibylle Itzerott and Sebastian Schmidltein were involved in formulating the research questions,

preparing the manuscript, and contributing to critical discussions. All authors were involved in the general paper review.

Conflicts of Interest

The authors declare no conflict of interest.

Chapter III: Determination of Spectral Gradients and Wavelength Features

This is the accepted version after peer review (Postprint) of the following article:

Neumann, C., Förster, M., Kleinschmit, B., Itzerott, S. (2016). Utilizing a PLSR-based band-selection procedure for spectral feature characterization of floristic gradients. IEEE Journal of Selected Topics in Applied Earth Observations and Remote Sensing, 9(9), pp. 3982 - 3996.

DOI: 10.1109/JSTARS.2016.2536199
Received: 09 June 2015 / Accepted: 17 February 2016 / Published: 28 March 2016

Abstract

The study introduces a new approach for the characterization of floristic gradients by hyperspectral features in a partial least squares regression (PLSR) framework. As ecological factors influence the composition of vegetation, our study is aimed to reveal related effects on spectral signatures. For this purpose, the variation of plant species in an open dryland area was projected into a three-dimensional ordination space using nonmetric multidimensional scaling (NMDS). Subsequently, ordination axes score rotations were performed in 180° semicircles and the waveband-specific correlation to spectral field measurements of reflectance, continuum removed, and first-derivative spectra were extracted. A bootstrapped PLSR modeling was applied over the entire rotation space using varying numbers of correlated spectral variables as input samples. On that basis, a new PLSR model suitability term was defined by isosurfaces that are spanned over ordination regions where PLSR latent vector (LV) number and PLSR R^2 variance is minimized. It incorporates model performance evaluation with feature characterization using weighted frequencies of spectral variable input in suitable ordination areas. Final PLSR suitability surfaces were transferred to image spectra to prove feature stability and model performance. Our investigation supports the assumption that spectral features are separable to distinct ordination space regions that can be related to individual species gradients. Thereby, the selection of an optimal PLSR model crucially depends on the spectral transformation technique. We further show that stable PLSR models can be derived in multiple ordination directions whereby an appropriate variable selection using suitability surface optimization reduces feature mismatch between field and image spectra.

1 Introduction

Remote sensing based vegetation mapping has become an important tool for monitoring habitats for nature conservation (Kerr and Ostrovsky, 2003; Turner et al., 2003; Wang et al., 2010). In particular, spatial vegetation patterns are used for the spatiotemporal characterization of biodiversity and the assessment of habitat quality in nature reserves worldwide (M. Bock et al., 2005; Corbane et al., 2015; Velázquez et al., 2010). Amongst recent developments in sensor technology, imaging spectroscopy provides high dimensional spectral feature spaces for the discrimination of indicator species or plant communities. This information can be utilized for identifying habitat types and assessing their conservation status (Cochrane, 2000; Lawrence et al., 2006; Oldeland et al., 2010a) using various algorithms from statistical machine learning theory (Ham et al., 2005; Melgani and Bruzzone, 2004). Hyperspectral signatures further enable a detailed specification of habitat stress induced by e.g. nutrient deficiency or pollutant contamination by relating spectral absorption

features to changes in chlorophyll, nitrogen, phosphorus and other foliar compounds (Hansen and Schjoerring, 2003; Sims and Gamon, 2002; Thenkabail et al., 2004). It is assumed that optical properties of plants can be linked with variations in foliar biochemistry (Gates et al., 1965; Ollinger, 2011). However, the derivation of distinct spectral characteristics to single plant species or plant communities is still problematic due to different plant states under varying environmental conditions (Price, 1994). Commonly, in the field of remote sensing a widely applied approach for the characterization of vegetation pattern and influencing factors is realized with classification of discrete vegetation units in the spectral feature space (Xie et al., 2008). Such methodology results in sharp boundaries between compositional vegetation patterns whereas continuous quantitative information, such as species abundance shifts, are aggregated into vegetation classes. With increasing degree of generalization, these vegetation classes thus unify spectral differences and therefore introduce additional sources of spectral within-class variance that impedes between-class differentiation (Rocchini et al., 2013). As a consequence, fine scale complexity, as evident in transitional changes in floristic composition along different spatiotemporal ecological gradients, cannot adequately be represented in classification.

The use of continuous floristic gradients described as a vegetation continuum in ordination spaces allows for a more detailed representation of compositional vegetation patterns by modeling gradual species shift directly along environmental gradients (Austin, 1985; Whittaker, 1967). It conflates plant responses to the abiotic environment and arising pattern in plant species composition. Basically, individual species cover stored in n-dimensional species x sample matrices are projected into abstract environmental spaces using different techniques of dimension reduction such as Non-metric Multidimensional Scaling (NMDS) (Kruskal, 1964), Correspondence Analysis (CA) (Hill, 1973) or Principal Component Analysis (PCA) (Hotelling, 1933). The variability of vegetation samples is thereby extracted in the form of floristic gradients that can be described by score coordinates of ordination space axes. Empirical coherence between spectral signatures and single ordination space axes, representing the floristic variation of vegetation, has been proven in various studies (Feilhauer et al., 2011; Oldeland et al., 2010b; Schmidtlein et al., 2007; Schmidtlein and Sassin, 2004; Thessler et al., 2005). In contrast to classification, this approach makes use of Partial Least Squares (Wold, 1966) in a regression framework (PLSR). It can handle multicollinearity that is evident in hyperspectral signatures due to redundant wavelength information in narrow spectral bands. However, the underlying relationship between spectral variables and varying gradient directions remains still unrevealed.

In an ordination space, the distribution of sample plots derived from indirect gradient analysis often reflects multiple environmental gradients that are not necessarily correlated parallel to the initial ordination score axes (Ter Braak and Prentice, 1988). In the field of vegetation

ecology it is a well-known fact that species replacement and abundance shifts can be described by different explanatory factors that varies in correlation strength and direction in an ordination result (Tahvanainen, 2004; Vitt and Chee, 1990). Whilst remote sensing-based gradient mapping approaches solely concentrate on predicting score vectors of the initial orthogonal ordination axes on the basis of image spectra, the connection between spectral feature responses and varying floristic gradients in different ordination directions remains still disregarded. However, the examination of ordination scores relative to spectral information across species abundance gradients offers a great potential for the indication of correlations with additional abiotic ecological factors. This is especially applicable as precise hyperspectral reflectance signatures for different plant species assemblages can be made available through spectral libraries (Bojinski et al., 2003; "SPECTATION," 2015; Zomer et al., 2009). On that basis, significant spectral features are detectable over empirical relations to changing foliar chemistry. Even though PLSR comprises well established feature selection approaches that have been proven to be valid in different fields of application (Mehmood et al., 2012), its usability for stable feature identification in vegetation science is only investigated in rare occasions (Cole et al., 2014; Fassnacht et al., 2014; Song et al., 2011). Especially, floristic gradient determination by means of spectral feature shifts in field measurements has not yet been intensively investigated.

In this study, we therefore introduce an approach to define floristic gradients by spectral features that are systematically derived for different ordination space topologies. For that purpose, we

a) present a new feature selection procedure for optimal PLSR model calibration,

b) prove the concept of the spectral determination of different gradient directions by an optimal predictive PLSR model on the basis of field spectroradiometer measurements.

c) test the transferability of features and models from field measurements to image spectra in order to provide stable predictions for spatial mapping purposes.

2 Material and Methods

2.1 Study Area and Floristic Inventory

The study was conducted in open dryland habitats on a former military training area, Doeberitzer Heide, located at 53° latitude and 13° longitude in the west of Berlin, Germany (Figure III-1). The study area encompasses 52 km² in which 27 km² are designated as Special Area of Conservation in the European Natura 2000 network. The abiotic background is mainly defined by glacial ground moraine deposits of the North German Plain. A distinctive small scale floristic heterogeneity is widely established on sandy, acid soil substrate. Typical plant communities are open pioneer grasslands (e.g. *Corynephorus canescens*), dwarf shrub

heathland (e.g. *Calluna vulgaris*) and sandy xeric grasslands (e.g. *Festuca ovina agg.*). Due to soil disturbances during military actions, local base enrichment (e.g. *Galium verum*, *Peucedanum oreoselinum*) and nitrate eutrophication (e.g. *Calamagrostis epigejos*) affecting species abundance and community composition. Structural changes by succession as degeneration stages, senescence or scrub invasion (e.g. *Populus tremula, Sarothamnus scoparius*) are mainly regulating floristic transition between typical plant communities. On the basis of expert knowledge, vegetation samples on 58 plots with a quadratic size of 1 m² were located within dominant inventories of major indicator species as well as along transition zones. The distribution of vegetation plots was chosen systematically to cover all dryland species and their possible transition that are likely to occur under the abiotic background of the entire study area. The semi-quantitative cover of all vascular plant species, mosses and lichens was estimated using the enhanced Braun–Blanquet scale (Reichelt and Wilmanns, 1973) that was transformed to average percent cover. For validation purpose, plant species cover was additionally recorded along 3 transects covering the main floristic transitions in 21 plots. In total 98 different species could be detected between June and August in 2011. See Neumann et al., 2015b for a detailed description of vegetation types, species distribution and gradients of the open dryland habitats in the study area.

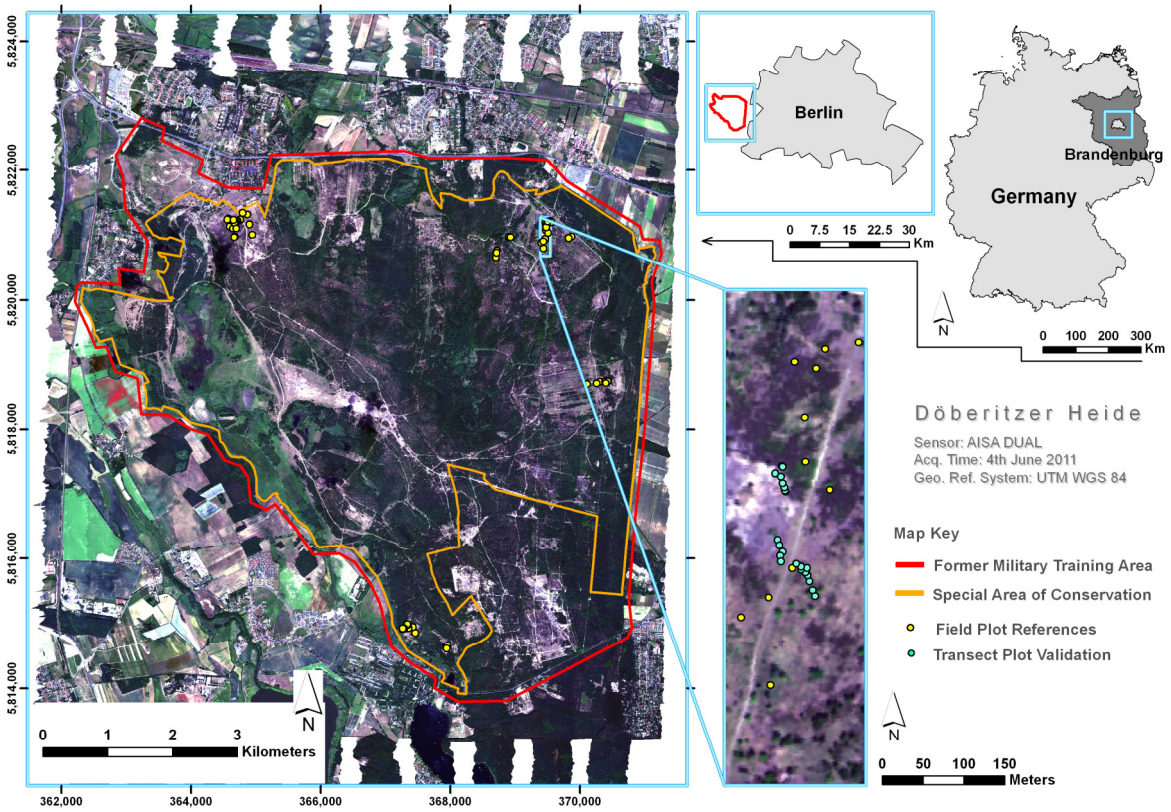

Figure III-1: *Spatial distribution of field plots for reference data collection in the study area visualized on AISA DUAL flight stripes, section of test area with transect plot locations*

2.2 Hyperspectral Imagery

Hyperspectral imagery was acquired with an AISA DUAL (UFZ Leipzig) imaging spectrometer ranging from visible (400 nm) to short wave infrared (2500 nm) in 367 spectral bands on 4th June 2011. Between 10.00 and 12.30 p. m. a total number of 22 flight stripes were recorded covering 300 samples per scanning line. After geometric coregistration using inertial measurement unit and automated ground control point allocation (SIFT) (Lowe, 2004), an image mosaic was generated with a final pixel size of 2 x 2 meter. Internal radiometric calibration was supplemented with spectral binning, smear correction and destriping (ROME) (Rogaß et al., 2011) to generate at sensor radiance. In order to obtain top of the canopy reflectance (TOC) a radiative transfer model (ATCOR-4) was implemented followed by an empirical line correction ELI (Smith and Milton, 1999). As reference for ELI post-calibration we made use of field spectra that were collected around acquisition time with an ASD field spectroradiometer (ASD inc.). Reference plots consisted of 3 dark and 3 light targets that were sampled in 25 transect measurements, respectively. The common ELI procedure was adjusted to polynomial regression until the best polynomial fit between image and reference spectra was found. To account for observed non-linearity effects at the UV-blue wavelength transition (< 440 nm), the first 10 bands were removed for further analysis. In summary, ELI post-calibration reduces the mean deviation between reference and image spectra by 5% in the visible-near infrared wavelength region (mean Root Mean Squared Error (RMSE) = 14 %) and by 9% in the shortwave infrared (mean RMSE = 8%). Reflectance signatures for ordination space plots were extracted from image mosaic as validation dataset.

2.3 Spectral Field Measurements

In order to provide similar conditions during overflight (image spectra) and field samples (field spectra) regarding plant species life states, plant phenological phases were estimated for index species from the Global Dataset (GDS, 2014) provided by the German Meteorological Service (Deutscher Wetterdienst - DWD) at 3 stations around Potsdam, Germany. Spectral field samples were collected with an ASD spectroradiometer for all 58 vegetation plots during midsummer phenological phase starting with flowering of large-leaved linden (Tilia platyphyllos) and ripeness of currant (Ribes) and ending with flowering of early apples (Malus) and ripeness of rowan (Sorbus aucuparia). Reflectance values were measured within a wavelength range from 350 to 2500 nm in 2151 spectral bands. On every field plot 25 reflectance signatures were collected at 1.4 m above canopy using an 8° foreoptic. The spectral information on the resulting footprint with a diameter of 0.2 m for single measurements was averaged over the entire 1 m² quadratic sampling area. Bands related to strong atmospheric water absorption (1335-1449, 1749-1999 and > 2399 nm) were then masked out. According to sensor-wavelength specific response functions, ASD field spectra were resampled to AISA spectral resolution resulting in 282 bands. The final 58 samples x

282 bands reflectance matrix was defined as predictor set A. On that basis 2 additional spectral predictor sets B and C were calculated using full-band transformation comprising Continuum Removal (Clark et al., 1987) in B and 1st Savitzky-Golay Derivation (Savitzky and Golay, 1964) in C, respectively.

2.4 Floristic Gradients

The final sites-by-species matrix was projected as a n-dimensional vegetation continuum using Bray-Curtis distances (Clarke and Warwick, 2001) for estimating species similarities on field plots. A Non-metric Multidimensional Scaling (NMDS) was applied to reproduce original sample plot similarities with ordination score axes. For this purpose, rank ordered similarities of the original matrix were iteratively regressed against ordination solutions until NMDS plot arrangement reaches a minimum in residual error or a maximum in goodness of fit, respectively. We used Kruskal's stress value (Kruskal, 1964) to proof reliability of the final ordination plot configuration. The resulting vegetation continuum was defined by 11 score axes that reached a minimal stress value of 11, which is assumed to be a good representation of original variance (Borg and Groenen, 2005; Kruskal, 1964). We restrict our analysis on the first three NMDS axes as they represent the main floristic variation for our study area (Figure III-2). Therein, major indicator species are well grouped to ordination plot regions with characteristic transitions to adjacent communities. While open pioneer grasslands and dwarf shrub heathland show clear separation pattern, sandy xeric grassland species are more variable forming broader transition pattern.

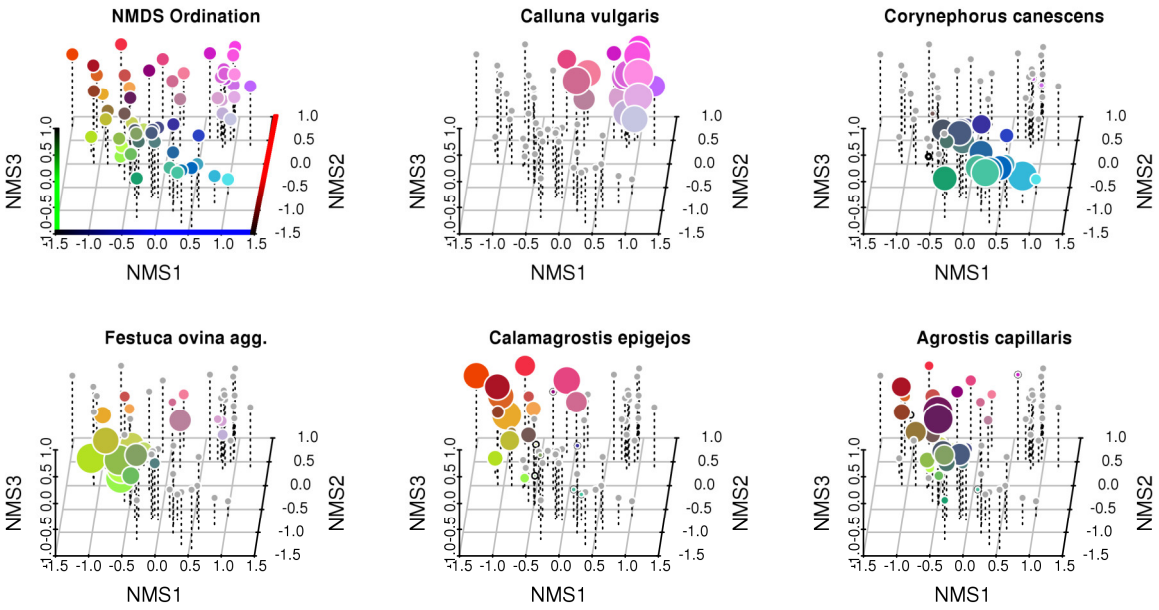

Figure III-2: *Exemplary NMDS ordination plot arrangement in RGB color space; dot size is positively correlated to species cover in field plots; concentrated species distribution (on top) as well as transitional species gradients (at the bottom) can be visualized*

2.5 Step 1: Ordination Space Rotation and Spectral Coherence Analysis

The final NMDS ordination space was rotated in 3 dimensions to identify spectral correlation in predictor sets A-C. Rotation is performed around origin of ordinates with rotation angles starting at 0 and progressing to 180 at a 0.5 degree step. Score values for field plots were re-calculated using rotation matrices in spatial directions [x, y, z] = [NMS1, NMS2, NMS3] with rotation angles [α, β, γ]. Thereby, one score axis R is always fixed and score coordinates can be derived for rotation angles of the remaining two axes:

$$\boldsymbol{R}_{(NMS1,\alpha)} = \begin{bmatrix} \mathbf{1} & \mathbf{0} & \mathbf{0} \\ \mathbf{0} & \boldsymbol{cos\alpha} & \boldsymbol{-sin\alpha} \\ \mathbf{0} & \boldsymbol{sin\alpha} & \boldsymbol{cos\alpha} \end{bmatrix};\ \boldsymbol{R}_{(NMS2,\beta)} = \begin{bmatrix} \boldsymbol{cos\beta} & \mathbf{0} & \boldsymbol{sin\beta} \\ \mathbf{0} & \mathbf{1} & \mathbf{0} \\ \boldsymbol{-sin\beta} & \mathbf{0} & \boldsymbol{cos\beta} \end{bmatrix};\ \boldsymbol{R}_{(NMS3,\gamma)} = \begin{bmatrix} \boldsymbol{cos\gamma} & \boldsymbol{-sin\gamma} & \mathbf{0} \\ \boldsymbol{sin\gamma} & \boldsymbol{cos\gamma} & \mathbf{0} \\ \mathbf{0} & \mathbf{0} & \mathbf{1} \end{bmatrix}$$

Axis specific rotated score values R were obtained in gradual rotation for every field plot in the ordination space. The new score coordinates were individually calculated by matrix multiplication on the direction vectors. For example, new score coordinates for 90° NMS1 rotation around fixed NMS3 axis results in shifted score values calculated by $\mathrm{R}_{(\mathrm{NMS3},90°)} = \mathrm{NMS1} \cdot \cos(90°) - \mathrm{NMS2} \cdot \sin(90°)$. As a result every rotation angle can be described by a unique score vector. These score vectors (n = 361) can now be regressed against the spectral variables stored in the predictor sets A-C for each angle direction, separately. Thereby, the spectral variables are defined as a predictor set of single wavelength bands (n = 282). Hence, each score vector was related to a single band by means of univariate linear regression for the predictor sets A-C, resulting in 361 x 282 x 3 coefficients of determination R^2 (Figure III-3-1). The R^2 in linear regression was used to identify the amount of score variance that can be explained by individual wavelengths. Finally, two R^2-matrices can be calculated for the rotation of two NMS axes. The procedure starts with the rotation of axis NMS1 around NMS2 and NMS3. Highest R^2 gradients were used as indicators for the selection of a preferred rotation direction. NMS1 was then rotated to the preferred direction and NMS2 was rotated around fixed NMS1 again until 180° are reached. In order to preserve axes orthogonality and sample point distances in the ordination plot, the NMS1 axis must be fixed in the second rotation. Following this procedure a complete spectral regression for different ecological gradients in a 3 dimensional NMDS representation can be achieved using ordination axes NMS1 and NMS2.

2.6 Step 2a: Spectral Feature Grouping

Spectral variables with correlation to particular gradient directions can be rank ordered according their specific R^2 values in linear regression (Figure III-3-2a). Thus, the strength in the relationship between single wavelength bands and rotated score vectors can be make visible. This information can be used in PLS regression to model different gradient directions. To maximize the explanatory power of PLSR models in different ordination space directions

it is necessary to define R^2 thresholds for significant spectral variable input. An optimal variable set that consist of different wavelength positions can be regarded as spectral feature group. Since possible features that describe specific axes rotations are not known before, a pre-selection of varying variable inputs into feature groups was performed according to the rank ordered R^2 percentiles. We define that a 99% percentile holds the 1% wavelengths with highest R^2 values; a 1% percentile holds 99% of all wavelengths but not the 1% with lowest R^2 values, respectively. Only percentiles > 50% were considered in order to restrict the analysis on high correlated spectral variables. This feature percentile grouping was implemented with both field and image spectra. It serves first to interpret the R^2 distribution for independent wavelengths in the rotation space, and second to compare the percent spectral predictor match between field and image feature groups in the same angle directions.

2.7 Step 2b: Spectral PLSR based Modelling

The following analysis steps are solely based on field spectra in order to prove the transferability of selected features in a PLSR framework to image spectra. For every percentile n = 1000 PLSR models were calibrated using bootstrapped samples of the spectral variables (bands) stored in the respective feature group (Figure III-3-2b). Thereby, the random exclusion of variables in bootstrapped samples can be used for the assessment of model stability and feature significance. For this purpose, the number of latent vectors (LVs) for PLSR R^2 saturation and the corresponding model R^2 is stored in every bootstrap calculation. Finally, the n = 1000 LV mean (LV_{boot}) and the R^2 variance ($VARR^2_{boot}$) was derived for 361 score vectors x 50 percentile feature groups. In addition the maximum PLSR R^2 ($PLSR_{R^2}$) was calculated for the respective feature groups using the complete number of included spectral variables without bootstrapping and LV minimization. We now define a new term, the PLSR model suitability ($PLSR_{suit}$), in order to assess the explanatory power and predictive stability of the PLSR framework in different ordination space directions. A suitable PLSR model is thereby assumed to achieve highest R^2 with a minimal number of latent vectors characterized by a stable combination of significant spectral variables in all bootstrap samples. Varying R^2s as well as an increased number of LVs for R^2 saturation are indicators for model instability and hence lead to a decrease in PLSR suitability. The negative influence of high LV_{boot} and $VARR^2_{boot}$ values can mathematically be expressed by reversed scaling of the original variable ranges: $_rLV_{boot} = -(LV_{boot}) - \min(-LV_{boot})$ and $_rVARR^2_{boot} = -(VARR^2_{boot}) - \min(-VARR^2_{boot})$. In consequence PLSR suitability is influenced in bootstrapping by regulating maximum explanatory power ($PLSR_{R^2}$) downward or upward, respectively. This behavior can be expressed by: $PLSR_{suit} = PLSR_{R^2} \cdot {}_rLV_{boot} + {}_rVARR^2_{boot}$ whereby $_rLV_{boot}$ is assumed to act as a gain factor and $_rVARR^2_{boot}$ as an error term addend. Generally, the maximum PLSR explanatory power has to be modified as effects of overfitting becomes more likely with an increased numbers of LVs. In contrast, the introduced error term represents a random effect in

model stability if spectral features are too small in the spectral range or randomly distributed in a way that their bootstrap exclusion leads to high PLSR R^2 variances. Spectral variable combinations that lead to suitable PLSR models under bootstrapped recombination can be defined as stable spectral features for distinct gradient regions. The final suitability distribution can be determined by isosurfaces on the rotation x percentile dimensions.

2.8 Step 3: Iterative Optimization for Feature Selection

Model suitability surfaces were used as weighting schemes for the spectral variables that are stored in the feature groups. For that purpose, the PLSR suitability surface was normalized between 0 and 1 and a weighted frequency table was calculated for the spectral variables. It is now possible to distinguish between two cases, a unique frequency weighting over the complete rotation x percentile space and single weighting schemes that can be extracted for different rotation angles. More precisely, spectral variables that occur more frequently in an ordination space direction where PLSR model suitability is increased benefits from higher table counts and weighting factors. This enables distinct spectral feature identification over their contribution to optimal PLSR ordination axes model. Nevertheless, in order to derive a final PLSR model with an optimal spectral variable combination (regarded as spectral features), an optimization procedure was introduced that maximize PLSR R^2 in the final model calibration via adjusting iteratively a) area of weighting scheme (PLSR suitability surface) and b) frequency thresholds for the inclusion of spectral variables (Figure III-3-3). In the rotation x percentile space, the procedure selects one suitability spot and the remaining gradient directions where mask out. In consequence, only spectral variables contributing to a distinct rotation direction were weighted according their suitability surface. Subsequently, the extent of the selected suitability spot was successively shrinked. For every extent step, weighted frequencies of spectral variables in corresponding feature groups were extracted and used as input variables for PLS regression. Simultaneously, the spectral input variables were reduced on the basis of their relative frequency thresholds ($0.05 < t < 0.97$) to define an optimal number of input variables that maximize PLSR R^2. This two-way optimization approach ends when the difference of two consecutive suitability surfaces tends to zero. The final PLSR model was consequently calibrated using a selected number of spectral input variables and related frequency weights from the relevant suitability surface. For an evaluation of feature transferability, the final suitability surface weighting was applied to the rotation x percentile space of the image spectra and the Pearson product-moment correlation between the frequency distribution of field and image spectral variables was estimated. Finally, field spectra based PLSR models were used to predict NMDS axes scores of reference plots using extracted image spectra at plot locations. Spatially explicit maps of axes scores for different ordination space direction were derived and related to the abundance of plant species in the validation transects.

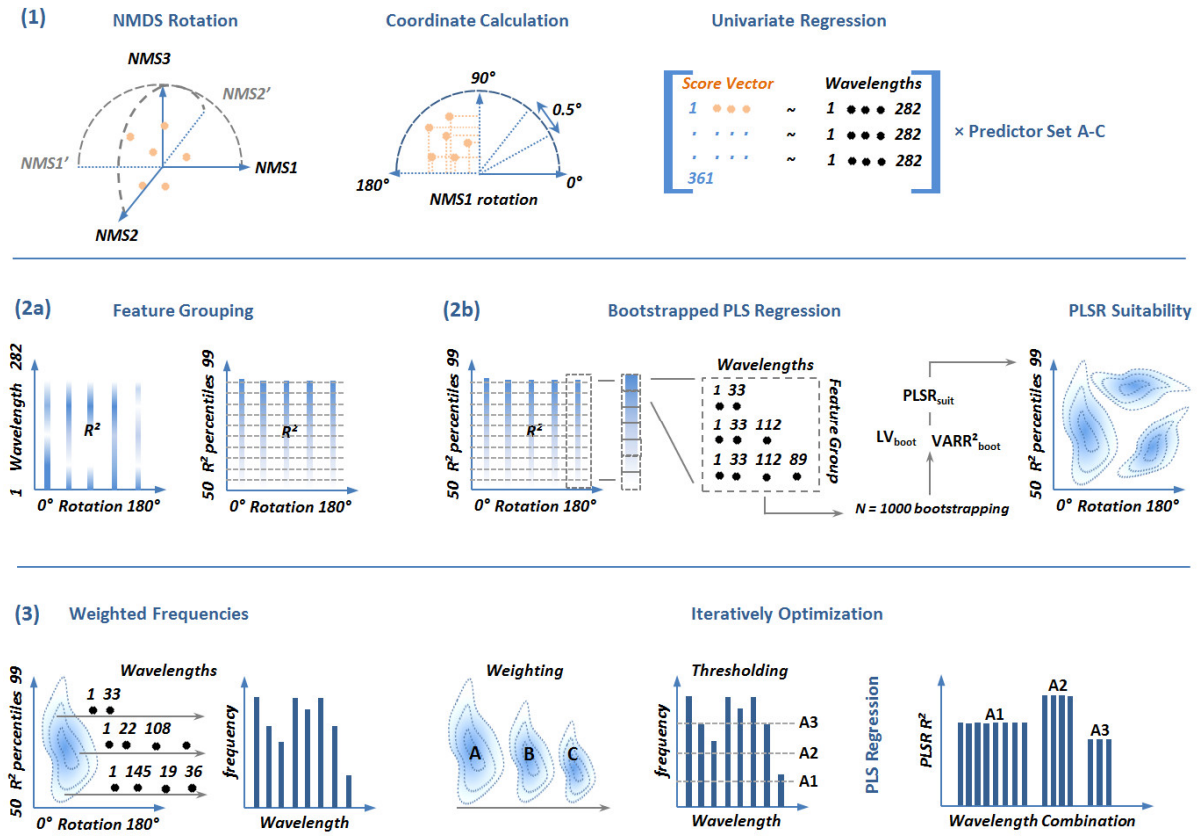

Figure III-3: *Methodological framework (step 1 – 3) for a PLSR based spectral feature selection in varying gradient directions within the NMDS ordination space*

3 Results

3.1 Step 1: Spectral Correlation Pattern in Rotated Ordination Space Configurations

Spectral wavelength specific responses to score vectors were visualized along 180° ordination axes rotation for field and image spectra, respectively (Figure III-4). The coefficients of determination (R^2) show distinct variations along band numbers in dependency on rotation angle. For every predictor set A - C regions with high R^2can be detected as possible spectral feature groups. In general, the correlation of field spectra with different gradients is stronger compared to image spectra. Regions with high R^2 are located at similar spectral areas with slight differences in feature density comparing field and image spectra for reflectance (set A) and continuum removal (set B). Reflectance spectra are correlated over a broad range between 40° and 110° whereas R^2 maxima can be achieved for the short wave infrared (SWIR). Spectral transformation, generally, enhanced spectral feature contrast. The feature distribution within these sets is more variable comprising higher incidence of deviation between field and image spectra, especially for derivative spectra. Continuum removed spectra (set B) show distinct spectral regions over the whole wavelength range (e.g. water absorption at 0.97, 1.20,

1.47 and 2.04 µm), mainly located between 45° and 90°. In contrast, wavelength features in derivative spectra (set C) occur in smaller isolated parts over the whole spectral range in varying gradient directions. Additional SWIR features particularly occur for floristic gradients above 110° using predictor sets B and C, with maximum correlation achieved in derivative spectra.

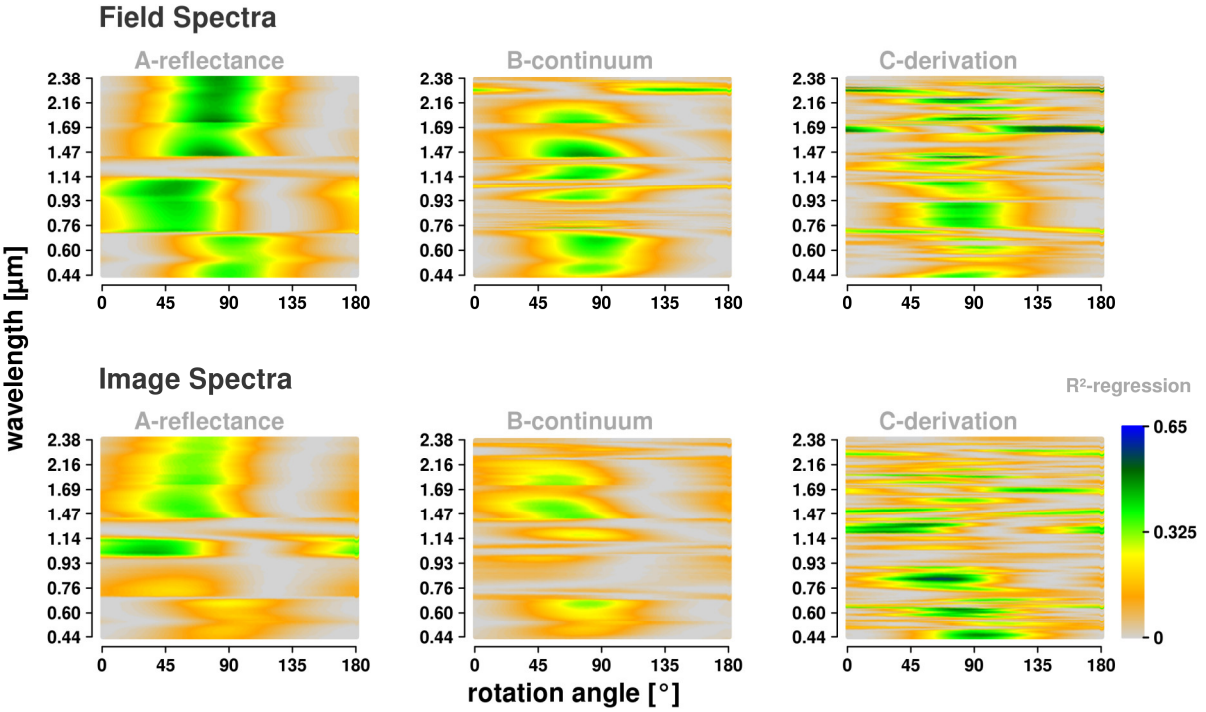

Figure III-4: *Field and Image spectra derivatives and wavelength dependent correlation (R^2) of spectral predictor sets A-C for NMS1 rotation around axes NMS3*

3.2 Step 2: PLSR Model Suitability Analysis

The model suitability ($PLSR_{suit}$) terms ($PLSR_{R^2}$, LV_{boot}, $VARR^2_{boot}$) were derived over all gradient directions on the basis of R^2 percentile classes (Figure III-5). Different response regions of single terms can be made visible in a rotation angle x percentile space. PLSR predictions on the basis of all spectral variables within selected feature groups ($PLSR_{R^2}$) reveal ordination space angles with high feature performances regarding gradient predictability. Therein, the explanatory power in PLSR is heterogeneously distributed depending on angle direction and percentile class. While the influence of included spectral variables around 85° for reflectance and continuum removed spectra and around 90° for derivative spectra is negligible, adjacent regions are limited to fewer variable inputs. This indicates a stronger potential of variable selection in these regions, except for a small correlation band at 145° in reflectance spectra. $PLSR_{R^2}$ typically reproduce single wavelength correlation (compare Figure III-4), whereas certain regions in the predictor set C (e.g. 110°) outperform single

feature R^2 in univariate regression. In general, $PLSR_{R^2}$ evaluated model performances are best in predictor set C. However, the number of latent vectors for R^2 saturation (LV_{boot}) and related R^2 variances ($VARR^2_{boot}$) in bootstrapped samples modifies initial $PLSR_{R^2}$ towards suitability regions ($PLSR_{suit}$)where stable PLSR models are expected (Figure III-6). Modification is mainly realized over an increased number of latent variables that is superimposed on high $PLSR_{R^2}$. Additionally, R^2 variance pattern reduce model suitability especially under the influence of a reduced set of spectral input variables (percentiles > 95%) that tend to overestimate explanatory power in small, isolated features. As a result, stable PLSR models are mostly distributed around 85° and 90° over a broad range of percentile classes. Additional suitable regions for specific variable compositions (percentile ranges) in different parts of the suitability surface can be detected for each predictor set.

The contribution of single spectral variables to stable PLSR models can be assessed by weighted predictor frequency over all feature groups (Figure III-6). Similar pattern as derived for rotated univariate regression R^2 (Section III-4.1) indicate the averaged influence of spectral features within the whole range of ecological gradients for NMS1 rotation. However, the comparison of spectral variable composition in percentile classes for field and image spectra (predictor match) reveals that there is still a need for model and gradient direction specific variable selection for the verification of spectral transferability characteristics. While variable composition in predictor sets A and B fit very well over a broad range of gradient directions, the spectral connection between set C is limited on only a view variables.

3.3 Step 3: Feature Selection

1) Rotation Angle Dependent Feature Occurrence: Spectral variables for optimal PLSR models can be derived in different gradient directions depending on suitability surface weights. There, a decomposition of overall predictor frequencies (Figure III-6), available for the entire ordination space, to distinct features for restricted ordination space regions can be made visible. Restricted ordination region were selected over the suitability extent optimization for NMS 1 rotation (Figure III-7). The best PLSR model regarding R^2 defines the final extent of a suitability surface. For every predictor set, 3 separate regions with maximum model suitability could be detected. According to initial surface extent and iteration number for best PLSR model fit, the final weighting area extent varies among percentile x rotation angle range.

The distribution of PLSR model suitability within the ordination space can be related to individual plant species gradients (see Figure III-2) and their correlation directions (Figure III-8). On the basis of changing species cover, the correlation to NMS1 axes scores varies as a function of the rotation angle.

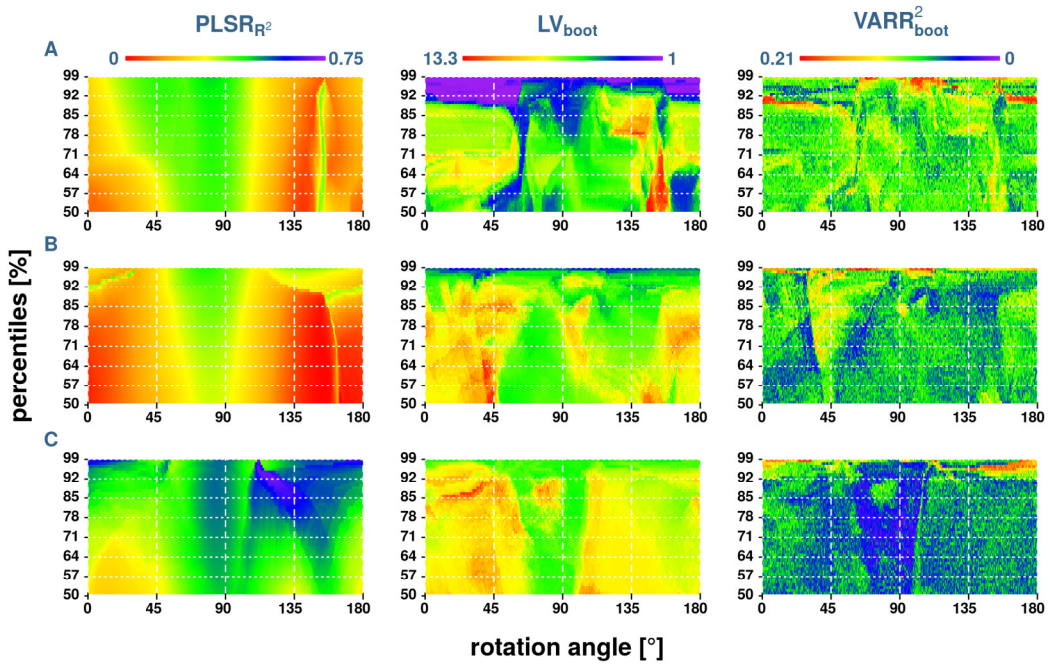

Figure III-5: *PLSR model suitability terms (PLSR$_{R^2}$, LV$_{boot}$, VARR$^2_{boot}$) in the rotation angle x R² percentile space for NMS1 rotation; color distribution correspond to feature groups of different spectral variable composition for predictor sets A (reflectance), B (continuum removal) and C (Savitzky- Golay derivation)*

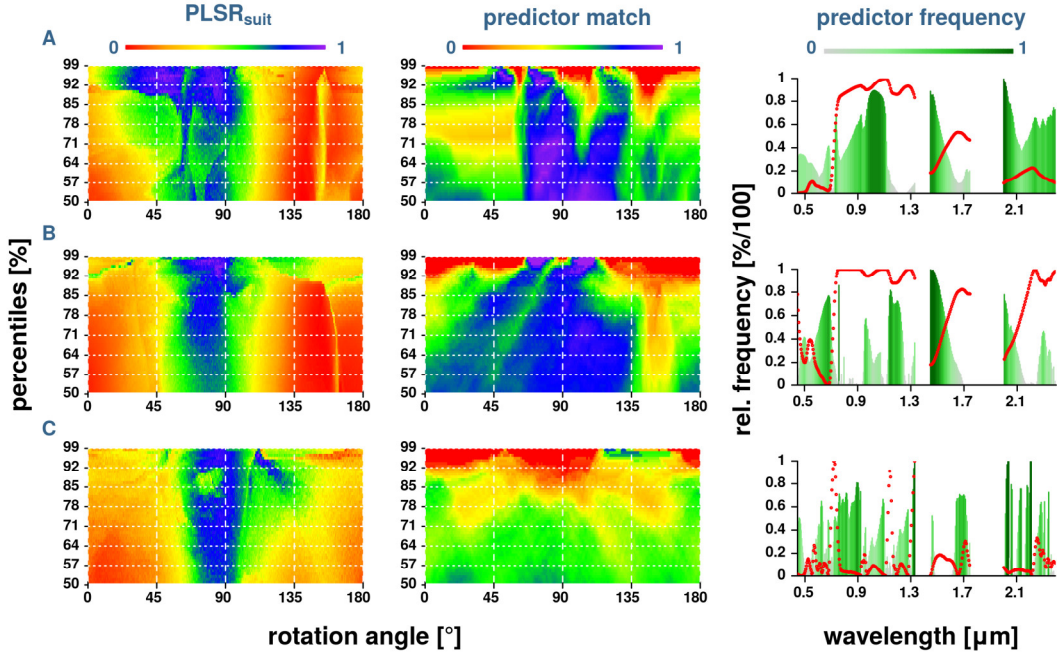

Figure III-6: *PLSR model suitability surface (PLSR$_{suit}$) for predictor sets A (reflectance), B (continuum removal) and C (Savitzky- Golay derivation) after combing model terms in the rotation angle x R² percentile space for NMS1 rotation; predictor match expressed as the percent fit of spectral variables in the feature groups of image and field spectra; spectral variable frequency using PLSRsuit as weighting surface*

For the selected species with concentrated distribution pattern, unimodal R^2 maxima occur around 135° (*Calluna vulgaris*) and 85° (*Corynephorus canescens*). More transitional species gradients are determined by two maxima, whereas, the R^2 distribution is spread around 45° (Festuca ovina agg., Calamagrostis epigejos) or below 45° and above 135° (*Agrostis capillaris*).

Every suitability region produces different spectral features, where sensitive spectral wavelengths are cumulated (Figure III-9). Thereby, feature variation occurs in response to different species and/or environmental gradients as well as a consequence of spectral transformation technique. First PLSR model for reflectance spectra is clearly determined by an absorption feature around 1.0 µm comprising water absorption and additional biophysical parameter (Thenkabail et al., 2013) at 1.07 µm. Water absorption at 1.5 and 2.05 µm overlaid with lignin and cellulose features in the SWIR-2 spectral region are most influencing variables for optimal PLSR model at 85° angle direction. Within a narrow gradient direction around 145°, stable models can be derived on the basis of NIR water absorption bands, green peak reflection and red edge inflection point.

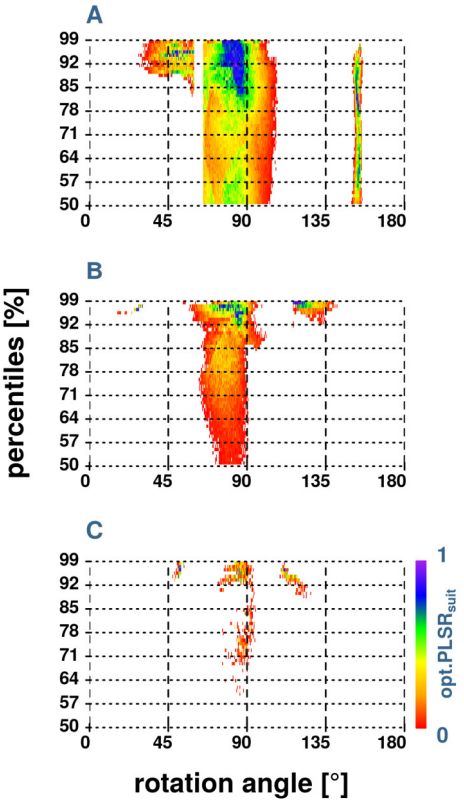

Figure III-7: *Optimized PLSR model suitability surfaces for NMS1 rotation; regions are selected on the basis of PLS R^2 maximization testing different spectral variable compositions in percentile classes*

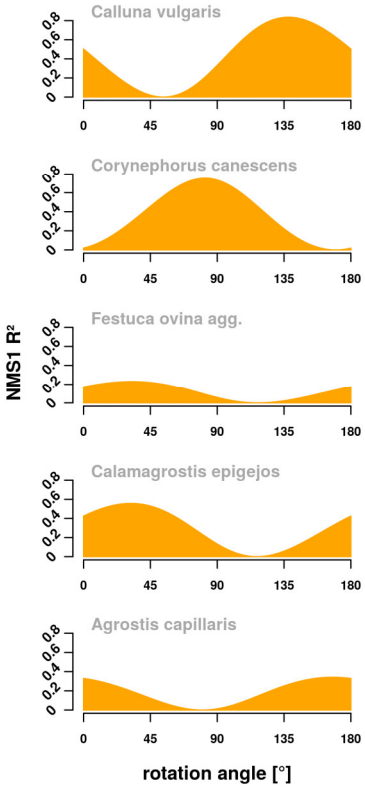

Figure III-8: *Correlation structure of major indicator species along NMS 1 axis rotation; Correlation maxima indicate the applicability of spectral feature selection to predict species abundance gradients*

Stable PLSR models for continuum removed spectra (set B) could again be derived for 85°. Therein, water absorption 1.5 and 2.05 µm equals selected reflectance features. Furthermore, NIR water bands and chlorophyll a & b absorption are additionally weighted for best PLSR selection. Models for 25° and 130° gradient directions are mainly based on an absorption feature at 2.30 µm. In general, features are clearly separated to distinct spectral regions. In comparison to Savitzky-Golay derivatives (set C), features are broader and less in number. For the 90° angle, predictor set C shares water absorption (1.35, 2.05 µm) and a lignin/cellulose (2.2 µm) feature with corresponding models of predictor sets A and B. Additional features are distributed over the whole spectrum with varying frequencies, whereas NIR plateaus between water absorption bands are preferentially identified. The red edge inflection point, known as an important vegetation characteristic for derivative spectra was only selected for the 48° gradient among other narrow features. A broad band feature around 2.35 µm occurs due to strong correlation at 120°. The resulting spectral variable weights for related angle directions could be used to predict extracted species abundance correlation depending on the predictor set.

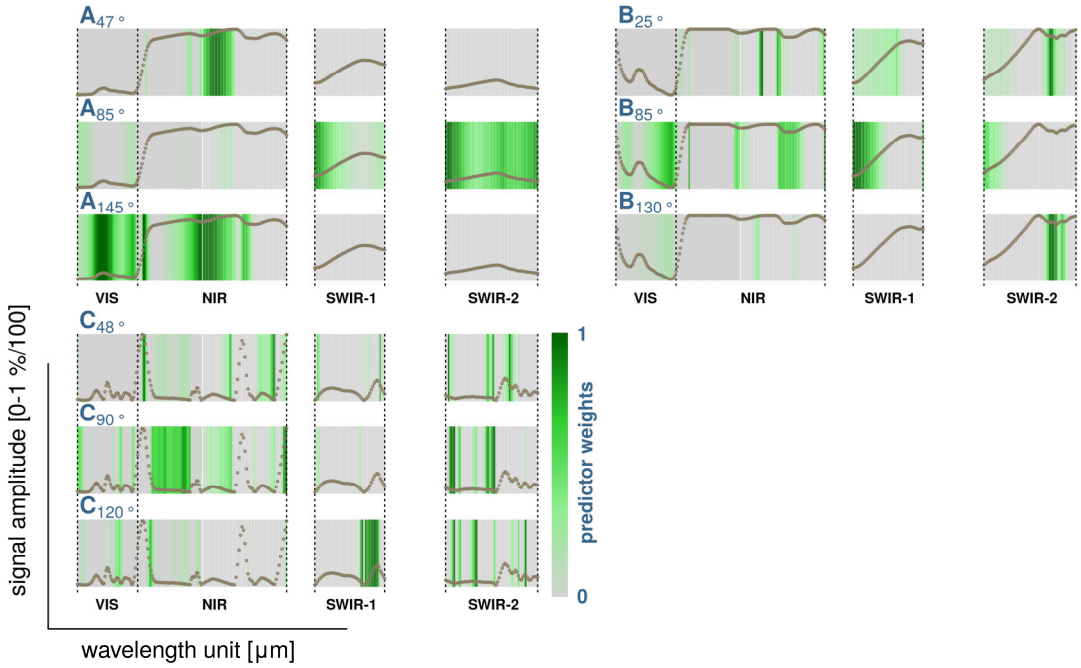

Figure III-9: *Spectral variable weights in NMS1 rotation for the 3 different PLSR suitability regions using spectral predictor sets (A-C); rotation angles for suitability regions are ordered ascendingly (0-180°) visualized in wavelength blocks*

Table III-1: *PLSR models for predictor sets A (reflectance), B (continuum removal) and C (Savitzky- Golay derivation) after optimization using weighted spectral variables within the 3 different PLSR suitability regions; nLV: number of latent vectors, nP: number of selected predictors, Icor: correlation of frequency weights with image spectra; green-selection of optimal PLSR model used for spatial mapping*

	nLV	nP	R^2	RMSE [%]	Icor
NMS1					
A	1	8	0.40	17.69	0.86
	3	7	0.59	18.30	0.94
	3	42	0.57	21.17	0.56
B	3	12	0.53	16.88	0.27
	3	98	0.61	17.83	0.85
	3	52	0.47	22.27	0.20
C	2	10	0.57	14.92	0.28
	1	4	0.51	21.22	0.35
	3	24	0.74	15.59	0.37
NMS2					
A	3	71	0.57	20.44	0.95
	3	74	0.56	20.22	0.88
B	1	6	0.33	24.32	0.93
	3	13	0.57	19.94	0.86
C	1	10	0.53	21.16	0.41
	1	5	0.52	21.03	0.39

2) PLSR Model Transferability: For selected PLSR suitability regions (Figure III-7), corresponding PLSR models were calculated performing optimization for variable selection within detected spectral features (Table III-1). In every predictor set the optimal PLSR model (according R^2) was selected for spatial mapping purpose (Figure III-10). In predictor sets A & B best PLSR models could be derived for the central gradient around 85°. While the reflectance model (set A) is determined by few SWIR features, the continuum model (set B) is based on a broad range of absorption over the complete spectrum (Figure III-10). The overall frequency weight distribution of both sets is highly correlated to gradient features from corresponding image pixels (Table III-1 Icor). Selected spectral variables for final PLSR models are located at matching position on high frequency weights (red dots Fig. 10). In contrast, best PLSR model for predictor set C is based on mainly one unique feature in the SWIR-1 region. Due to additional narrow band features that appear over the whole spectrum, overall correlation to weighted spectral variables in image spectra (Icor Table III-1) is decreased. PLSR models for NMS2 rotation are less variable. In summary, their explanatory power is lower than NMS1 axes models. Selected features are mainly located at spectral region that are comparable to NMS1 rotation at 85° with slight variations. Likewise, image feature correlation is maximized in predictor sets A and B. In general, PLSR models after

optimization show higher performance than univariate wavelength correlations, with predictor set C achieve best performance.

Although overall feature stability is more evident for reflectance and continuum removed spectra, a $PLSR_{suit}$ selection during optimization can reduce initial spectral variables for derivative spectra (set C) to a meaningful variable set for prediction. The feature density as displayed in weighted frequencies (Figure III-10) is thereby focused to single variables on frequency maxima, which remain in the final models. Such variables often better reproduce feature location from field to image spectra. This can be proven with high accuracies achieved in external validation, applying selected spectral variables and derived PLSR models to corresponding image spectra (Table III-2). Derivative spectra significantly outperform reflectance and continuum removal in NMS1 rotation, owing to a reduced set of significant input feature variables; although overall frequency fit (Icor) is weaker. In contrast, accuracy for NMS2 score prediction is maximized for reflectance spectra. In general external transfer of field spectra calibrated PLSR models did not impair predictive accuracy.

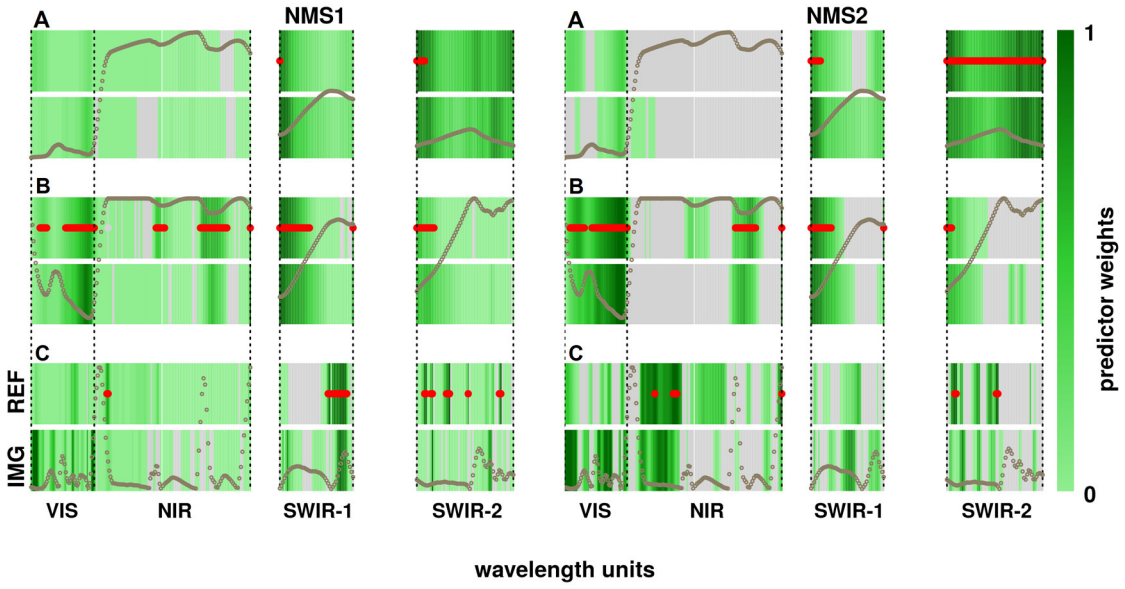

Figure III-10: *Spectral variable frequency weights in NMS1 and NMS2 rotation for best selected PLSR models in comparison to image spectra weights (REF - field spectra, IMG - image spectra) using spectral predictor sets (A-C); red points - selected spectral variables after optimization*

3.4 Gradient Mapping

The selected PLSR models for different ordination space directions are applied to image spectra. Each model generates different pattern of NMDS axes scores according to the input predictor variables and predicted rotation angle (Figure III-11). The spatial distribution of axes scores can be related to plant species abundance data from independent transect plots.

While reflectance and continuum spectra (set A, B) maximize *Corynephorus canescens* correlation at NMS1 85° rotation, derivative spectra (set C) produces variant score pattern by maximizing the prediction of *Calluna vulgaris* abundance at NMS1 120°. Sandy xeric grassland species are less explainable in selected gradient directions even though *Festuca ovina agg.* shows quite good correlation (R^2 = 0.50) using SWIR features from reflectance signatures. PLSR models for NMS2 rotation again maximize the predictive differentiation in the main transition between open pioneer grasslands-dwarf shrub heathland-sandy xeric grassland whereas a clear score vector shift can be observed for NMS2 171° rotation. In general, major differences in predicted ordination axes scores arise from axis rotation (see Figure III-11 NMS1 120° and NMS2 171°) that reveal additional floristic gradients from NMDS ordination.

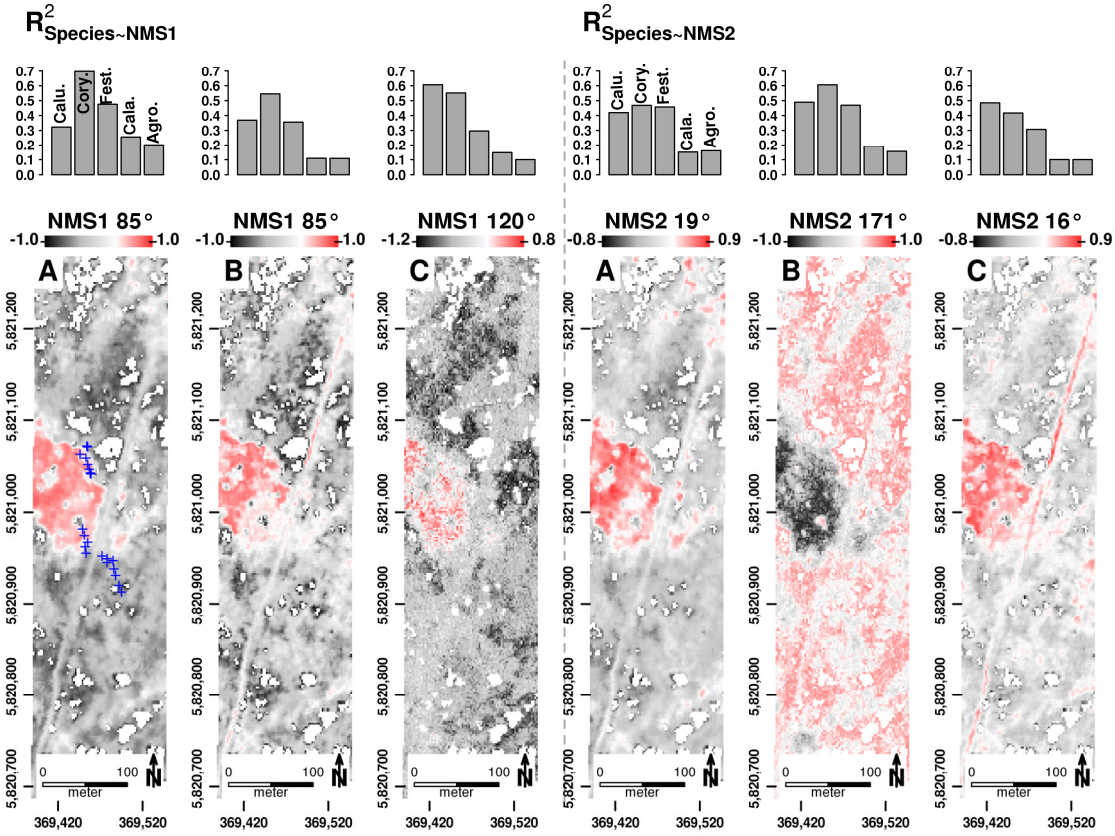

Figure III-11: *Spatial mapping of NMDS axes scores using selected PLSR models in varying rotation angles; Axis score-R^2 relation of the major indicator species derived from transect plant species surveys (blue crosses); Calu.-Calluna vulgaris, Cory.-Corynephorus canescens, Fest.-Festuca ovina agg., Cala.-Calamagrostis epigejos, Agro.-Agrostis capillaris*

Table III-2: *Accuracy assessment applying selected field spectra based PLSR models to image spectra for NMDS axes score prediction of sample plot ordination; Root Mean Squared Error and R² between NMDS ordination scores and predicted scores; corresponding scatterplots for observed (x-axis) against predicted (y-axis) score values*

	RMSE [%]	R^2	Scatter A	Scatter B	Scatter C
NMS1					
A	18.05	0.63	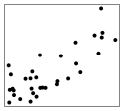	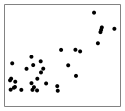	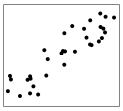
B	17.92	0.64			
C	13.25	0.81			
NMS2					
A	18.19	0.65	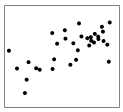	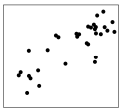	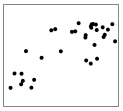
B	21.40	0.44			
C	20.05	0.58			

4 Discussion

The presented study demonstrated that a rotation of initial ordination score axes is capable of revealing additional gradient specific spectral responses. In particular, variance pattern on the first ordination axis preserve different ecological gradients that can be explained by distinct spectral features. It is important to keep in mind that NMDS ordination does not maximize floristic variance at ordination axes. In fact it should be considered as "species composition restoration" (De'ath, 1999). As a consequence, axis rotation does not violate methodological assumptions for species projection. It is rather an opportunity to reveal external gradients that influences species replacement in sample gradients. Hence, spectral gradient analysis for mapping purpose can have a high potential in explaining processes gradually affecting species composition (e.g. cover, fitness) as demonstrated in a few studies (Kooistra et al., 2004; Smith et al., 2004). On that account, we primary developed a methodology for selecting an optimal set of spectral features for the prediction of gradients in a rotated ordination space. Further research effort is needed for a clear semantic determination of such abstract gradients in order to understand the link between spectra, plant species and environmental factors. In our investigation second NMDS axes provided less variation in gradients shown by minor feature shift in axes rotation. A relatively small floristic heterogeneity within the complexes of Gray hairgrass - Calluna heath - Sandy xeric grass on slightly varying soil substrate are limiting structural variance pattern in ordination result. Feature selection in NMS2 rotation led to PLSR models with decreased explanatory power, although main gradients are well described by correlated spectral variables. This behavior is also evident in comparable studies (Feilhauer et al., 2011; Schmidtlein et al., 2007). However, this cannot be considered as a general

behavior of NMDS ordination. Plant diversity and environmental factor richness are also proved in higher dimensions (Kahmen et al., 2005) implicating appropriate spectral response. Further dimension inclusion (3 + n dimensional NMDS ordination) combined with multiple axes regression on external factors are suggest in order to retrieve differentiated plot configurations.

It is interesting to note that the floristic composition as reflected in species abundance shift can be assigned to selected suitability regions for different ordination space directions. Therein, selected spectral features for stable PLSR models can be used to describe plant species correlation along distinct floristic gradients (compare Figure III-7, 8, 9, 11). However, a direct transfer to spatial plant species abundance mapping needs to be supported by additional information about the abiotic background and structural canopy characteristics. An evaluation of spectral feature locations in different transformation techniques provides a first hint on separating single species gradients from background signals. Recent studies often aggregate such information over a broad range of vegetation characteristics using empirical relations between leaf chemical parameter and canopy derived spectral variables e.g. chlorophyll (Jago et al., 1999), nitrogen (Townsend et al., 2003), water (Clevers et al., 2008) concentration. Only few studies have already shown the potential of one dimensional species responses to spectral proxies e.g. vigor gradients (Artigas and Yang, 2005) or to abiotic predictor variables (Evans and Cushman, 2009). The approach introduced in this study, allows for a more detailed description and differentiation of floristic pattern and related environmental gradients in a multi-species environment that is often affected by ecological processes at different complexity levels. On the basis of ordination, multiple predictions for different gradients can be made possible. The potential of spatial mapping can directly be assessed via PLSR suitability surfaces in NMDS ordination. An appropriate feature selection as introduced in the optimization procedure can further help to assess the applicability of different spectral transformation techniques used in an optimal PLSR model for spatial prediction purpose.

The investigation of different spectral transformation techniques for feature occurrence revealed differences in shape and location for gradient specific spectral feature distribution. While reflectance and continuum spectra occupy broadly connected regions, derivative features are narrow and much in number. For similar gradient directions different feature locations with significant influence on stable PLSR models could be detected. Thereby, small band information can provide strong features for PLSR modelling which additionally indicates a high potential of pre-selected absorption features (vegetation indices, distinct band depth normalization) for gradient predictions (Kokaly and Clark, 1999; Mutanga and Skidmore, 2003). On the other hand transferring feature location becomes complicated for increased spectral variances that are often characteristic for heterogeneous image pixels.

Additional features may occur in pixel representations due to plant stress, phenology shift or vegetation structure changes (e.g. life-form, canopy height, litter, senescence). Possible causes are a) inappropriate pixel size for floristic variability reproduction, b) spatial non-stationarity effects or c) time gaps between spectral sampling and overflight (Feilhauer and Schmidtlein, 2011; Rocchini et al., 2013). In consequence, gradient specific spectral features can be weakened or even shifted for pixel sizes that are not capable of resolving the spatial variance of plant species. In Fig. 4 such effects are made visible through shifts in correlation maxima in distinct wavelength regions between field and image spectra. A significant increase in model transferability can be achieved when multiple features are reduced to few spectral variables via the optimization procedure introduced here. Despite the irregular distribution of selected features among different spectral transformations, optimized $PLSR_{suit}$ selected features are reproducible from field to image spectra to a great extent. This is especially applicable using hyperspectral reflectance signatures that provide broad range wavelength regions in small spectral sampling units. Spectral samples can systematically be tested on stable feature combinations in a predictive PLSR framework using proposed bootstrapped testing. As shown in (Kokaly and Clark, 1999), predictive features were not necessarily related to center wavelengths. However, except for edges at 0.45 and 0.65 µm, selected wavelengths are located at expected chemical bonds in foliage material (Curran, 1989).

Our investigation has indicated that a PLSR based modeling of plant characteristics in a vegetation continuum is further variable in gradient direction for best model selection. As a function of spectral transformation different directions are more or less sensitive to spectral characteristics. By now only little research effort was made in order to understand observed variations of feature location in different spectral transformation. Recent comparative studies support our findings in foliage chemical constituent prediction (Huang et al., 2004; Shi et al., 2003). Commonly, spectral transformation in vegetation mapping is based on (pre-) testing of model performance in the statistical framework that was chosen for a specific application (Cho et al., 2007). Physical based evidence of feature location is often relegated to the background. In our investigation we offer a first step towards a combined method for model performance estimation and feature characterization in the field of gradient mapping that has not yet been carried out. Depending on ordination space angles, a distinct region extent is iteratively detected and allocated feature variables are selected on the basis of predictive accuracy and stability parameters in PLSR model calibration. The resulting PLSR model performances (Table III-2) are comparable to NMDS axes models using more or less similar species inventories from a heathland area (Feilhauer et al., 2011), bearing in mind that common gradient mapping approaches are exclusively based on image spectra not on field spectra like in this study.

Furthermore, it must be considered that there is a generalization effect in ordination when no adequate projection of additional plant parameter can be realized on gradient axes. To minimize external prediction errors for hyperspectral vegetation mapping, comprehensive spectral information of different plant states over the complete growing season are needed to cover near overflight conditions. For that purpose existing spectral libraries (Bojinski et al., 2003; "SPECTATION," 2015; Zomer et al., 2009) should continuously be extended by hyperspectral signatures. In this context, hyperspectral cameras mounted on Unmanned Aerial Vehicles (UAV) offer a great potential in flexible collection of spatially high resolved vegetation spectra as shown in e.g. (Calderón et al., 2013; Zarco-Tejada et al., 2013). In addition, recent developments in hyperspectral satellite sensor technology e.g. EnMAP (Guanter et al., 2015) or HyspIRI (Abrams and Hook, 2013) will allow for a better representation of vegetation dynamics in large areas and small time intervals. However, effective spectral feature characterization algorithms are needed in particular, when spectral library information is transferred to these rather coarse spatial pixel sizes (30 m).

5 Conclusions

Within this study we showed that an axes rotation in NMDS ordination is capable of extracting spectral responses for different floristic gradients. Depending on rotation angles, spectral variables form distinct features according their correlation to floristic composition in the ordination space. We introduced a new PLSR feature selection procedure that incorporates model stability and predictive accuracy assessment in spectral bootstrap samples over the complete 180° gradient space. It can be used to enable selective testing of gradient directions and PLSR model performance evaluation, simultaneously. The proposed approach is seen as a contribution in understanding physically based feature sensitivity under spectral and spatial sensor constrains, especially in a complex species environment. Our results make clear that an ideal feature composition for the description of a specific floristic gradient cannot be found in a 1-dimensional correlation structure in ordination. A 2-dimensional weighting scheme taking into account the ordination space angle and feature variance, did in fact explain single gradients with the highest PLSR model accuracy. Therein, selected features are stable from field to image spectra to a large extent which indicates a good transferability for spatial mapping purpose. The method developed will enable a deeper understanding of the relations of foliage chemistry and floristic gradients via spectral response evaluations. Thus, the derivation of surface characteristics from plant species spectra, especially in UAV or satellite (Environmental Mapping and Analysis Program - EnMAP) based hyperspectral imagery show great potential for the determination of ecological processes that influence species diversity.

Acknowledgments

We would like to thank Dr. Angela Lausch and Dr. Daniel Doktor (The Helmholtz Centre for Environmental Research - UFZ) for providing the imaging spectrometer AISA DUAL, organizing the overflight campaign and giving technical and scientific input for an optimal calibration of reflectance data. The mapping of plant species was conducted by Gabriele Weiss (ecostrat GmbH) with the aid of student field worker Josefine Wenzel. Special thanks to Gabriele Weiss for extensive manuscript review. Our thanks also go to all student field workers that were involved in spectroradiometer measurements during the summer months. We are also grateful to Elisabeth Kuehl, Joerg Fuerstenow and Peter Nitschke (Sielmanns Naturlandschaften) for enabling a secure and permanent field plot access. This work was funded by the Deutsche Bundesstiftung Umwelt (DBU) and the Environmental Mapping and Analysis Program (EnMAP).

Chapter IV: Determination of Calibration Performances and Spatial Mapping

This is the accepted version after peer review (Postprint) of the following article:

Neumann, C., Itzerott, S., Weiss, G., Kleinschmit, B., Schmidtlein, S. (2016). Mapping multiple plant species abundance patterns - A multiobjective optimization procedure for combining reflectance spectroscopy and species ordination. Ecological Informatics, 36, pp. 61 - 76.

DOI: 10.1016/j.ecoinf.2016.10.002
Received: 04 August 2016 / Accepted: 11 October 2016 / Published: 19 October 2016

Abstract

Nature conservation and ecological restoration crucially depends on the knowledge about spatial patterns of plant species that control habitat conversion and disturbance regimes. Especially, species abundances are capable of indicating early development tendencies for setting habitat management strategies. This study demonstrates the transfer of field spectroscopy to hyperspectral imagery to map multiple plant species abundances in an open dryland area using two imaging spectrometers in two different phenological phases. We show that species abundances can partially be described by multiple gradients forming different coordinates in a contour map. For this purpose, species abundances were projected into an ordination space using non-metric multidimensional scaling and subsequent spatial interpolation. It was demonstrated that different gradients can be modeled in a Partial Least Squares regression framework resulting in distinct spectral features for certain gradient directions. We combine both objectives in a multiobjective NSGA-II procedure to maximize the quantitative determination of species abundance in ordination and spectral predictability in related field spectra, simultaneously. NSGA-II was finally used to select optimal spectral models for n = 35 single species that were transferred to hyperspectral imagery for mapping purpose. We can show that abundance predictabilities can be evaluated on the basis of individual model performances that hold different spectral features for each species in a designated phenological phase. Finally, we present spatially explicit multi-species maps for the best n = 18 and abundance maps for n = 8 models that could be linked to patterns of species richness, coexistence, succession stages and habitat type conditions.

1 Introduction

Recent advances in sensor technology open up new possibilities from plant community towards distinct plant species mapping. It has been recognized that spatially explicit information on the distribution of plant species serve as important indicators for an estimation of ecosystem functions such as habitat suitability (Ustin and Gamon, 2010) and thus lead to a refined understanding of ecosystem processes (He et al., 2015a; Maestre et al., 2012; Pasari et al., 2013). Especially nature conservation and restoration is based on monitoring and sustainable management systems that implement indicator and target species as habitat assessment parameter (M. Bock et al., 2005; Corbane et al., 2015; Fancy et al., 2009). Thereby, single plant species discrimination is facilitated by imaging spectrometers as they provide dense spectral information that can be related to distinct features of leaf biochemistry, anatomy and physiology (Asner, 1998; Gates et al., 1965; Ollinger, 2011). Several studies have shown the potential of hyperspectral classification algorithms for the identification of tree species (e.g. Asner et al., 2008; Clark et al., 2005; Cochrane, 2000; Feret and Asner,

2013), crop and crop-weed species (e.g. Borregaard et al., 2000; Rao et al., 2007; Thenkabail et al., 2013) and individual invasive species (e.g. Chance et al., 2016; Hamada et al., 2007; Lawrence et al., 2006; Pengra et al., 2007) whereas only a few studies exist for individual species detection in open grassland habitats (Day et al., 2006; Irisarri et al., 2009; Schmidt and Skidmore, 2001).

It is important to point out that different habitat types often co-occur in relatively complex multi-species environments. Transitions between types and hence habitat quality change is driven by continuous species shifts in varying compositions. Single species can contribute as favorable quality indicators or disturbance factors depending on their abundances in different plant communities. Thus, for an effective management and understanding of habitat conditions and their drivers, spatiotemporal patterns and dynamics of plant abundances in different habitat types are required to assess development tendencies of habitat conversion (Hodgson et al., 2011). However, quantitative plant species mapping between varying habitat types and transitions have not been sufficiently investigated so far. Currently, only a few studies have examined vegetation abundance mapping in categories such as percent green vegetative cover (McGwire, 2000) and plant functional types (Cole et al., 2014), at the level of tree species (Barbosa et al., 2016; Plourde et al., 2007) or for dominant stands of herbaceous plants (Lu et al., 2009; Parker Williams and Hunt, 2002; Underwood, 2003). Variances of plant species abundance patterns are thereby commonly mapped in fractional cover classes using spectral classification methods (Marvin et al., 2016; Underwood, 2003), spectral unmixing (Plourde et al., 2007) or linear regression (Cole et al., 2014; Lu et al., 2009). However, these studies are based on a few (2-4) pre-selected species or broader species categories. Imaging spectroscopy for mapping multiple species inventories has never been realized so far. Especially with regard to diversity measures, a more holistic approach, would effectively contribute to an advanced assessment of potentials and limitations in ecosystem mapping.

The particular challenge for multi-species mapping arises from an inherent complexity of interactions between plant traits and taxonomical integrity (Lausch et al., 2016). Regarding the concept of the individualistic continuum (Gleason, 1926), species are distributed according to an individual behavior that is controlled by the variation of inner-species interactions and external abiotic gradients. Hence, species abundance can only be modeled in a multifactor environment since spectral responses are affected by multiple species transition in different gradient directions. From an ecological point of view a solution was defined by the vegetation continuum concept (McIntosh, 1967) that is determined by species assemblage projections into the n-dimensional environmental space using abstract gradients (Austin, 1985). Plant species samples from floristic field surveys are therein arranged along different gradient directions that represent species composition shifts. These gradients can be understood as coordinate axes forming n-dimensional ordination spaces as a representation of

species sample similarities and transition induced by environmental factors. Thereby, non-variance maximizing methods such as non-metric multidimensional scaling (NMDS) (Kruskal, 1964) are interpretable as species composition restoration (De'ath, 1999) along ordination space axes. This approach is capable of representing floristic gradients with significant relations to habitat quality estimates that can further be related to hyperspectral reflectance signatures (Feilhauer et al., 2014; Neumann et al., 2015b; Schmidtlein et al., 2007).

Although the ecological community is well aware of spatial interpolation methods to quantify species abundances in an ordination space (Hauser and Mucina, 1991), the resulting multi-species variance patterns have not yet been systematically related to spectral features for spatial mapping purposes. This is particularly interesting with regard to the growing number of spectral libraries for vegetation (Bojinski et al., 2003; "SPECTATION," 2015; Zomer et al., 2009) that could be utilized to calibrate transferable models for new spaceborne imaging spectrometers such as Environmental Mapping and Analysis Program (EnMAP) (Kaufmann et al., 2008). At the present time there are only a few studies testing the transferability of spectral library data to image pixels for vegetation mapping (Siegmann et al., 2014; Thorp et al., 2013; Zomer et al., 2009). They make use of common classification approaches such as endmember mixture analysis or spectral angle mapper. At the moment there is no spectral feature transfer algorithm in a regression framework published. Thus, our study wants to investigate the relationship between species abundances and spectral responses over a habitat gradient that is projected as a vegetation continuum in an ordination space. We implement a multiobjective optimization procedure to answer the following research questions:

1) What proportion of species abundance can be explained by projected samples in an unconstrained NMDS ordination? Are there species abundance patterns that can be delineated by sample gradients in such an NMDS ordination?
2) Are there significant spectral features that can be related to abundance patterns in an NMDS ordination? Are these features stable and transferrable from field spectra to image predictions?
3) How persistent are derived abundance maps when applying spectral library based species models to different hyperspectral sensors in varying phenological phases?

For this purpose we analyze the species distribution in an open heathland area composed of different habitat types that are protected in the European Natura 2000 network. In this actively managed area it is important to know to what extent single species abundances can be spatially mapped as they provide crucial information on habitat conversion. The study is based on spectral and floristic field surveys as well as on two different hyperspectral imaging sensors. It will be shown how multi-species abundance patterns in an ordination can be related to spectral features solving a multi-objective genetic optimization procedure for spatial mapping purpose.

2 Material and Methods

2.1 Study Area and Floristic Field Survey

The study was conducted on a former military training area, Doeberitzer Heide, at 52° 30' latitude and 13° 03' longitude in the west of Berlin (Figure IV-1). The area is located in the North German Plain that was formed by glacial and periglacial erosion and deposition during the Pleistocene. Our study focus on open dryland plant communities that have become established on ground moraine deposits located at higher ground levels. These areas were intensively shaped by long-term military actions, which have lasted for over 100 years. In consequence, permanently open dryland habitats have arisen from tree removal, fires from bombardments, soil disruption and translocation. On sandy, acidic soil substrates that mostly exhibits thin organic topsoil layers, dwarf shrub heaths have established that are affected by nitrate eutrophication (*Calamagrostis capillaris*) and local base enrichment (e.g. *Galium verum, Peucedanum oreoselinum*). Following the end of military usage in 1991, the open training fields has left undisturbed. Since then, processes of natural succession, particularly, invasion by grasses and woody species mainly control dynamics of habitat conversion.

As of 2004 an active nature conservation management was implemented by the nature foundation Sielmanns Naturlandschaften gGmbH. Particular emphasis is placed on big mammals grazing such as European bison (*Bison bonasus*), wild horse (*Equus ferus przewalski*) and sheep flocks in conjunction with active tree removals for open dryland regeneration and establishment. Pioneer stages are artificially constructed by vegetation layer removal and soil profile disruptions using heavy vehicles. Heathlands are periodically mown, shrubs and young trees are cut and organic material is completely removed to minimize nutrient accumulation. As a result, multiple species transitions are generated leading to small-scale floristic mosaics and interpenetrations driven by various successional trajectories. Vegetation can be grouped to a main pioneer grassland (*Corynephorus canescens*) – sandy xeric grassland (*Festuca ovina agg.*) – heathland (*Calluna vulgaris*) complex that is interpenetrated by grass (e.g. *Agrostis capillaris, Calamagrostis epigejos*), herbs (e.g. *Rumex acetosella, Euphorbia cyparissias*), mosses and lichens (e.g. *Cladonia spec., Polytrichum piliferum*) and shrubs (e.g. *Populus tremula, Sarothamnus scoparius*). The main complex is designated to a Special Area of Conservation in which the Natura 2000 habitat types 2330 (Inland dunes with open Corynephorus and Agrostis grasslands), 6120 (Xeric sand calcareous grasslands) and 4030 (European dry heaths) are protected and forced to preserve their conservation status (Neumann et al., 2015b).

In summer 2011, floristic field samples were systematically collected for dominance stands and plant species in various typical transitions. The fractional percent cover of vascular plant species, mosses and lichens was mapped translating the enhanced Braun-Blanquet scale

(Reichelt and Wilmanns, 1973). Sample plot size was set to 1 square meter. For calibration purpose, 32 sample plots were located in different open dryland habitats distributed over the entire study area (Figure IV-1). The plot selection was based on expert knowledge to cover known species variability. A validation data set was acquired along 3 transect surveys comprising altogether 21 single square plots along typical transitions between habitat types. In total, 35 different plant species were mapped resulting in a 32 sites x 35 species matrix for further analysis.

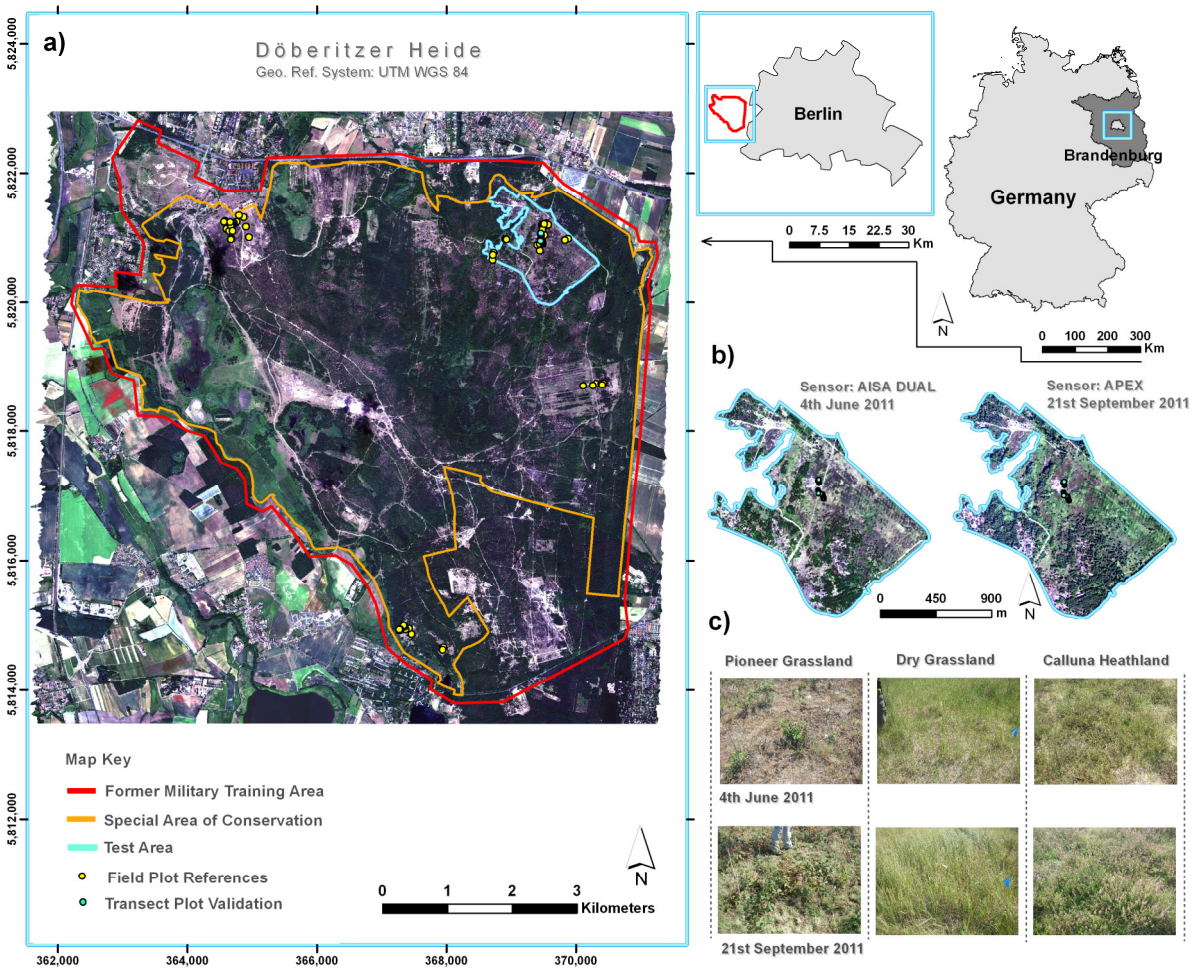

Figure IV-1: *a) location of study area and sample plot distribution; b) RGB-true-color composites of test area for AISA and APEX acquisition times; c) images of the three main plant communities in the two phenological phases during the spectral sampling period*

2.2 Hyperspectral Imagery

Hyperspectral imagery was recorded during two airborne overflight campaigns with two different sensors within different phenological phases. The first overflight was carried out between 10.00 and 12.30 UTC (Coordinated Universal Time) on 4th June 2011 using an AISA DUAL (UFZ Leipzig) imaging spectrometer ranging from visible to short wave

infrared (VIS - SWIR: 400 nm - 2500 nm) in 367 spectral bands. Flight stripes are relatively small covering 300 samples per scanning line. The second overflight was realized on the 21st of September with an APEX imaging spectrometer covering the same VIS-SWIR spectral range in 288 wavebands. Acquisition time was set between 08:27 and 09:12 UTC scanning 1000 samples per line. While AISA imagery represents dry conditions during midsummer, APEX was acquired after a warm-humid period in midautumn showing vital and grown vegetation stands.

Inner geometric rectification was performed on the basis of inertial measurement units on board of the airborne platforms, followed by an automated ground control point allocation (SIFT) (Lowe, 2004) and a subsequent coregistration. The final image mosaics were resampled to 2 m (AISA) and 2.5 m (APEX). At sensor radiance was derived from internal radiometric calibration coefficients accompanied by spectral binning, smear correction and destriping (ROME) (Rogaß et al., 2011). On that basis, a radiative transfer model (Atcor-4) (Richter and Schläpfer, 2002) was applied to retrieve top-of-canopy reflectance spectra. Additionally, spectral wavebands were corrected to overflight conditions using reference targets for empirical line calibration (Eli) (Smith and Milton, 1999). Reference targets, consisting of 3 dark and 3 bright transects of 25 single measurements that were collected with an ASD field spectroradiometer during overflight time. The first 10 AISA wavebands were removed due to observed non-linearity effects at the UV-VIS transition in Eli calibration. The initial number of wavebands was further reduced at atmospheric water absorption bands (1335-1449, 1749-1999 and > 2399 nm) resulting in n = 282 AISA and n = 237 APEX wavebands.

In order to obtain valid data for predictions within the calibration range of dryland communities, shadow and tree pixels were masked out applying principal component clustering on image pixels of the test area. Thereby, images of the first (brightness for shadow removal) and second (greenness for tree removal) principal component were clustered using hill-climbing unsupervised classification (Rubin, 1967). Tree and shadow classes were manually grouped to create the final mask.

2.3 Spectral Field Sampling

Spectral field samples were taken twice for all 32 vegetation sample plots in order to derive spectral models for the two sensors. The sample periods were restricted to the same phenological phases as indicated for the respective overflight time (Fig. 2). Measurements were conducted with an ASD spectroradiometer (ASD inc.) that collects relative reflectance spectra (VIS-SWIR: 350 nm – 2500 nm in 2151 wavebands) related to a white reference panel. The entire 1 m² sample plot area was sampled in 25 single measurements at 1.4 meter above vegetation canopy using an 8° foreoptic. Singe measurements were averaged for each

plot and resampled to sensor specific waveband response functions. The main atmospheric water bands were removed. On the basis of spectral absorption, figure 2 illustrates the phenological phase shift between the two sampling periods. APEX averaged spectra in midautumn is characterized by an increased pigment absorption at 450 nm and 650 nm and stronger water absorption in the SWIR region that indicates more vital vegetation stands in comparison to AISA acquisition time (compare Figure IV-1-c).

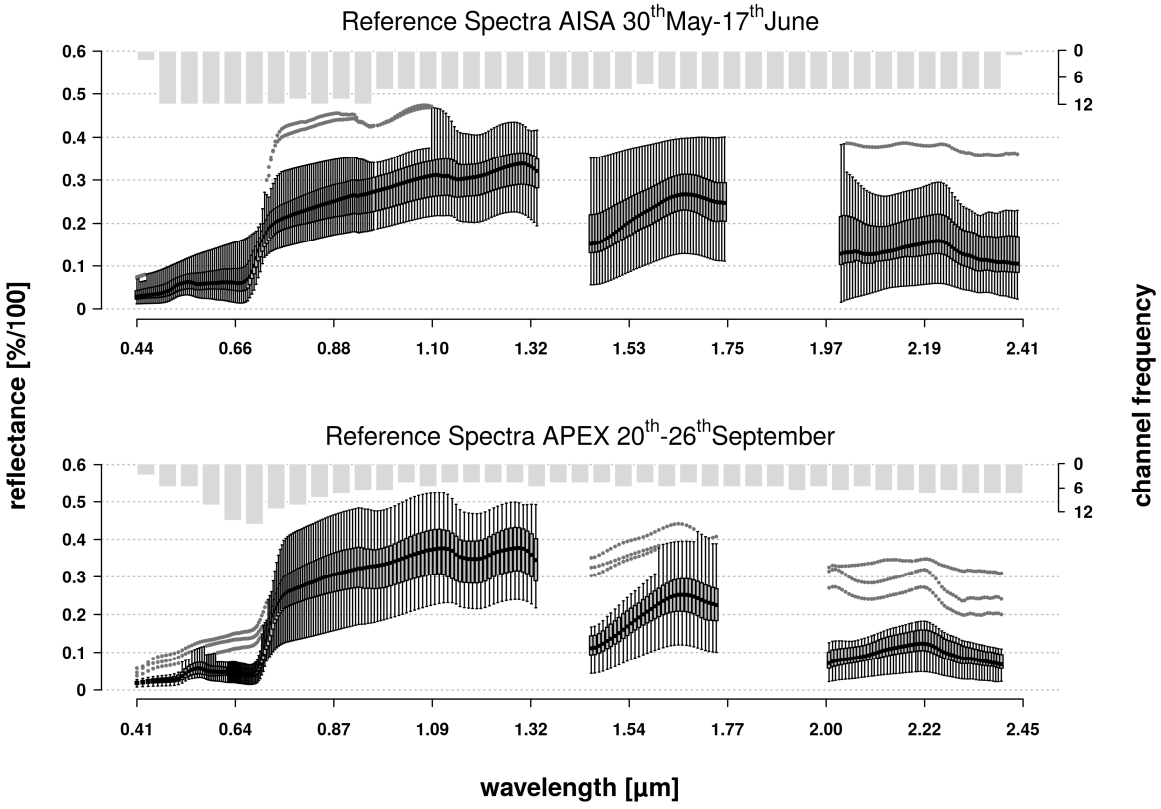

Figure IV-2: *Waveband specific box-whisker plots for n = 32 reference field spectra resampled to AISA and APEX spectral resolution; grey bars: absolute frequency of sensor waveband density*

2.4 Spectral Variables

Reflectance spectra from field measurements were transformed to narrowband vegetation indices and wavelength specific normalized absorption depths (Table IV-1). The distribution of indices and absorption bands was selected such as to represent information over the full spectral range. Known wavelengths for index calculation and shoulder definition for absorption features were extracted by taking the nearest waveband in the respective sensor domain. For band depth normalization a continuum removal was applied by linearly interpolating a convex hull between absorption shoulders (Clark et al., 1987). Subsequently, the original waveband reflectance was divided by the continuum line and finally normalized

over the area between the shoulders (Table IV-1) (Curran et al., 2001). In consequence, each absorption feature consists of normalized wavebands that characterize absorption depths in selected spectral regions. The final set of spectral variables, hence, was composed of single index values and normalized wavebands belonging to individual absorption features.

In PLS regression, results depends on the predictor variable scaling that is determined by their given ranges (variances) (Wold et al., 2001, 2002). Typically, different variable units cause different variable variances that determine their importance in explaining response vectors. In order to eliminate a priori variable importance weighting, predictors are typically auto-scaled by dividing them by their standard deviation (SD) and subtracting the variable mean (VM). As vegetation indices are not calculated in the same units, we applied an auto-scaling to standardize index variances to SD = 1. Absorption features are expressed in the same units but hold different wavelength importances regarding their explanatory power in the absorption center or at the absorption edge. A decrease in wavelength importance to the edge of known absorption wavebands was preserved by dividing each waveband SD by the maximum SD in the respective feature range. Thus, features were made comparable to vegetation index variances with maximum SD = 1 that decrease to SD = 0 at the edge of absorption.

2.5 Conceptual Framework of Modeling Approach

Plant species abundances from field surveys were initially stored into a sample x species matrix that was further translated to sample similarities which were then projected to an NMDS ordination space (Figure IV-3-1). On the basis of resulting score coordinates, for each species f different continuous 2-dimensional abundance contour grids were calculated in varying ordination space dimensions $a_{1\ldots n}$ and directions $z_{1\ldots n}$ by means of variography in a regression-Kriging framework (Hengl et al., 2007a; Neumann et al., 2015b; Odeh et al., 1995). Since different NMDS ordination space dimensions and directions provide different score coordinates due to varying sample arrangements, rotated and recombined score vectors could be used to set up correlations to spectral variables measured at sample plot locations (Figure IV-3-2). For each score axis suitable PLSR model regions were defined that hold significant and stable spectral features for sample gradient predictions (Neumann et al., 2016). In the final NSGA-II optimization each species was evaluated according the minimum distance to the optimal Pareto solution (utopia point) where spectral predictability as well as the fit of the abundance contour grid is maximized (Figure IV-3-3). The resulting modulation parameters were finally used to calibrate PLSR models with selected spectral variables and a related abundance grid that can be transferred to imagery for mapping purpose.

Table IV-1: *Spectral variables derived for species model calibration using reflectance bands with minimum distance to wavelengths R; spectral regions are grouped together according information provided by wavelength range*

Spectral region & formula	Designation	Abbr.	Reference
Plant Water Absorption			
$R900/R970$	Wetness Index	WI	Penuelas et al., 1997
$R857 - R1241/R857 + R1241$	Normalized Differenced Wetness Index	NDWI	Gao & Bo-cai, 1996
$R1094 - R1205/R1094 + R1205$	Normalized Differenced Wetness Index 2	NDWI2	Serrano et al., 2000
$R1650/R820$	Moisture Stress Index	MSI	Hunt et al., 1989
$R802 + R547/R1657 + R682$	Disease Water Stress Index	DSWI	Galvao et al., 2005
$R850 - R2218/R850 + R2218$	Leaf Water Content	LWC	Hunt et al., 1987
Chlorophyll Absorption			
$R850 - R710/R850 + R680$	Leaf Chlorophyll Index	LCI	Datt & Bisun, 1999
$3[(R700 - R670) - 0.2(R700 - R550)(R700/R670)]$	Transformed Chlorophyll Absorption Ratio	TCARI	Haboudane et al., 2002
$TCARI/(1 + 0.16)(R800 - R670)/(R800 + R670 + 0.16)$	Optimized Soil Adjusted Vegetation Index	OSAVI	Huete, 1988
$R780 - R710/R780 - R680$	Maccioni	Macci	Maccioni et al., 2001
$1.2(R700 - R550) - 1.5(R670 - R550)\sqrt{R700/R670}$	Triangular Chlorophyll Index	TCI	Hunt et al., 2011
$R754 - R709/R709 - R681$	MERIS Terrestrial Chlorophyll Index	MTCI	Dash & Curran, 2004
Pigment Absorption			
$R800 - R445/R800 - R680$	Structure Intensive Pigment Index	SIPI	Penuelas et al., 1995
$R531 - R570/R531 + R570$	Photochemical Reflectance Index	PRI	Penuelas et al., 1995
$1/R510 - 1/R550$	Chlorophyll Reflection Index	CRI	Gitelson et al., 2001
$1/R550 - 1/R700$	Anthocyanin Reflectance Index	ARI	Gitelson et al., 2001
$R680 - R500/R750$	Plant Senescence Reflectance Index	PSRI	Merzlyak et al., 1999
$\sum_{i=6\ 00}^{7\ 00} R_i / \sum_{j=5\ 00}^{6\ 00} R_j$	Red Green Ratio Index	RGRI	Gamon & Surfus, 1999
Cellulose Absorption			
$0.5(R2020 + R2220) - R2100$	Cellulose Absorption Index	CAI	Daughtrry et al., 1996
Lignin Absorption			
$\left[\begin{matrix} log(1/R1754) - \\ log(1/R1680) \end{matrix}\right] / \left[\begin{matrix} log(1/R1754) + \\ log(1/R1680) \end{matrix}\right]$	Normalized Difference Lignin Index	NDLI	Serrano et al., 2002
Nitrogen Absorption			
$\left[\begin{matrix} log(1/R1510) - \\ log(1/R1680) \end{matrix}\right] / \left[\begin{matrix} log(1/R1510) + \\ log(1/R1680) \end{matrix}\right]$	Normalized Difference Nitrogen Index	NDNI	Serrano et al., 2002
$R1510 - R660/R1510 + R660$	Normalized Difference 1510 Ratio	NRI15	Herrmann eta al., 2010
$R700 + 40\left[\left((R670 + R780/2) - R700\right)/R740 - R700\right]$	Red Edge Inflection Point	REIP	Vogelmann et al., 1993
Band Depth Normalized Absorption Features			
$R_i' = R_{i\ [refelctance]}/R_{i\ [conex\ hull]}$ $for\ R_i \ldots R_n$	R 408 … R 518	P1	Mutanga & Skidmore, 2003
	R 550 … R 750	P2	
	R 920 … R 1000	W1	
	R 1116 … R 1284	W2	
$(1 - R_i/R_i')/\int_{R_i}^{R_n} R_{i..n\ [convex\ hull]}$	R 1634 … R 1786	C1	Kokaly & Clark, 1999
	R 2006 … R 2196	C2	
	R 2222 … R 2378	C3	

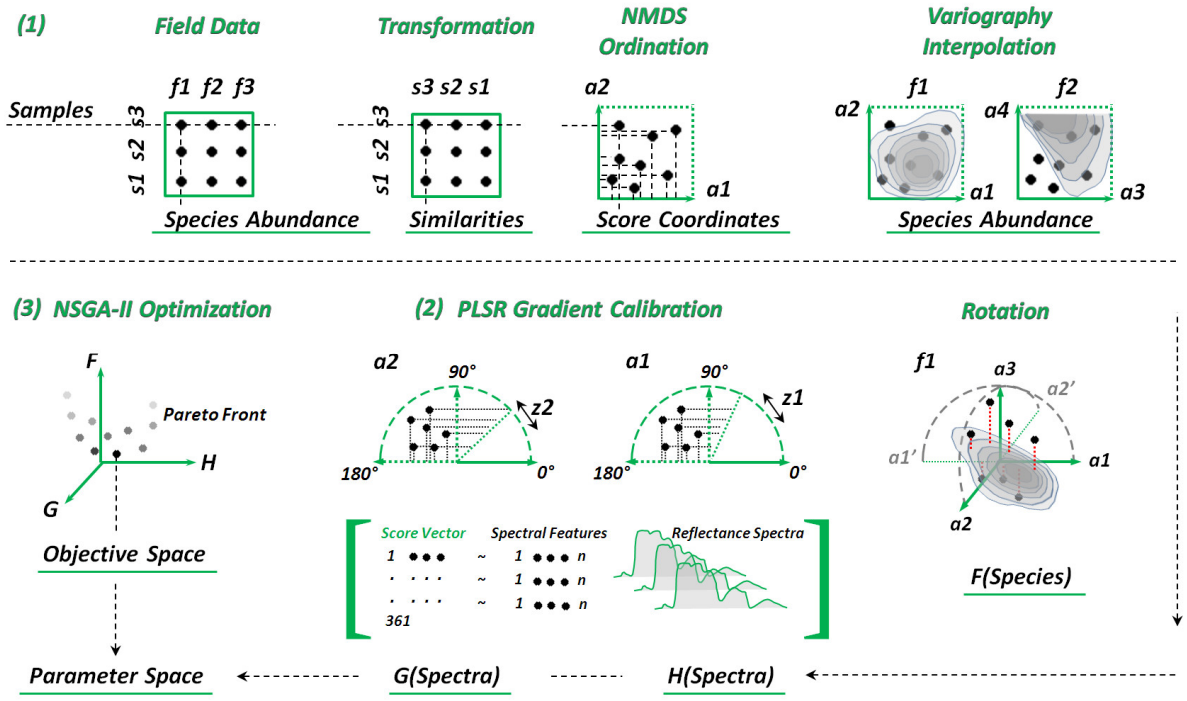

Figure IV-3: *Conceptual model framework comprising the method workflow: (1) plant species abundance modelling in NMDS ordination, (2) PLSR feature selection from field spectral variables, (3) multiobjective NSGA-II procedure to optimize parameters for the spectral prediction of species abundances*

2.6 Species Abundance Variance in NMDS Ordination

According to the individualistic hypothesis (Gleason, 1926), single species abundances from field surveys were transferred from the initial sample x species matrix into a gradient space. On the basis of varying abundance patterns, the similarity between field samples was calculated using the Bray-Curtis distance measure (Clarke and Warwick, 2001). The resulting similarity matrix; the greater the distance, the lower the similarity; was used as a criterion for projecting field samples into an ordination space. For this purpose, we applied non-metric multidimensional scaling procedure that relocates samples until the deviation between original similarities and the similarity of ordination space sample configuration is minimized (Kruskal, 1964). The best solution supplied 11 ordination space axes that define the new sample coordinates on the basis of ordination axis scores.

Therein, each sample point is determined by a characteristic species composition and related abundance values. Hence, abundances are distributed as point patterns (spatial random variable) in the NMDS ordination space. For an individual species, the abundance distribution was thus modeled as a contour map on a grid that was spanned between different score axes combinations in varying directions (Neumann et al., 2015b). We can consequently define an

objective function F that examines the deviation between sample abundances and abundances predicted for the contour grid for different rotations z_x, z_y of two ordination axes a_x and a_y:

$$\mathbf{F}(a_x, a_y, z_x, z_y) = R_T^2 + \left[(1 - R_T^2) \times \left[\mathrm{R}_\mathrm{V}^2 - \left(\mathrm{R}_\mathrm{V}^2 \times \frac{\mathbf{c_0}}{\mathbf{c}}\right)\right]\right]$$

It can be solved over two variance terms that model (a) the bivariate linear trend of abundance patterns in a two dimensional ordination space representation:

$$R_T^2(a_x, a_y, z_x, z_y) = 1 - \frac{\sum_i (p_i - f_i)^2}{\sum_i (p_i - \overline{p})^2}$$

In this case, for the observed abundance $p_1 \ldots p_n$ with mean: $\overline{p} = \frac{1}{n}\sum_{i=1}^{n} p_i$ a trend surface model was fitted: $f = \beta_x a_x(z_x) + \beta_y a_y(z_y) + \varepsilon$ using different rotation angles $z_{x,y} \in [1 \ldots 180]$ of available ordination space axes $a_{x,y} \in [1 \ldots 11]$ in a linear regression framework with regression coefficients $\beta_{x,y}$ and an error term ε. The proportion of variance $(1 - R_T^2)$ that cannot be explained by the regression plane $\mathbf{f}$ was modeled in a second variance term (b) that approximates the spatial configuration of the residuals ε:

$$R_V^2(a_x, a_y, z_x, z_y) = 1 - \frac{\sum_i (\gamma_i - f_i)^2}{\sum_i (\gamma_i - \overline{\gamma})^2}$$

Therein, the spatial variance of regression residuals ε can be described on the basis of their locations u in different distance classes h wich results in empirical semivariances $\gamma_1 \ldots \gamma_n$ with mean: $\overline{\gamma} = \frac{1}{n}\sum_{i=1}^{n} \gamma_i$ according: $\boldsymbol{\gamma}(\mathbf{h}) = \frac{1}{2n(h)}\sum_{i=1}^{n(h)}[\varepsilon(u_i) - (\varepsilon(u_i + h)]^2$. In order to model the error distribution, 19 different variogram models were fitted against the empirical simivariances $\boldsymbol{\gamma}(\mathbf{h})$ and the model with minimal sum of squared error was selected for calculating the variance function f (Hiemstra et al., 2009; Pebesma, 2004). Since there may be variance effects at small distances that cannot be explained by the variogram model, this so called nugget effect $\mathbf{c_0/c}$ had to be removed from the explainable error variance. The modeled residual distribution is based on the ordination axes and rotation that are inherited by the trend surface model. In consequence, the parameter space to be estimated for the first objective function consisted of the chosen ordination space axes number (a_x, a_y) and a preferred direction of rotation (z_x, z_y).

2.7 PLSR Suitability Surface Selection

In an NMDS ordination space, the sample configuration is determined by score axes coordinates. Score axes in an NMDS result can be rotated in a way such as different rotation angles reflect different sample gradients. Each rotation angle thereby points towards a specific gradient direction that can be described by score coordinate vectors of the samples. These score vectors were related to the spectral variables collected for the samples in the field. It

was now assumed that species replacement and abundance variations along sample gradients of different rotation angles can be assigned to specific spectral features. In Neumann et al., 2016 it was shown that different gradients in rotated NMDS ordination spaces can be modeled by PLSR based spectral predictor selection in combination with predictive accuracy and stability evaluation. Our second objective function was thus defined in a modified PLS regression framework in order to model sample gradients using optimal spectral predictors. For the purpose of generating the NMDS coordinate system for the final 2-dimensional contour grid of abundance distribution (see section 3.2), PLSR was applied to two ordination axes a_x, a_y and respective directions z_x, z_y, separately. This results in two objective functions G_x and H_y predicting a 2-dimensional representation of abundance gradients as calculated in the objective F. The PLS regression for gradient x was defined in G_x:

$$\boldsymbol{G(a_x, z_x, w_x t_x) = y = XWq + \varepsilon}$$

The case presented here refers to a coordinate vector **y** that is predicted by **X** = sample × spectral predictor matrix, **W** = weights for X-scores to project latent variables **T = XW**, **q** = loading vector for response decomposition, that is estimated by regressing **T** against **y** according to $\boldsymbol{y = Tq + f}$, **f** = residuals between observed and modelled response (Höskuldsson, 1988; Wold et al., 2001). A crucial factor is the selection of significant spectral features in X that a) maximize PLSR explanatory power and b) minimize model complexity to prevent overfitting. For this purpose, a model suitability term $PLSR_{suit}$ was introduced by Neumann et al., 2016:

$$\boldsymbol{PLSR_{suit}(a_x, z_x) = [PLSR_{R^2}]_{sv} \times [-T_{boot}]_{sv} - [VARR^2_{boot}]_{sv}}$$

Here, for a given axes a_x, the PLSR coefficient of determination $\mathbf{PLSR_{R^2}}$ was calculated for different numbers of selected spectral variables **sv** in all angle directions $\boldsymbol{z_x \in [1 \ldots 180]}$. Concurrently, the averaged number of latent variables $\mathbf{T_{boot}}$ and the mean variance of R^2 $\mathbf{VARR^2}$ in bootstrapped samples extracted from the initial sv combination was used to evaluate PLSR model suitability over a complete ordination axes rotation. Hence, $PLSR_{suit}$ point towards sample gradients that can be characterized by stable PLSR models with strong predictive power. Finally, the PLSR suitability area for a_x over z_x was used to determine an optimal predictor set X for the prediction of a certain sample gradient in the PLS regression framework:

$$\boldsymbol{X(a_x, z_x, w_x t_x) = w_x(PLSR_{suit}) \leq t_x}$$

A PLSR suitability area can be used as weighting scheme on the frequencies of selected input spectral variables **sv** in order to select spectral features that maximize explanatory power of underlying PLSR models. Thereby, different model calibrations can be tested iteratively by successively shrinking suitability weighting $\mathbf{w_x}$ and including only spectral variables below

varying thresholds $\mathbf{t_x}$ on the frequencies. The final parameter space inherits $a_{x,y}$ and $z_{x,y}$ from the species abundance function $F_{x,y}$ and additionally assigns $w_{x,y}$ and $t_{x,y}$ for an optimal spectral predictor combination to solve the objectives G_x and H_y.

2.8 NSGA-II Optimization

In order to model single species abundance variations it is necessary to specify sample gradients that are capable of delineating species shift along effective spectral features. Therefore, the overall goal is to maximize species variance patterns in $F_{x,y}$ and spectral predictability in G_x and H_y, simultaneously. In consequence, for each plant species an optimal parameter space $P \in [a_x, a_y, z_x, z_y, w_x, w_y, t_x, t_y]$ should be defined in a multi-objective optimization procedure. We applied the Non-dominated Sorting Genetic Algorithm (NSGA-II) (Deb et al., 2002) that defines a number of Pareto-optimal solutions on the basis of solving the objective functions. The Pareto optimality was used as multiple equivalents of non-dominated solutions can be expected in a complex multi-species environment. In that respect, non-dominance can be achieved by finding solutions that cannot be improved on any objective without being degraded in one of the other objectives. The NSGA-II algorithm thereby iteratively approximates the Pareto front via an evolutionary approach that compares the fitness and diversity of parent and child populations by solving the objectives with tunable parameter values (chromosomes). The fitness of individuals was estimated by sorting the rank order of non-dominated solutions. In order to guarantee spread of solutions (diversity), individuals with same ranks but located in less crowded areas (higher value of distance to neighboring solutions) are preferred. The child populations are created on the basis of search points from only the fittest parent individuals that survive, so that the chromosomes are passed to the next generation. We used 140 generations until a convergent Pareto front was achieved. The maximum number of population members was set to n = 40 individuals incorporating processing time and convergence tuning. The final Pareto set that was displayed as Pareto front in the objective space (Fig. 4). Due to evolutionary learning approach, the introductions of elitism on the sorted non-dominated solutions and a crowding distance comparison, NSGA-II has proven to be a fast and less parameter intensive multi-objective optimization procedure in a wide range of studies (Ferringer and Spencer, 2006; Khare et al., 2003; Yusoff et al., 2011). We used a NSGA-II implementation from the R-CRAN package mco version 1.0-15.1 (Mersmann, 2014). In the present study it was finally required to obtain one best Pareto solution for each species from the Pareto front in the objective space. For this purpose, the Euclidean distance between all Pareto front individuals and the Utopia point, where all objective function values are maximized, was calculated. In case of utopia solution, objective values from species variance $F_{x,y}$ as well as spectral predictabilities G_x, H_y, would result in the absolute value of 1 which indicates that species and spectral variance can completely be explained (Fig. 4, upper left). The final parameter space was subsequently

extracted for the individual solution with minimum distance to utopia point. These parameters were used to identify species dependent spectral features from field spectra based PLSR models. The resulting models were transferred to hyperspectral imagery to spatially map individual plant species.

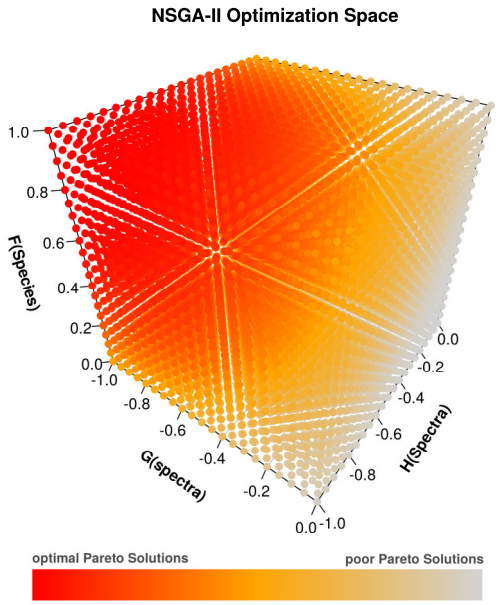

Figure IV-4: *Possible Pareto solutions in the 3-dimensional objective space; utopia point is reached in the upper left corner for F(Species) = 1, G(Spectra) = -1, H(Spectra) = -1 where species and spectral variance are fully explained by model equations*

3 Results

3.1 Optimization and Objective Space

According to the minimum distance to utopia point over all Pareto solutions from NSGA-II optimization, a sorted rank order of individual species distances could be visualized for the two sensors in different phenological phases (Figure IV-5). The lower the distance to utopia the better a plant species can be modeled in the three objective functions, simultaneously. In general, AISA/June spectra outperformed APEX/September spectra for most plant species. The sorted rank order between species varied considerably, reflecting different optimal predictabilities due to plant growth status in different phenological phases. The indicator species for Pioneer Grassland (*Corynephorus canescens*), its succession stadium (*Cladonia spec.*) and Calluna Heath (*Calluna vulgaris*) showed persistent patterns of high model performances in both sensors. Furthermore, high performances in both objective spaces were achieved for the grassland species *Rumex acetosella* and *Poa angustifolia*. In the upper range of objective performances, only one grassland species, *Agrostis capillaris*, was better explained using APEX spectra. Variations in the lower performance range regarding species

rank order were stronger with a few species, e.g. *Ornithopus perpusillus*, *Agrimonia eupatoria,* having higher APEX based model performances.

We subsequently depicted the three species, *Calluna vulgaris, Corynephorus canescens* and *Cladonia spec.*, with highest performance in both objective spaces in order to display the distribution of all population members in the resulting Pareto-Front for comparison (Figure IV-6). Such visualizations can be used for a detailed interpretation of species behavior in the objective space and thus for selecting an appropriate model configuration from the related parameter space.

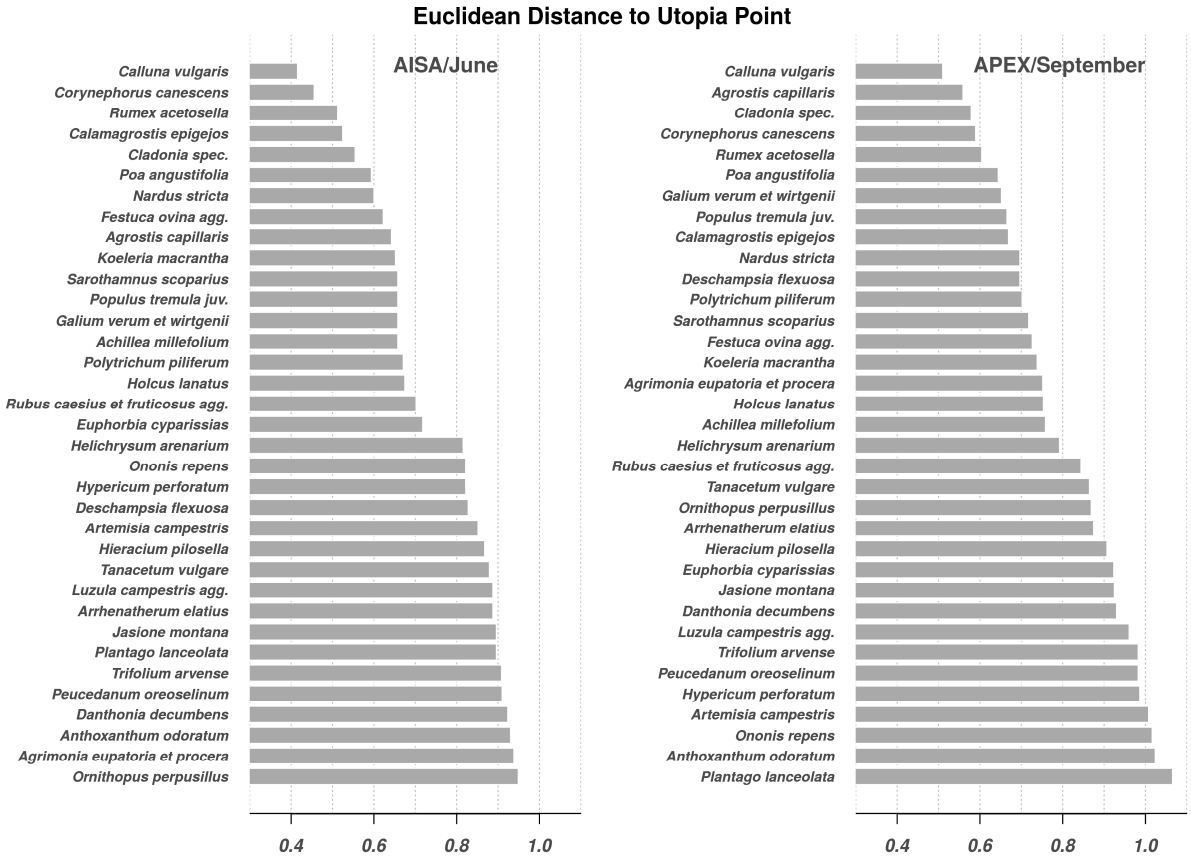

Figure IV-5: *Utopia point distance of individual plant species abundances in field spectra calibration of AISA spectra acquired around June and APEX spectra acquired around September in 2011*

For example, *Calluna vulgaris* abundance could completely be modeled in the ordination space ($F \approx 1$), independently of the spectral models. The same behavior was observed for *Corynephorus canescens*, where Pareto sets showed the best abundance model fit at the same locations where optimal spectral model were fitted. The behavior of *Cladonia spec.* Pareto sets is more variable with maximum abundance objective values for lower spectral objective values. Here, for AISA models the final non-dominated solutions were wide spread in the objective space. However, it can clearly be seen that AISA based objectives outperform

APEX objectives due to a weaker spectral coherence in the second spectral model (axis H(spectra)). Finally, we used the minimum Euclidean distance to utopia point for the extraction of objective function parameters that subsequently were used to map species abundances on hyperspectral imagery.

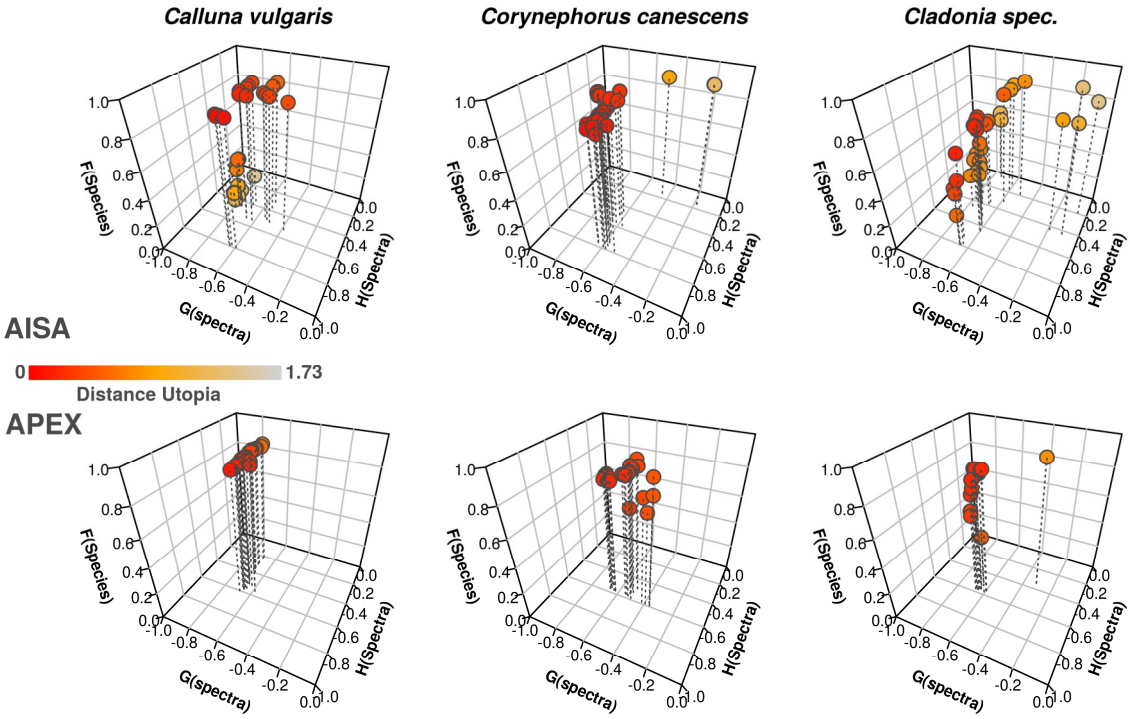

Figure IV-6: *Sensor comparison of Pareto-Front representations after NSGA-II optimization of the population members used for the main dryland indicator species; utopia point (red saturation) is again located in the upper left part of the objective space*

3.2 PLSR Feature Selection from Parameter Space

The optimal Pareto solution with lowest distance to utopia point defines the final composition of variables in the parameter space for each species. This was used to extracts spectral features that maximize species abundance explanation at ordination axes NMS1 (a_x) and NMS2 (a_y). The inclusion of spectral variables as species independent spectral features was visualized for the two sensors (Figure IV-7, 8). Differences could be made visible with relation to phenological phase shifts and spectral sensor configuration. For this purpose the first five species visualized for APEX are the same as modeled with AISA spectra. APEX spectral models showed less features in the first water absorption bands at 0.96 µm resulting in only few selections of water supply based vegetation indices. In contrast, AISA spectra for the best species objectives were not determined by the CAI cellulose index, however, the related absorption feature around 2.1 µm was selected occasionally. Whereas the low spectral APEX resolution in the VIS-Blue area resulted in only a few selected variables in comparison

to AISA, the denser spectral sampling interval in the red edge had less influence for feature identification. In general, there was no stable feature configuration for a certain species found over the two phenological phases. However, spectral variables were predominately selected for the SWIR absorptions at 1.68 and 2.30 µm and for the second water absorption at 1.68 µm. Spectral indices variations were higher according their frequency of selection. For AISA phase, most frequently used indices were MSI, TCARI/OSAVI, TCARI and NRI1510 and for APEX phase TCARI/OSAVI, RGI and TCI. Intra-species comparison revealed similar feature distributions between *Calluna vulgaris* and *Cladonia spec.* for both sensors and between *Rumex acetosella* and *Agrostis capillaris* in APEX and between *Calamagrostis epigejos* and *Festuca ovina agg.* in AISA, respectively.

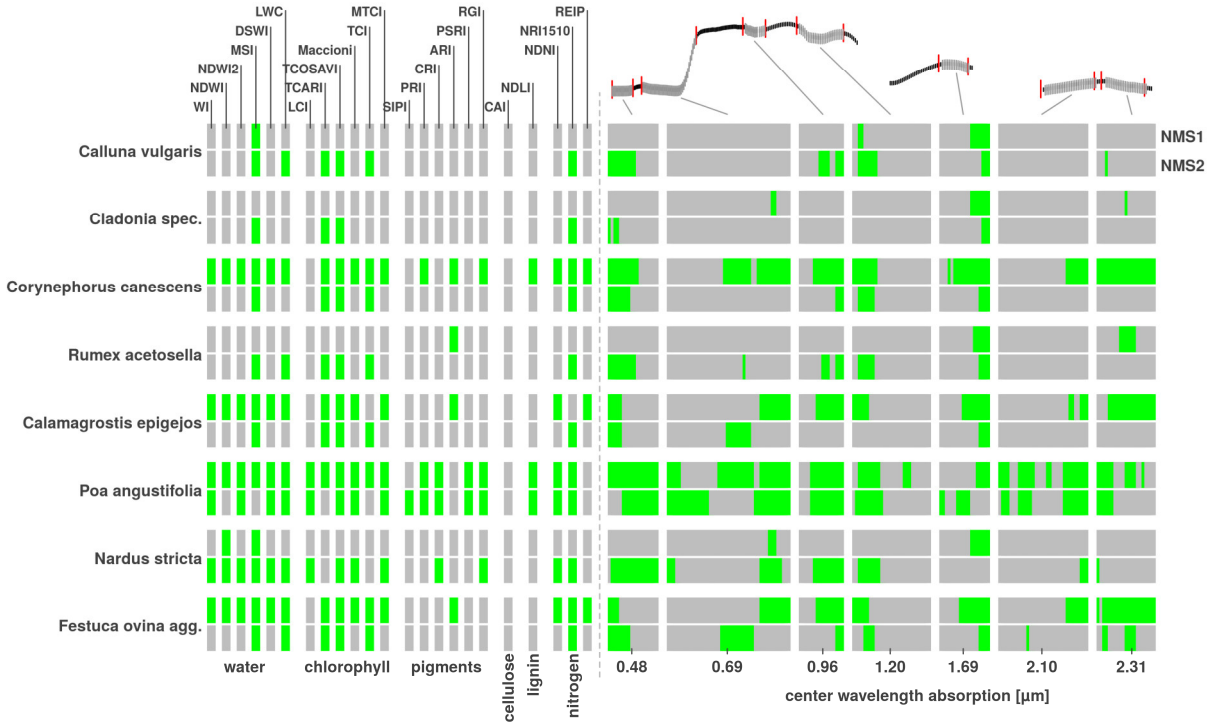

Figure IV-7: *AISA selected spectral variables for objective space solution with minimum distance to utopia point in dependency of single plant species and ordination axes; green-selected variable; grey-initial feature distribution*

3.3 Species Mapping

The final parameter composition from best Pareto solutions were selected in order to calibrate field spectra based species models. The 18 best AISA species models according to the minimum distance to utopia (Fig. 5) were then applied to spectral variables extracted from image spectra for mapping purpose. Every pixel was thereby assigned to n=18 individual abundance values between 0 and 100 %. This procedure was used for a spatial evaluation of species coexistence patterns assuming that only pixels with maximum individual plant species

abundances below 100% allow for multi-species establishment (Figure IV-9). In general, it can be stated that the lower the mapped pixel abundance maximum the higher the probability of species coexistence. Thereby the respective dominant species was capable of indicating particular habitat types (1. Max Figure IV-9-b). We were able to spatially explicitly distinguish between open pioneer stands (e.g. *Corynephorus canescens, Cladonia spec., Agrostis capillaris*), heathlands (*Calluna vulgaris*) and dry grasslands (*Festuca ovina agg., Calamagrostis epigejos*) whereby maximum species diversity was reached in grassland communities (Figure IV-9-a,b). Furthermore, plant associations and thus habitat type compositions were made visible by plotting lower level pixel abundances (Figure IV-9-c). For example, *Calluna vulgaris* was mostly mapped together with *Nardus stricta*. Pixels of open pioneer stands always got high abundance values of *Corynephorus canescens, Cladonia spec.* and *Agrostis capillaris*. In addition, high abundances of *Rumex acetosella* (1. Max) were mapped sparsely in grassland communities mostly on pixel in which *Festuca ovina agg.* achieved high abundance values (2. Max). The abundance of *Rumex acetosella* was decreased when it was mapped together with *Agrostis capillaris*.

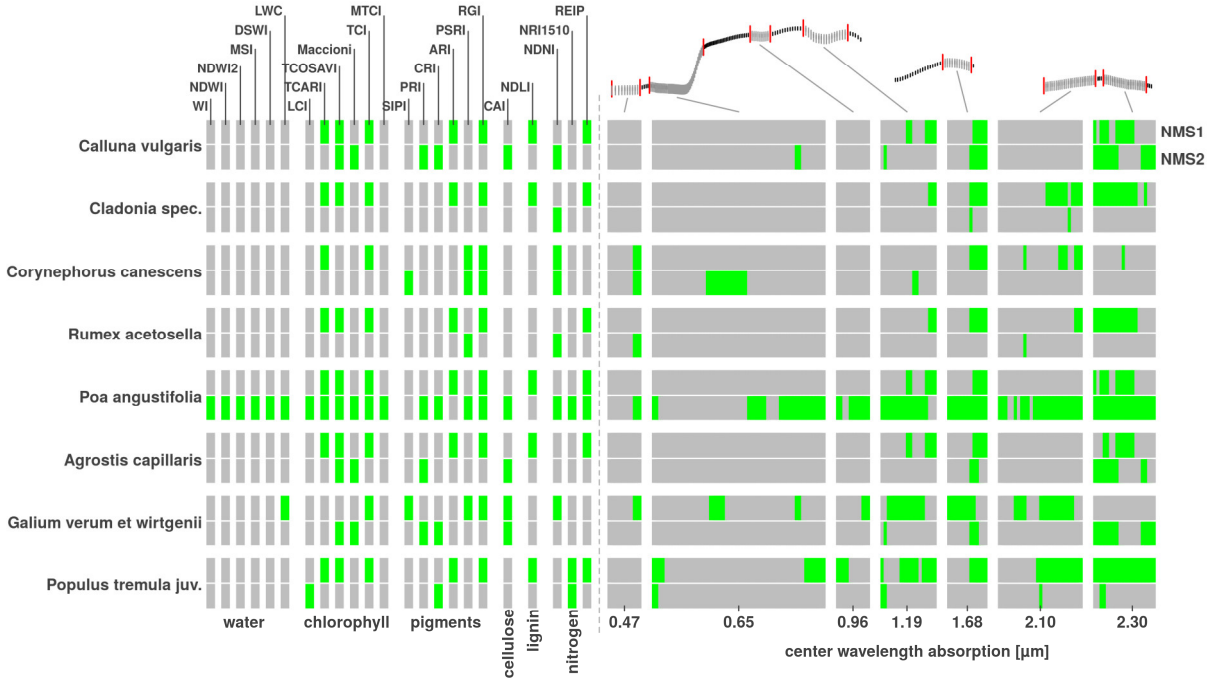

Figure IV-8: *APEX selected spectral variables for objective space solution with minimum distance to utopia point in dependency of single plant species and ordination axes; green-selected variable; grey-initial feature distribution*

Individual species abundances with highest model performances were visualized for open dryland complex (Figure IV-10) and for sandy xeric grassland species interpenetration (Figure IV-11). The open dryland complex was clearly separable into Heathland (*Calluna vulgaris*) and Pioneer stands (*Corynephorus canescens*) whereas *Cladonia spec.* was mapped in both

stands. *Rumex acetosella* thereby could form high abundances in adjacency to Corynephorus and Cladonia stands but not on pixels were Calluna vulgaris occurrences were detected. Dry grassland complexes could be characterized by different grass and herb species in small scale interpenetration patterns with maximum abundances < 15 % at the 2m pixel scale (Figure IV-11). Each grassland species holds a unique spatial abundance patterns with different abundance maxima locations. Thereby, different zones of overlap could be made visible. For example, *Agrostis capillaris* was mapped together with *Calamagrostis epigejos* in the north-west of our study area; however, in other locations both species were clearly separable into different habitats. *Festuca ovina agg.* was mapped over the whole grassland area with transition to Calluna heath stands. Only low abundances were mapped for *Poa angustifolia* that was particularly close to stands of Festuca and Calamagrostis in the central area. *Agrostis capillaris* grasslands could be mapped within Calamagrostis and Festuca stands, whereas occurrences were also detectable in open pioneer stands with missing occurrences of typical grassland species.

Table IV-2: *Model performances achieved for internal cross-validation at Pareto-solution with minimum distance to utopia point in F, G, H; external validation results for species abundance at transact plots with N – presences mapped in percent abundance range*

	Calluna vulgaris	*Corynephorus canescens*	*Cladonia spec.*	*Rumex acetosella*	*Calamagrostis epigejos*	*Poa angustifolia*	*Nardus stricta*	*Festuca ovina ag.*	*Agrostis capillaris*
R^2 F(Species)	0.91	0.83	0.65	0.78	0.76	0.79	0.81	0.54	0.49
R^2 G(Spectra)	0.64	0.64	0.67	0.59	0.62	0.75	0.61	0.65	0.64
R^2 H(Spectra)	0.81	0.77	0.73	0.77	0.71	0.48	0.59	0.75	0.80
R^2 [transect plots]	0.89	0.71	0.90	0.32	0.51	NA	NA	0.35	0.37
N [presence]	13	7	8	16	8	NA	NA	11	12
Range [%]	5-80	1-15	1-65	1-25	1-30	NA	NA	2-20	1-25

The coefficient of determination R^2 for the optimal Pareto-solution of the 9 best species models (see Figure IV-6, 7) for AISA varied considerably in different objectives (Table IV-2). There was always one main gradient in the ordination that exhibits significant better spectral predictabilities. The grassland species *Festuca* and *Agrostis* were mainly downgraded in the optimization due to a weak abundance representation in the ordination (low F values). The terrestrial mapping of abundances in transect plots was subsequently linearly regressed against mapped pixel abundances. Due to a relatively small number of presences in the

validation plots, *Poa angustifolia* and *Nardus stricta* had to be excluded from transect validation. Best performances were achieved for *Cladonia spec., Calluna vulgaris* and *Corynephorus canescens* and *Calamagrostis epigejos* as best grassland species. The terrestrial abundance range of *Corynephorus* most notable differed from mapping results.

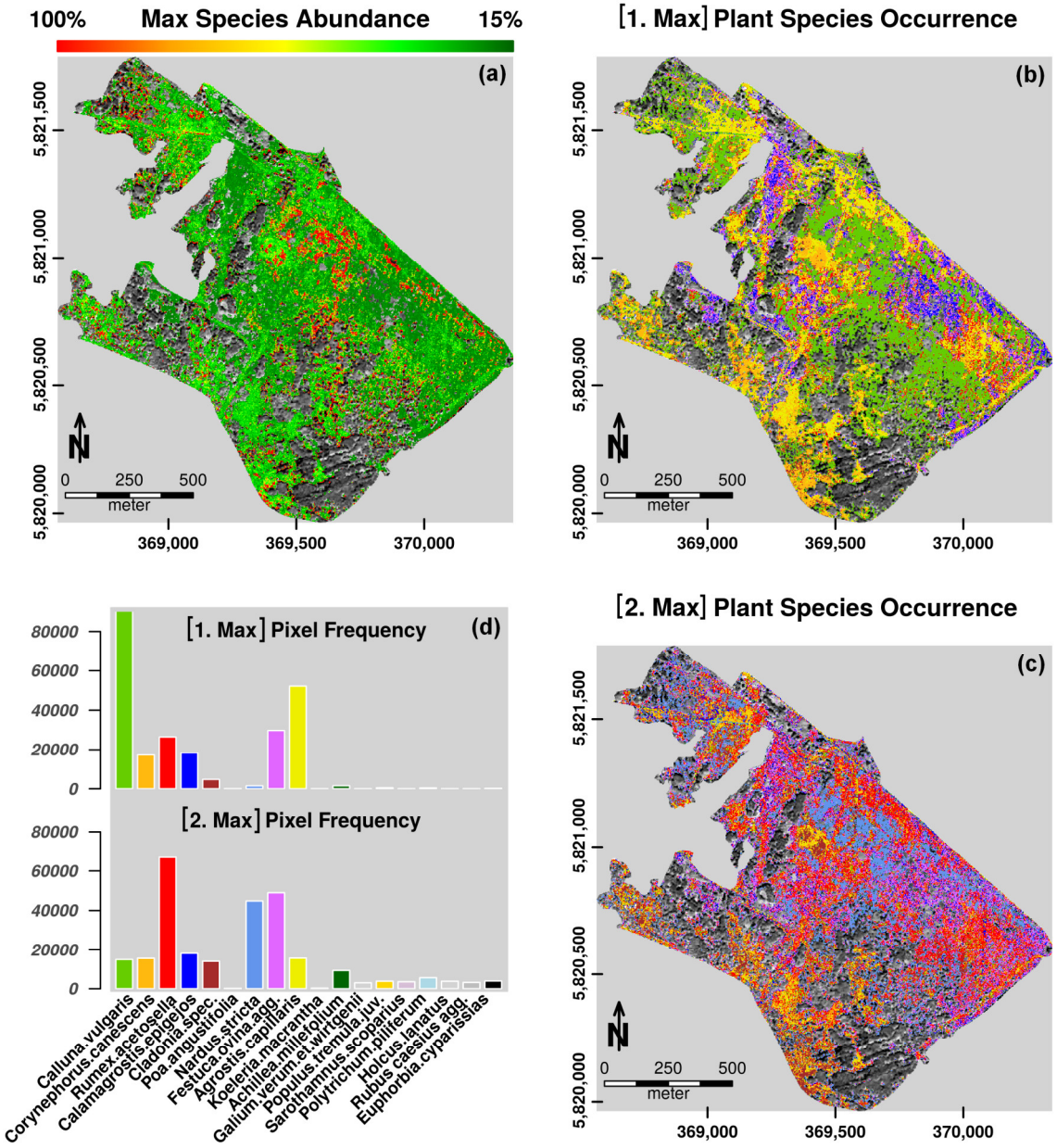

Figure IV-9: *a) maximum plant species abundance values that can be achieved in a single image pixel applying field spectra based optimization models to AISA image spectra for n = 18 species, b) 1. Max represents dominating species with maximum abundance values in the respective pixel, c) 2. Max represents coexisting species having second highest abundance values in the respective 1. Max pixels, d) color legend for mapped species with highest abundances (b), second highest (c) visualized as image pixel frequencies over the entire test area*

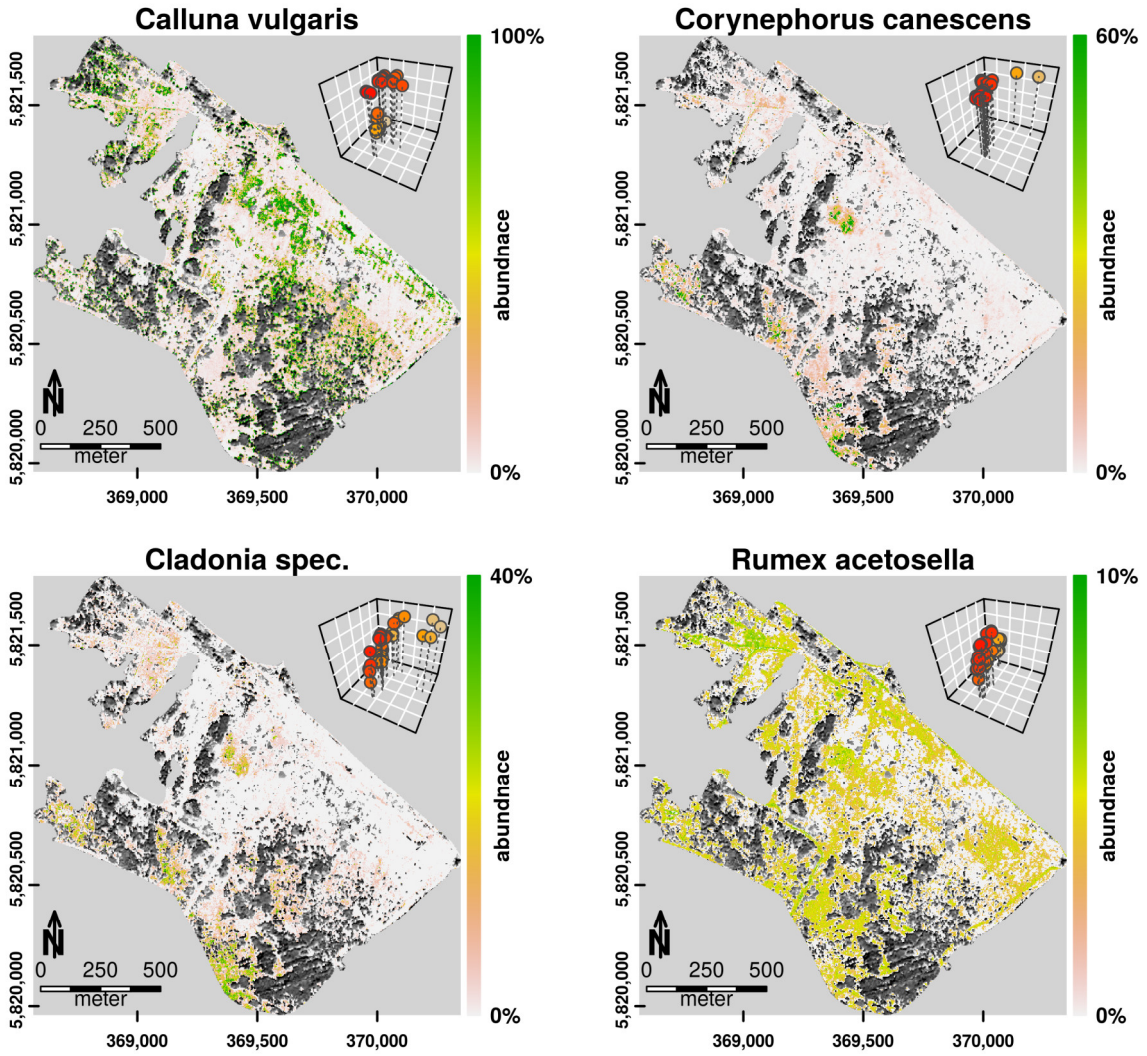

Figure IV-10: *Open dryland species abundance distribution on the basis of field spectra models transferred to AISA imagery for the four most abundant species with highest model performances; parameter sets for model calibration were extracted from nearest utopia solution in NSGA-II Pareto sets displayed in the upper right*

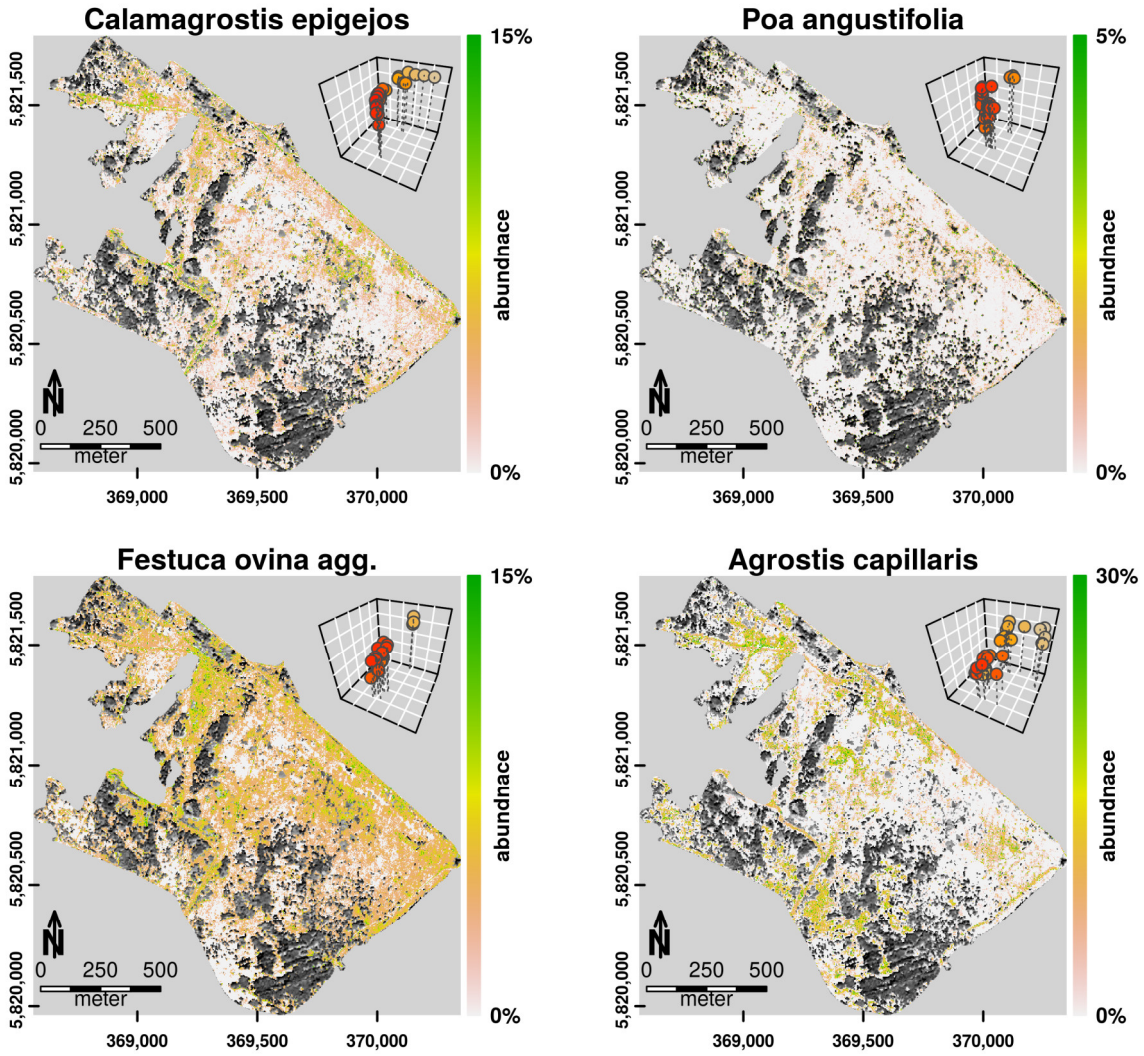

Figure IV-11: *Dry grassland species abundance distribution on the basis of field spectra models transferred to AISA imagery for the four most abundant species with highest model performances; parameter sets for model calibration were extracted from nearest utopia solution in NSGA-II Pareto sets displayed in the upper right*

4 Discussion

4.1 Multi-Species Mapping

In our study we present a procedure to assess spectral predictabilities of single species abundances in a complex multi-species environment. We understand this work as a contribution to a more holistic approach of ecosystem characterization by hyperspectral reflectance signatures. Therein, an ecoregion can coherently be described by ecological gradients that modify plant species composition in a vegetation continuum. The multiobjective Pareto-optimization finally reveals to what extent individual species abundances can be explained out of this continuum by spectral information. It crucially differs

from conventional mapping strategies that a priori select a particular set of species that is then tested against spectral features for model calibration (e.g. Clark et al., 2005; Dudley et al., 2015; Underwood, 2003). Such models are often affected by feature overlays in mixed signatures. In particular, species detection success is reduced with increased side complexity due to increased spectral and species richness (Andrew and Ustin, 2008). Ordination space projections, in contrast, model species occurrences and replacement coherently as a whole. Spectral responses can be multidirectional and thus enable a more differentiated evaluation of species-spectral responses. The proposed optimization procedure can therefore provide a more detailed view into side characteristics and arising mapping possibilities.

4.2 Species Patterns and Dynamics

Species abundances are directly relatable to the species cover that can be resolved at the spatial pixel scale. Due to subpixel diversity of different species overlap, patterns of coexistence, associations and canopy structures can be made visible. The mapping of fine scale structures of plant community composition and related development stages thereby allow for a detailed assessment of successional trajectories under the influence of management efforts. It is, for example, interesting to see that *Cladonia spec.* can be associated with heath and pioneer stands, but also disappears in some areas of the same habitat types. Here, it can be shown that both associations of lichens a) in pioneer stands as indicator for succession and b) in heathlands as indicator for degeneration phases are possible realizations in our study area. Natural succession of sandy dune communities towards heather establishment is often indicated by lichens growth that is further triggered by factors such as surface stability or soil acidity (Alvin, 1960; Christensen, 1989). The final association between Calluna heath and Cladonia is relatively stable even under reforestation (Alvin, 1960). However, in dense Calluna canopies during the building phase, lichens and other species are almost completely suppressed until Calluna reaches its mature or degeneration stadium where the persisting Cladonia association will show trough the collapsing canopy (Barclay-Estrup and Gimingham, 1969; Watt, 1955) which thus enables spectral features identification in the lower vegetation layers (Delalieux et al., 2012). We can further show that at a 2 meter spatial pixel scale *Calluna vulgaris* is still capable of developing dominance stands whereas *Corynephorus* is always associated with bare ground cover resulting in maximum pixel abundance values of 60%. The form of association between lichen populations and pioneer/heath stands also leads to reduced maximum vegetation cover of *Cladonia spec.* of 40% in a 2 meter pixel representation. In contrast, *Rumex acetosella* holding generally low abundances values < 10% that mainly indicates an open pioneer – grassland transition since association between *Corynephorus canescens* and different grass species exist while it mostly disappears in heathland communities. Although, Marrs (1986) reported *Rumex* and birches as the only other higher plants records in different British

heathlands, our study area comprises much higher species diversity that may replace these Rumex associations with various grass invasions within the degeneration and building phases of *Calluna*.

The behavior of coexistence and dominance can be spatially visualized for grass and herb species as well. They are distributed more heterogeneous with transition to different other community types and plant species assemblages. In this context, grassland species such as *Agrostis capillaris* or *Calamagrostis epigejos* form high density patches with abundances > 10%. Again, at some locations these two species appear together in other parts of the study area they do not (see Section IV-4.3 & Figure IV-11). Such behavior can be seen as individual species response to external factors that reveal whether an association/plant community really exists. In this case it is supposed that the distribution of *Calamagrostis epigejos* is presumable controlled by nitrate deposition in soils and thus enables an invasive spread into different habitats (Süβ et al., 2004). Another interesting finding about the grass species distribution is that *Agrostis capillary* coexists with *Corynephorus* and *Cladonia* in open pioneer stands but not with *Calluna vulgaris*. Grass encroachment of heather is rather indicated by *Festuca ovina agg.* that in fact grows together with Calluna. Further research is needed in order to understand this kind of selective behavior.

4.3 Spectral Transferability

Our study presents an approach to transfer spectral features for species abundance coherences from field sampling to image spectra by means of evolutionary optimization. The PLSR based spectral models are validated internally by using 1000 bootstrapped samples in order to select significant and stable features for high predictive accuracies (Neumann et al., 2016). In Neumann et al., (2016) it was further proven that certain gradient directions in an NMDS ordination space are defined by unique species replacements that can be assigned to suitable spectral feature spaces in a PLS regression framework. Since species replacement in multiple directions inherits spectral patterns of transition, such features are better representative for mixed image pixel signatures. Furthermore, the species abundance itself is not directly modeled in a linear relation between field plots and measured spectra. Abundance distributions are projected into the n-dimensional ordination space of multiple species transition that can be delineated by different spectral gradients. The spectral variability is therefore extracted for specific gradients separated from the actual species abundance that is related post hoc in the optimization process.

However, for a successful image transfer, patterns of transition have to be covered by spectral field measurements on plots that are capable of resolving the actual floristic heterogeneity in image pixels. That is assuming an appropriate atmospheric modeling to retrieve valuable canopy reflectance values in the imagery and spectral normalization on known absorption

wavelength regions. Such regions produce highest accuracies in internal calibration as they are directly relatable to the ecophysiology of vegetation. In our study, for example, the mean deviation of indices and spectral absorption features between image pixels and reference plots varies between 5-12%.

Spectral sampling additionally needs to be carried out in near overflight conditions. Otherwise spectral signatures will be affected by individual plant growth, phenology and canopy structure changes that can rapidly be influenced by short-time weather conditions. An adequate timing of field work and data acquisition is thus of utmost importance to overcome spatial non-stationary effects (Feilhauer and Schmidtlein, 2011). Many scientists are well aware of possible feature shifts due to spatial non-stationary, vegetation layer overlay or vitality and plant structural parameter variations on the pixel scale that will be inherent for transferring field spectra to images (Andrew and Ustin, 2008; Feilhauer and Schmidtlein, 2011; Okin et al., 2001). However, it has been found strong evidence that, generally, significant empirical relations between plant species composition and reflectance spectra can be established (Feilhauer et al., 2010; Feilhauer and Schmidtlein, 2011; Schmidt and Skidmore, 2001). The success of model transfer, then particularly depends on a spectrally dense characterization of possible habitat conditions under which a species may form varying abundance patterns. In this context, spectral databases in conjunction with open data archives open up new potentials for providing dense vegetation characteristics that can be used to extensively train multivariate models at the field and image scale (Dudley et al., 2015; Neumann et al., 2015a; “SPECTATION,” 2015).

4.4 Validation

In our study we solely include reference samples that were collected ± 18 days around image acquisition. Besides dominance stands and typical plant communities, we further sampled all known transitions between communities. For this purpose the plot size was selected so that single species shifts could be detected within the spatial scale of floristic variation in our study area. However, since ecological processes inherit properties of fractal geometry (e.g. Johnson et al., 1992; Levin, 1987; Palmer, 1988) it is hardly possible to set up fully representative samples. Moreover, species turnover along gradually changing scales as evident in species-area curves (Nekola and White, 1999; Williamson, 1990) show that the fractional cover of single species varies substantially between different observation scales. These findings must be reviewed critically for an external validation of plant species abundances by remote sensing approaches. In our study, 1 m² transects plots were compared to 2 m geocoded and hence, resampled image grid representations. Due to coordinate inaccuracies for plot locations (GPS ± 3 m) and the broader 2 m mapping scale along with the mentioned distance decay in species turnover, the species cover in image pixels can be expected to be shifted with regard to field plot records. However, the coefficient of

determination between predicted species abundances and field plot abundances still matches very well for e.g. *Cladonia spec (*$R^2 = 0.90$), *Calluna vulgaris* ($R^2 = 0.89$) and *Corynephorus canescens (*$R^2 = 0.71$). Dry grasslands are affected more by scaling effects resulting in weaker abundance correlation between $R^2 = 0.51$ (*Calamagrostis epigejos*) and $R^2 = 0.32$ (*Rumex acetosella*).

In view of the scaling issues influencing external validation interpretability, we propose the use of the introduced optimization criterion for an evaluation of potential mapping success. The distance to utopia thereby comprises independent cross-validation procedures in the different objectives separately: a) The final species ordination is validated regarding pattern significance (1000 random permutations), configuration stability (1000 bootstrapped samples) (Knox and Peet, 1989; Neumann et al., 2015b; Pillar, 1999) and the stress criterion from 1000 random configurations (Kruskal, 1964); b) The PLS regression of score axis coordinates is validated for spectral feature significance, feature stability and predictive accuracy using 1000 bootstrapped samples (Neumann et al., 2016). Thus, both methods are validated independently and subsequently joined in the optimization in order to extract an overall validation criterion. This procedure overcomes conventional modelling approach where the training data is directly fitted onto the response variable and hence, resulting model performances are directly related to the calibration parameters.

4.5 Sensor and Phenology Comparison

According the minimum distance to utopia via the NSGA-II optimization, the performance of species abundance predictions is maximized in the midsummer phenological phase for AISA spectra. This time period can be considered as the species peak phase for mid-European dry grasslands where most plant species appear during May passing into late development stages in June (e.g. *Festuca ovina agg., Rumex acetosella, Koeleria macrantha*). Several studies have shown that late phases of plant development, such as flowering and adolescence growing, provide stronger evidence for spectral discrimination due to species traits enhancement (Andrew and Ustin, 2008; Feilhauer et al., 2010; Laba et al., 2005). Such phases are relatively stable. Short term weather variations like drought or heavy rainfall events are only capable of shifting the phenological response by a few days (Jentsch et al., 2009). In late September 2011 after good growing conditions, species like *Calamagrostis epigejos, Galium verum or Agrostis capillaris* show optimal plant development stages. At this time they are superimposed with degenerated dry grassland species that hold their optimum in the midsummer phase. The existence of only a few superimpositions of leaves and therefore more exceptional masking of species in the ground strata can be seen as one possible reason for a better predictability of AISA midsummer spectral gradients. However, we may also have seen here an effect of spectral sensor configuration that allow for an increased AISA spectral resolution a more precise spectral description of species gradients. Further analysis on similar

sensors in different phenological phases or on different sensor in the same phenological phase offer great potentials for revealing sensor constraints and phenological feature shifts for the determination of floristic gradients.

Nevertheless, the sorted rank order of single species according their optimization success in the objective space for one sensor, already allows an evaluation of species mapping capabilities in a certain phenological phase. Thereby, our study confirms that the dryland species *Calluna vulgaris* and *Corynephorus canescens* can generally be mapped very well due to a high spectral contrast in relation to the surrounding grassland communities (Delalieux et al., 2012; Förster et al., 2008; Spanhove et al., 2012). Moreover, there are other surprising species candidates such as *Cladonia spec.*, *Rumex acetosella* and *Poa angustifolia* with good model performances in both phenological phases. In contrast, species like *Agrostis capillaris, Galium verum* or *Festuca ovina* show clear preferences to one phenological phase for optimal mapping conditions. Species order variation is increased in the lower objective performance regions. A detailed analysis of species rank order and resulting mapping products over different phenological phases hold great opportunities for the characterization of processes and dynamics in ecological systems. Further research is needed in order to understand the form of organization of plant species that is interrelated with ecological processes in an ecoregion.

5 Conclusions

In a multi-species environment, single plant species abundance patterns can be quantified by applying spatial correlation functions on projected sample gradients in an NMDS ordination. Thus, each species holds a unique abundance distribution in different ordination dimensions and directions that can be related to field spectral signatures. Spectral models can subsequently be used to map individual plant species abundances on hyperspectral imagery. We show that finding an optimal spectral model for individual plant species abundance patterns in an ordination can be translated into a multi-objective optimization procedure. It incorporates abundance quantification and multivariate spectral calibration in order to find predictive spectral features for mapping purpose. For the first time, the species inventory over different habitats will be evaluated as a whole according individual spatial predictabilities of plant species abundances. In consequence, for a number of confident models, multi-species mapping has proven to deliver valid species distributions for open dryland communities. Patterns of coexistence, transition and dominance could be mapped to a great extent. We believe that these spatially explicit abundance patterns provide a relevant contribution towards the detection of fine-scale ecosystem responses that will refine the assessment of habitat conversion and disturbance. Future research is needed in order to identify sensor constraints and phenology influences for optimal model performances.

Acknowledgments

We gratefully thank Dr. Angela Lausch and Dr. Daniel Doktor (The Helmholtz Centre for Environmental Research-UFZ) for providing AISA imagery and Maximilian Brell (German Research Centre for Geosciences-GFZ) for AISA image pre-processing. We further express our gratitude to the Sielmanns Naturlandschaften gGmbH, namely Angela Kuehl, Joerg Fuerstenow and Peter Nitschke, for enabling a secure and permanent field plot access. A special thanks goes to all the student field workers, comprising spectral measurements during the summer 2011. This work was funded by the Deutsche Bundesstiftung Umwelt (DBU, grant: 26257-33/0) and the Environmental Mapping and Analysis Program (EnMAP, grant: 50EE0946).

Chapter V: Synthesis

1 Main Conclusions

This thesis investigates the potentials of hyperspectral remote sensing for the spatial mapping of plant species to support efforts in nature conservation and ecosystem restoration. It is demonstrated how vegetation can be defined as a continuum of individual plant species transitions that can further be utilized for the derivation of habitat management parameters (chapter II). Evidence is provided on the existence of coherent relationships between species gradients and spectral reflectance signatures (chapter III). Spatially explicit maps on individual species abundance patterns could finally be derived by combining patterns of gradual species shift with corresponding spectral features from field references (chapter IV). On these points, the research questions raised in chapter I-3 are answered in detail according to each chapter (II: V-1.1, III: V-1.2 and IV: V-1.3) in the following.

1.1 Habitat Type Characterization and Conservation Status Assessment

Question-I: An NMDS ordination can be used as a numerical method for the representation of continuous vegetation patterns that originate under the boundary conditions within a region of the natural environment. Since the number of different plant species increase by increments of geographical distance and hence the similarity of species composition decreases (Nekola and White, 1999; Williamson, 1990), an NMDS ordination space needs to be based on ecologically defined areas of distinct plant formations. Such areas (e.g. ecoregion, biome) are characterized by ecosystems of common processes, species interactions and arising dynamics of vegetation patterns which make them distinguishable from other geographic locations. Measures of ecological restoration have to be systematically selected and applied in accordance with these area characteristics in order to realize a targeted control of habitat development.

Question-II: Within this thesis it could be shown that open dryland communities of the study area can fully be described by NMDS ordination. Patterns of Natura 2000 habitat types as well as multidirectional transitions between types are reproducible on the basis of field plot samples and their arrangement in the ordination space. It was proven that projected patterns are stable and differ significantly from random sample permutations and thus deliver a meaningful characterization of the area's species composition. A random exclusion of species assemblages has no significant influence on the topology of sample gradients in the ordination result (II: Section 3.1).

Questions III-IV: On the basis of stable sample gradients in the final NMDS ordination space, the thesis further introduces a new rule-based approach for the quantification of habitat type characteristics that are needed for the assessment of habitat management strategies (II: Section 2.4). An ordination space thereby holds species abundance values on every sample plot. The distribution of species and their abundance variations can be modeled in an

ordination sample structure using spatial correlation functions and geostatistical Kriging (II: Section 2.5). On that basis it is now possible to map probability surfaces for the occurrence of certain habitat types and habitat pressure indicators that are directly defined over species composition and abundance shifts. For the first time this thesis shows that habitats can be determined as a continuum of probabilities. A Natura 2000 habitat type is thus more likely if an a posteriori defined species composition pertains. A decrease in habitat type probability is affected by species turnover through succession, invasion or disturbances that can be modeled likewise by setting the characteristic species indicating potential pressures. Habitat type and pressure probabilities are consequently attributed to functional relationships between species, transition and triggering processes that are assigned to samples and their projection in the NMDS ordination space (Figure II-4).

Question-V: If there is evidence of habitat type probability variations and responsible pressure indicators in the sample continuum of an NMDS ordination result, an itemized conservation status assessment can be introduced. One can directly "ask" the ordination space about the reason of the decrease in habitat type probability, and hence a deterioration of conservation status. Different ordination space regions will then give different answers about the species turnover that leads to specific pressure. The thesis gives evidence that different pressure probabilities can be modeled within an ordination space (Figure II-6) that can be incorporated into a conservation status assessment scheme (Figure II-7). Due to the inter-polation of probabilities over multidirectional sample gradients, the final conservation status; favorable (A: excellent; B: good) and unfavorable (C: adverse) after (LANA, 2015; Zimmermann, 2015); is gradually assignable. Hereby, early development tendencies and directions can be detected within transitions between the assessment categories that deliver valuable information for the implementation of management practice.

Question-VI: The probability delineation of habitat characteristics in an NMDS ordination can further be assigned to spectral reflectance signatures. It can be shown that image spectra at locations of field plot samples are related to probability variations in the NMDS ordination space (Table II-4b). In consequence, it was shown that continuous measures of habitat type qualities can be transferred to spatially explicit maps of Natura 2000 habitat types and conservation states (Figure II-8). In this manner habitat management is made possible with recourse to species turnover extracted from ordination. Hence, one of the major breakthroughs thereby is the detached mapping of sample gradient positions and the post-hoc attribution of habitat characteristics from the final ordination space. It enables a detailed examination of the spatial characteristics of habitat transition and provides early estimates about development trends.

1.2 Spectral Feature Characterization of Floristic Gradients

Question-I: In complex multi-species environments the extraction of distinct spectral signatures for plant species detection is often impeded by an increased spectral variability (Andrew and Ustin, 2008). This thesis demonstrates that spectral features can be modeled dynamically along multiple floristic gradients in an NMDS ordination (chapter III). The complexity of spectral responses was thereby broken down into different gradients of floristic transition. For this purpose, a 3-dimensional NMDS ordination space rotation with simultaneous PLSR-based spectral feature extraction was newly introduced. It was shown that different directions in a rotated NMDS ordination space generate different patterns of spectral responses. Each wavelength of field spectroscopic data collected for samples in the ordination exhibits a unique correlation behavior depending on the rotation angle and spectral transformation technique (Figure III-4). Moreover, the study revealed coherencies between the correlation behavior of field and image spectra that opened up new perspectives for an appropriate feature selection approach.

Question-II: In spite of the skepticism whether plant species can uniquely be described by spectral reflectance signatures (Feilhauer and Schmidtlein, 2011; Price, 1994), the thesis presents a novel procedure for the identification of stable spectral features for the delineation of floristic gradients (III: Section 2.5-2.8). The procedure uses a modified PLSR framework that combines feature selection with stability evaluation in a gradually rotated NMDS ordination space. On that basis, a new concept for the examination of gradient predictabilities was developed. The so-called PLSR suitability designates areas in a NMDS ordination where the explanatory power of stable feature combinations is maximized (Figure III-6). Two interesting findings could be derived from such suitability areas. On the one hand, each NMDS ordination space dimension holds distinct and clearly delineated areas of high PLSR-based predictive abilities. Such suitable areas are further defined by a unique set of grouped wavelength regions. On the other hand, the wavelength position of these spectral features and related predictive accuracies crucially depend on the spectral transformation applied a priori (Figure III-9).

Questions III-IV: Narrow waveband features as provided from e.g. Savitzky-Golay derivatives may outperform broad band reflectance and continuum removed absorption features due to more precise relations to the ecophysiology of plants. However, it was shown that narrow wavelength regions often disappear when applying suitability modeling to the scale of pixel spectra (Table III-I). Such feature dissimilarity would impede the transferability of PLSR models to hyperspectral imagery. The thesis demonstrates that a feature selection using optimization on the suitability area extent and wavelength weights can significantly increase the success of model transfer. Iterative thresholding can thereby be used to reduce an initial feature distribution to a meaningful set of spectral variables for spatial mapping. It was further

ascertained that the finally mapped floristic gradients can be related to patterns of plant species abundances of the major indicator species in the study area.

1.3 Plant Species Abundance Modeling

Question-I: In the continuum of plant species, unique patterns of abundance distributions will be formed in different dimensions of a NMDS ordination result. The thesis demonstrates that the proportion of explainable abundance variance can be approximated for individual species via contour grids fitted on the sample plots by means of geostatistical modeling. The maximum variance that could be explained by sample arrangement in NMDS ordination ranges from 91% (*Calluna vulgaris*) in heathlands, 83% (*Corynephorus canescens*) in pioneer stands and 81% (*Nardus stricta*) in dry grasslands (Table IV-II).

Question-II: A novel approach was developed that combines abundance approximation with accordant spectral feature attribution in a genetic, multiobjective optimization procedure. In the objective space, the thesis introduces a new criterion (distance to utopia point) for maximizing abundance explanation and field spectroscopy based predictabilities for n = 35 species (IV: Section 3.4). Thus, in each species optimization a Pareto solution can be found that optimally combines species and spectral modeling and extract related modulation parameters that can be used for the model transfer to hyperspectral imagery. This straightforward analysis procedure provides a novel framework to evaluate the performance characteristics for multi-species mapping.

Question-III: From the evaluation procedure, compelling evidence was found for the transferability of n = 18 species models in which n = 8 species were selected for spatially explicit abundance mapping. In particular, heathland (e.g. *Calluna vulgaris* R^2 = 0.89, *Cladonia spec.* R^2 = 0.90) and pioneer stands (e.g. *Corynephorus canescens* R^2 = 0.71) achieved high accuracies in external validation whereas complex grassland assemblages often complicate abundance assessment (*Calamagrostis epigejos* R^2 = 0.51, *Festuca ovina agg.* R^2 = 0.35) (Table IV-II). However, on the open dryland test site, plausible and meaningful patterns of plant species coexistence in different habitat types could be mapped successfully. Multiple abundance patterns on the subpixel scale were able to reveal characteristic plant associations, habitat type encroachments and particularly the status of different successional trajectories (IV: Section 4.3 & 5.2).

Question-IV: It was further shown that the predictive ability of most species crucially depends on the phenological phase. There is strong evidence that species traits enhancement during the species peak phase for mid-European dry grasslands leads to better model performance due to an enrichment of spectral contrasts between the plant species (Figure IV-5). The current findings expand prior investigations on the abundance mapping of few (2-4) pre-selected invasive species in relatively species-poor environments (Lu et al., 2009; Parker

Williams and Hunt, 2002; Underwood, 2003) towards multi-species ecosystem inventory mappings. Especially with regard to measures of biodiversity and ecosystem functioning, the proposed approach will contribute to a detailed and thus refined understanding of holistic ecosystem processes.

2 Applications and Future Research

The ecological continuum of plant species properties, related spectroscopic responses and inferable species and habitat mapping facilitate a number of further applications, particularly, in the fields of ecology and spectroscopy with implications for forthcoming satellite missions and growing environmental data archives. The following section addresses practical consequences for habitat management and monitoring as part of the ecological restoration process (Section V-2.1) and expands on ecological process dynamics that are responsible for faunistic habitat formations (Section V-2.2). It is further discussed to what extent a remote sensing based mapping result can be assigned to terrestrial mapping units and which concepts have to be reconceived for the interpretation of spatial information (Section V-2.3). Finally, the science of spectroscopy from space is complemented by new insights, requirements and potentials for future operationalization (Section V-2.4).

2.1 Ecosystem Monitoring

As mentioned in section I-1.3, one of the key components in ecosystem restoration and, hence, habitat management practice, is the implementation of spatially explicit monitoring systems. The developed methodological framework allows an integration of different monitoring aspects for the analysis of spatiotemporal pattern dynamics:

1) Habitat type definition and conservation status assessment was enabled through reproducible functional relationships between species composition and habitat conditions in a multidimensional NMDS ordination result. It supports terrestrial mapping activities by a more flexible definition of mapping units that makes field survey categorization better revisable since ordination space measures define a standardized metrology of vegetation classification (Bonham, 2013b). It helps to generate objective units for the designation of potential areas within the planning process of terrestrial field surveys.

2) Furthermore, the mapping dimensionality is enlarged towards multiple species transition and stressor mechanisms as investigated in coupled human-earth system research (DeFries, 2008). In consequence, ecosystem resilience to multiple stressor regimes can be evaluated in complex landscapes. Multiple factor complexes and species interactions can be defined as integrated bioindicators for monitoring habitat conversion as required in the Natura 2000 network reports (Ostermann, 2008; Vanden Borre et al., 2011), national biotope mapping

initiatives (Gao et al., 2012; Qiu et al., 2010) or protected area conservation (Nagendra et al., 2013).

3) Within the scope of this thesis it could also be demonstrated that the significance of spectral discriminability between species and habitats can be incorporated in the screening and scoping process of appropriate bioindicators for long-term protected area monitoring. It was shown that the vital signs concept of U.S. national parks (Fancy et al., 2009) can be complemented by spectrally distinct habitat parameters in order to provide crucial knowledge about the status and trends of park resources (Luft et al., 2014). Such ad hoc integration of spectral predictabilities in an area's vegetation continuum during the design phase of monitoring programs is seen as the next step towards a refined linkage between researchers, decision makers and the public.

4) The mapping of multiple species patterns, abundance variations and accordant multidirectional transition allows for a detailed estimation of ecosystem biodiversity. It has been recognized that an increased biodiversity loss by human impact degrades ecosystem functioning and thus reduces essential ecosystem services (Hooper et al., 2005; Loreau, 2001; Schlapfer and Schmid, 1999). The developed mapping procedure delivers spatial information about patterns of species richness, diversity measures, coexistence or community structures that are required by recent biodiversity inventory programs such as NILS, Sweden (Ståhl et al., 2011), NeoMaps tested for Venezuela (Ferrer-Paris et al., 2013), the U.S. NEON network (Kelly and Loescher, 2016) and global databases such as GBIF (Otegui et al., 2013) or PREDICTS (Hudson et al., 2014). The mentioned programs are mostly point sample-based and would highly benefit from supplementary spatially explicit data. The European GEO BON initiative provides thereby an initial framework that joins earth observation, existing monitoring networks and different aspects of biodiversity in harmonized databases and observation systems (Scholes et al., 2012). Derived species data from mapped ordination space structures in selected areas by imaging spectroscopy would potentially facilitate the filling of existing gaps, the verification of data consistencies and potentially increase the level of detail for automated inventory programs.

5) One of the most important advantages of gradient mapping via the ordination space continuum is the possibility of post hoc floristic gradient characterization. Since sequential species replacement along certain gradient directions can be described by spectral feature occurrences, the underlying exogenous factor that defines the vegetation status and species composition can be modeled as well. Mapped species gradients thus indicate a certain environmental background that gradually varies in accordance with the species turnover. Such information can be utilized in order to derive proxies for soil moisture, soil pH and fertility (Ellenberg, 1988; Ellenberg et al., 1991) that can be mapped in hyperspectral imagery (Möckel et al., 2016; Schmidtlein, 2005), for soil contamination by heavy metals in river

floodplains (Kooistra et al., 2004), in agriculture, induced by mine waste deposition or in urban, industrial areas and for soil salinity (Zhang et al., 2011). The monitoring of plant stress at the human-environment interface consequently delivers early endangerment signals involving the root zone of soils.

Future research is particularly needed at the level of spatiotemporal pattern formation. Neighboring effects, spatial interdependencies, forms of species organization and temporal resiliencies are still not fully understood. Much more effort has to be put into pattern interpretation and epistemological deduction in conjunction with the ecological community as commenced in Section IV-5.2. Especially, the influence of biodiversity on ecosystem functioning and the driving forces for species extinction and invasion requires long-term experiments that would highly benefit from reproducible and consistent spectroscopic mapping approaches. A close integration of derived spatial knowledge in habitat management programs for large area monitoring is predestinated to generate detailed insights into controlling impacts and trends.

2.2 Habitat Modeling

Spatially explicit data on the distribution of plant species and plant traits induced by external factors are applicable for the modeling of floristic and faunistic habitat properties. There are implications for the distribution of animals, their movement patterns and metapopulation dynamics:

1) An additional outcome of this thesis is a published investigation about the modeling of the occurrence probability of the butterfly species *Hipparchia statilinus* in the study area (Luft et al., 2016). The developed approach was thereby transferred towards presence/absence projections in the 3-dimensional NMDS ordination space. It was shown that *Hipparchia* presences are determined for certain areas in the vegetation continuum. Such regions were again be described using iso-surfaces from Indicator Kriging and spectral signatures for NMDS score coordinates that were further transferred to image pixels. As a result the occurrence probability for the butterfly species was predicted on hyperspectral imagery as the position in the vegetation continuum. In consequence, each pixel could be re-projected to the NMDS ordination space in which the habitat properties are determined over distinct floristic gradients. Finally, conclusions about the expected species composition and related exogenous gradients such as relief parameter or canopy structure were assigned to the mapped habitat distribution. Thus, the developed approach has proven to offer an integrative method for the simultaneous mapping of animal occurrences and driving habitat parameters that could be utilized for the modeling of habitat distributions for different other species.

2) The introduced optimization procedure for multi-species abundance mapping proposes a complement to conventional species distribution modeling (SDM). Species occurrence

probabilities are thereby substituted by multiple abundances whereby the environmental factor response is deducible from NMDS ordination space arrangements. The actual mapping is realized over spectral responses to variations in species composition and related environmental influences. This methodological strategy can help to overcome the lack of spatial predictor variables to fully capture habitat characteristics and the known spatial bias of presence/absence data in conventional SDM approaches (He et al., 2015b). Imaging spectroscopy of plant traits and gradient structures further contribute indirectly to an improved fine-scale species mapping by going beyond recent predictor categories (Pradervand et al., 2014), or directly by mapping species occurrences with hyperspectral reflectance signatures (Skowronek et al., 2016).

3) The spatial distribution of species and habitat suitability estimates raises important implications for recent research in the field of movement ecology. In order to understand why, where and how species move, it is of utmost importance to allocate external factor dynamics (Nathan et al., 2008). By now, it is mostly unknown how spatial and temporal environmental variability affects movement paths and how movement patterns can contribute to maintain ecosystem functioning (Jeltsch et al., 2013). Habitat composition, condition and transition may form critical triggers for pathways of species exchange in metapopulations. In this context, the fine thematic resolution that can be achieved by means of imaging spectroscopy entails a high potential for the examination of small scale and high frequency movement (Nathalie Pettorelli et al., 2014; Rose et al., 2015).

4) A relatively new and controversially debated topic in the ecological community is the intentional movement of species into suitable habitats, commonly referred to as assisted colonization. Due to the ubiquitous human impact on ecosystems worldwide, deliberations about species translocation and reintroduction are made in order to preserve metapopulation networks and dynamic systems (Seddon, 2010). The fundamental concept beyond species relocation is an ad hoc prediction of favorable habitat ranges in which a species can persist under specific environmental conditions (Loss et al., 2011). Here, the developed approach of determining habit parameters, species distribution and spectral predictabilities from NMDS ordination offers a potential tool for the spatially explicit characterization of suitable areas for distinct species relocation. The mapping unit thereby, is not restricted to probable habitat units. Moreover, additional information can be extracted from multiple ordination space gradients that will enable a detailed evaluation of habitat resiliencies for e.g. climate change adaption or stress tolerance. Even though complementary adaption strategies, e.g. enhancing connectivity, reducing pollutant immission or suppress species invasion are suggested (Lawler and Olden, 2011), the proposed methodological framework in this thesis may open new perspectives for the discussion about anthropogenic ecosystem design in the light of preserving and understanding the diversity of ecosystem processes.

2.3 Transferability and Scaling Effects

One major issue for applied methods in imaging spectroscopy is the often raised question about the transferability of developed mapping procedures into similar areas or even into different ecosystems. In the following sections, basic aspects of empirical model transfer are dissected especially in the frame of ecological scaling problems:

1) An NMDS ordination result represents the vegetation continuum of an ecologically distinct area (Section V-1.1). Species association, transition and abiotic gradient allocation are therein relatively stable (Section II-3.1). Thus, by applying the same approach to a similar area, an analogous ordination space structure can be expected. New species data do not necessarily have to be collected, which implies a general transferability of the developed method to other military training areas that are located at ground moraine deposits of the European northern lowlands. In contrast to the wide range of national vegetation classification schemes (Jongman et al., 2001), a species ordination could provide a valuable method for the characterization of transboundary ecosystem networks. Here in particular, ecosystem properties are not defined beforehand by classification rules or indicator approaches (M. Bock et al., 2005), but rather described as a species continuum that forms under the boundary conditions of selected ecoregions. However, the extent of a region in which the application of ordination techniques provides interpretable patterns of species interactions needs to be defined carefully depending on the underlying landscape complexity. The more ecological niches an ordination encompasses, the higher is the generalization effect in the final pattern projections. Future research has to be conducted in order to understand the multiple dimensionality of NMDS ordination for complex landscapes.

2) The directional spectral predictability of species gradients in an NMDS ordination allows for a robust evaluation of mapping potentials. It delineates distinct species gradients in such a way that significant spectral features are established. These features will be reduced to a meaningful set of stable predictors for PLSR modeling (Section III-3.3). It was shown that the final spectral feature set from field spectroscopy is preserved in image spectra to a great extent. Robust features are absolutely essential for calibrating recent machine learning algorithms since they prevent model overfitting (Somers and Asner, 2013). Many studies therefore implement pre-selected spectral indices for stable predictions (Oldeland et al., 2010a; Thenkabail et al., 2013). Often, feature allocation is disregarded completely in predictive mapping (Atzberger et al., 2010; Lawrence et al., 2006; Roth et al., 2015). However, transferability in fact can only be approached if research provides knowledge about the significant spectral responses that need to be exposed for further interpretation of species characteristics. The developed feature selection procedure will be particularly helpful to form a basis for pattern analysis in field spectroscopic data with regard to multiple floristic gradients. Plant species mapping is thereby enabled over different spectral characteristics that

are condensed in an empirical PLSR approach. Since plant species gradients cannot be modeled distinctly due to the huge number of taxonomical differing varieties and the variability of plant sates driven by exogenous factors (Section I-2.1), a given magnitude of uncertainty in model transfer will still depend on the density and range of statistical sampling that is conducted at the field scale (Section IV-5.3).

3) This thesis argues the case for an ecosystem perspective in data sampling. A wide range of different environmental parameter samples in conjunction with comprehensive plant traits sampling will enable systematic applications of recent data mining procedures for ecosystem mapping. The generation of open data archives for multiple processing routines, a better link between ecological field work and remote sensing capacities as well as an intensification of collaboration and communication between research and conservation practice forms the basis for wider range transferability and network applications (N. Pettorelli et al., 2014; Rose et al., 2015; Turner et al., 2015) as partly realized in GEO-BON (http://www.earthobservations.org /geobon.shtml), CRSNet (http://www.remote-sensing-biodiversity.org/networks/crsnet) or CEOS Biodiversity (http://www.ceos.org). As a contribution to shared network policies, within the scope of the thesis, two open data archives were generated and made freely accessible. A spectral library that incorporates vegetation surveys, field spectroscopic measurements and additional relief and soil parameters was supplied ("SPECTATION," 2015). Furthermore, the thesis provides hyperspectral imagery and linked field data on a web server that is complemented by standardized metadata protocols (Neumann et al., 2015a). Recent developments in spectroscopic database infrastructures (Bojinski et al., 2003; Kelly and Loescher, 2016; Zomer et al., 2009) and reinforced interdisciplinary networking will help to validate existing models, identify significant ecological measures and enable an advanced statistical testing of new methodologies and future imaging spectrometers.

4) One of the main issues that often complicate the transfer of spectral mapping procedures into conservation practice is the information itself that can be provided by imaging spectroscopy. Thereby the pixel unit integrates continuous biotic and abiotic properties based on sub-pixel entities that are transferred into information over an external model of inherent functional relationships. It crucially differs from terrestrial mapping units which are based on subjective perceptions and knowledge recombination in an internal modeling process at the level of the expert's mind. Since terrestrial sampling units have to cope with fractal properties of scale dependent species turnover (Johnson et al., 1992; Nekola and White, 1999; Palmer and White, 1994), the conflict rises in comparing mixed pixel information (e.g. species abundance, coexistence, spatial non-stationary gradients) during validation (Section IV-5.4). New dedicated validation frameworks are required in order to bridge the scales between field based point sampling and image based spatial continua that incorporate additional criteria

such as intentions of use, pattern plausibility, reproducibility of results or transferability to other settings (Aspinall, 2002; Vanden Borre et al., 2011).

2.4 Implications and Constraints for Prospective Imaging Spectrometer

Plant species and habitat mapping will become increasingly important for biodiversity conservation and ecological restoration from local to global scales. This chapter addresses new imaging technologies for the monitoring of local habitat management practice and coming hyperspectral satellite missions and arising implications for global conservation network policies.

1) Recent developments in the field of Unmanned Aerial Vehicles (UAV) allow for advanced sensor designs that unify high spatial resolutions (5-50 cm) with narrow spectral sampling intervals of continuous VIS-NIR-SWIR records into pushbroom scanning systems. Such systems are predestinated for fine-scale ecosystem characterizations, especially for supporting and evaluating local management activities and its influence on large scale pattern dynamics as observed in e.g. abandoned mountain meadow management (Herben et al., 1993; Krahulec et al., 2001). Evidence has been found that fine-scale spatial patterns of habitat parameters can help to better manage population viabilities since they have shown to provide optimal landscapes metrics to represent animal species abundances and habitat suitabilities (Fernández et al., 2003; Razgour et al., 2011). In this context, the developed approach provides a tool that joins common habitat parameter ordination at small-scale habitat ranges (Mattoni et al., 2000; Titeux et al., 2004) with recent hyperspectral information in order to derive fine-scale spatial patterns of habitat properties. Even though the ecological community highly favor UAV applications since they can deliver scale-appropriate measurements of ecological phenomena (Anderson and Gaston, 2013), critics are argued on safety, privacy and data security issues that need to be investigated in order to implement a good ethical practice for nature conservation efforts (Sandbrook, 2015).

2) The next generation of satellite hyperspectral imaging sensors promises great advances in regional to global scale ecosystem mapping. Based on the encouraging experiences in distinct species mapping from EO1 Hyperion imaging spectroscopy (Papeş et al., 2010; Pengra et al., 2007; Ramsey III et al., 2005), plant species gradient delineation, habitat quality assessment and habitat suitability modeling, as demonstrated in this thesis with airborne hyperspectral imaging, are likely to supply important methodological components for satellite based monitoring systems. The upcoming Environmental Mapping and Analysis Program (EnMAP) (Guanter et al., 2015; Kaufmann et al., 2008) will be the next operational space mission with a continuous VIS-SWIR spectral sampling in an improved signal-to noise ratio on 30 m spatial pixel sizes and an increased swath width of 30 km that allows a revisit time of 4 days. One of the main aspects of upcoming hyperspectral sensing from space will be the decreased spatial

resolution in comparison to airborne or UAV imaging. Thereby, the applicability of the developed approach depends on the spatial observation scale in which ecological processes influence landscape dynamics. The NMDS ordination itself generates a scale invariant representation of ecological interdependencies. The superimposed spectral model reflects dominance stands and transition that will be expressed by the modeled ecological context. The final model transfer to the image scale actually assumes that the local variance of species coexistence can be mapped within an appropriate spatial resolution. Otherwise the ecological process structure will be blurred in mixed pixel representations. In consequence, transition will be mapped in e.g. every 30 m pixel that can be considered to be real in images due to the calibrated spectral responses. However, such species maps will have only little relevance for distinguishing terrestrial habitat units if species turnover is differentiated at smaller scales. It is well known that each ecosystem exhibits unique patterns of local variance that need to be defined beforehand in order to allocate representative pixel scales (Woodcock and Strahler, 1987). On the other hand, one can integrate spatial mapping results into perceptions of refined ecosystem understandings (Section V-2.3 (4)) by defining spatially explicit ecosystem variables that prove their explanatory power with regard to terrestrial ecosystem processes. This is where another enlightening research field opens up new opportunities for satellite imaging spectroscopy. The first steps are done by introducing global, standardized and harmonized monitoring systems for biodiversity as realized in the concept of Essential Biodiversity Variables (EBV) (Pereira et al., 2013). The process of translating different EBVs into satellite based measurements and to evaluate their scalability have just getting started (O'Connor et al., 2015; Paganini et al., 2016; Pettorelli et al., 2016; Proença et al., 2016). The thesis contributes an applied methodological framework for realizing these coming monitoring requirements and for testing detailed and scale-adequate mapping routines.

References

Abrams, M.J., Hook, S.J., 2013. NASA's Hyperspectral Infrared Imager (HyspIRI), in: Kuenzer, C., Dech, S. (Eds.), Thermal Infrared Remote Sensing. Springer Netherlands, Dordrecht, pp. 117–130.

Adam, E., Mutanga, O., 2009. Spectral discrimination of papyrus vegetation (Cyperus papyrus L.) in swamp wetlands using field spectrometry. ISPRS J. Photogramm. Remote Sens. 64, 612–620.

Adam, E., Mutanga, O., Rugege, D., 2010. Multispectral and hyperspectral remote sensing for identification and mapping of wetland vegetation: a review. Wetl. Ecol. Manag. 18, 281–296.

Akaike, H., 1973. Information Theory and an Extension of the Maximum Likelihood Principle. B Petrov B Csake EdsSecond Int. Symp. Inf. Theory Akademai Kiado, Budapest.

Alvin, K.L., 1960. Observations on the Lichen Ecology of South Haven Peninsula, Studland Heath, Dorset. J. Ecol. 48, 331.

Anderson, K., Gaston, K.J., 2013. Lightweight unmanned aerial vehicles will revolutionize spatial ecology. Front. Ecol. Environ. 11, 138–146.

Andrew, M., Ustin, S., 2008. The role of environmental context in mapping invasive plants with hyperspectral image data. Remote Sens. Environ. 112, 4301–4317.

Apitz, S.E., Elliott, M., Fountain, M., Galloway, T.S., 2006. European environmental management: Moving to an ecosystem approach. Integr. Environ. Assess. Manag. 2, 80–85.

Aplin, P., 2005. Remote sensing: ecology. Prog. Phys. Geogr. 29, 104–113.

Armitage, R.P., Kent, M., Weaver, R.E., 2004. Identification of the spectral characteristics of British semi-natural upland vegetation using direct ordination: a case study from Dartmoor, UK. Int. J. Remote Sens. 25, 3369–3388.

Aronson, J., Clewell, A.F., Blignaut, J.N., Milton, S.J., 2006. Ecological restoration: A new frontier for nature conservation and economics. J. Nat. Conserv. 14, 135–139.

Artigas, F.J., Yang, J.S., 2005. Hyperspectral remote sensing of marsh species and plant vigour gradient in the New Jersey Meadowlands. Int. J. Remote Sens. 26, 5209–5220.

Asner, G.P., 1998. Biophysical and Biochemical Sources of Variability in Canopy Reflectance. Remote Sens. Environ. 64, 234–253.

Asner, G.P., Braswell, B.., Schimel, D.S., Wessman, C.A., 1998. Ecological Research Needs from Multiangle Remote Sensing Data. Remote Sens. Environ. 63, 155–165.

Asner, G.P., Jones, M.O., Martin, R.E., Knapp, D.E., Hughes, R.F., 2008. Remote sensing of native and invasive species in Hawaiian forests. Remote Sens. Environ. 112, 1912–1926.

Aspinall, R.J., 2002. Use of logistic regression for validation of maps of the spatial distribution of vegetation species derived from high spatial resolution hyperspectral remotely sensed data. Ecol. Model. 157, 301–312.

Atzberger, C., Guérif, M., Baret, F., Werner, W., 2010. Comparative analysis of three chemometric techniques for the spectroradiometric assessment of canopy chlorophyll content in winter wheat. Comput. Electron. Agric. 73, 165–173.

Ausden, M., 2007. Habitat Management for Conservation. Oxford University Press.

Austin, M.., 2002. Spatial prediction of species distribution: an interface between ecological theory and statistical modelling. Ecol. Model. 157, 101–118.
Austin, M.P., 1986. The theoretical basis of vegetation science. Trends Ecol. Evol. 1, 161–164.
Austin, M.P., 1985. Continuum concept, ordination methods, and niche theory. Annu. Rev. Ecol. Syst. 39–61.
Barbosa, J., Asner, G., Martin, R., Baldeck, C., Hughes, F., Johnson, T., 2016. Determining Subcanopy Psidium cattleianum Invasion in Hawaiian Forests Using Imaging Spectroscopy. Remote Sens. 8, 33.
Barclay-Estrup, P., Gimingham, C.H., 1969. The Description and Interpretation of Cyclical Processes in a Heath Community: I. Vegetational Change in Relation to the Calluna Cycle. J. Ecol. 57, 737.
Beier, W., Fürstenow, J., 2001. Übersicht zu den bisher nachgewiesenen Pflanzen-und Tierarten auf dem ehemaligen Truppenübungsplatz Döberitz. Döberitzer Heide Mit Ferbitzer Bruch–Beiträge Zum Naturschutz Zur Landsch. Zur Gesch. 11, 5–25.
Bestelmeyer, B.T., Trujillo, D.A., Tugel, A.J., Havstad, K.M., 2006. A multi-scale classification of vegetation dynamics in arid lands: What is the right scale for models, monitoring, and restoration? J. Arid Environ. 65, 296–318.
Blackburn, G.A., 2006. Hyperspectral remote sensing of plant pigments. J. Exp. Bot. 58, 855–867.
Bock, M., Rossner, G., Wissen, M., Remm, K., Langanke, T., Lang, S., Klug, H., Blaschke, T., Vrščaj, B., 2005. Spatial indicators for nature conservation from European to local scale. Ecol. Indic. 5, 322–338.
Bock, M., Xofis, P., Mitchley, J., Rossner, G., Wissen, M., 2005. Object-oriented methods for habitat mapping at multiple scales – Case studies from Northern Germany and Wye Downs, UK. J. Nat. Conserv. 13, 75–89.
Bojinski, S., Schaepman, M., Schläpfer, D., Itten, K., 2003. SPECCHIO: a spectrum database for remote sensing applications. Comput. Geosci. 29, 27–38.
Bonham, C.D., 2013a. Measurements for terrestrial vegetation, Second Edition. ed. Wiley-Blackwell, Chichester, West Sussex ; Hoboken, NJ.
Bonham, C.D., 2013b. Monitoring and Evaluation, in: Measurements for Terrestrial Vegetation. John Wiley & Sons, Ltd, Oxford, UK, pp. 217–235.
Borg, I., Groenen, P., 2005. Modern multidimensional scaling: Theory and applications. Springer, NY, USA.
Borregaard, T., Nielsen, H., Nørgaard, L., Have, H., 2000. Crop–weed Discrimination by Line Imaging Spectroscopy. J. Agric. Eng. Res. 75, 389–400. doi:10.1006/jaer.1999.0519
Braun-Blanquet, J., 1964. Pflanzensoziologie Grundzüge der Vegetationskunde. Springer Vienna, Vienna.
Burrows, C.J., 1991. Processes of Vegetation Change. Springer Netherlands, Dordrecht.
Calderón, R., Navas-Cortés, J.A., Lucena, C., Zarco-Tejada, P.J., 2013. High-resolution airborne hyperspectral and thermal imagery for early detection of Verticillium wilt of olive using fluorescence, temperature and narrow-band spectral indices. Remote Sens. Environ. 139, 231–245.
Cantarello, E., Newton, A.C., 2008. Identifying cost-effective indicators to assess the conservation status of forested habitats in Natura 2000 sites. For. Ecol. Manag. 256, 815–826.
Carter, G.A., 1994. Ratios of leaf reflectances in narrow wavebands as indicators of plant stress. Int. J. Remote Sens. 15, 697–703.

Carter, G.A., 1993. Responses of Leaf Spectral Reflectance to Plant Stress. Am. J. Bot. 80, 239–243.
Carter, G.A., Knapp, A.K., 2001. Leaf optical properties in higher plants: linking spectral characteristics to stress and chlorophyll concentration. Am. J. Bot. 88, 677–684.
CBD, 1992. United Nations Convention on Biological Diversity. Int. Leg. Mater. 818.
Chance, C.M., Coops, N.C., Crosby, K., Aven, N., 2016. Spectral Wavelength Selection and Detection of Two Invasive Plant Species in an Urban Area. Can. J. Remote Sens. 42, 27–40.
Cho, M.A., Skidmore, A., Corsi, F., Van Wieren, S.E., Sobhan, I., 2007. Estimation of green grass/herb biomass from airborne hyperspectral imagery using spectral indices and partial least squares regression. Int. J. Appl. Earth Obs. Geoinformation 9, 414–424.
Christakos, G., 1984. On the Problem of Permissible Covariance and Variogram Models. Water Resour. Res. 20, 251–265.
Christensen, S.N., 1989. Floristic and vegetational changes in a permanent plot in a Danish coastal dune heath, in: Annales Botanici Fennici. JSTOR, pp. 389–397.
Clark, M., Roberts, D., Clark, D., 2005. Hyperspectral discrimination of tropical rain forest tree species at leaf to crown scales. Remote Sens. Environ. 96, 375–398.
Clark, R.N., King, T.V.V., Gorelick, N.S., 1987. Automatic continuum analysis of reflectance spectra, in: Proceedings, Jet Propulsion Laboratory. Presented at the Third AIS workshop, JPL Publication, Pasadena, California, pp. 138–142.
Clarke, K.R., 1993. Non-parametric multivariate analyses of changes in community structure. Austral Ecol. 18, 117–143.
Clarke, K.R., Warwick, R.M., 2001. Change in Marine Communities: An Approach to Statistical Analysis and Interpretation, 2nd ed. PRIMER-E Ltd, Plymouth, UK.
Clements, F.E., 1916. Plant succession: an analysis of the development of vegetation. Carnegie Inst. Wash. No. 242.
Clevers, J.G., Kooistra, L., Schaepman, M.E., 2008. Using spectral information from the NIR water absorption features for the retrieval of canopy water content. Int. J. Appl. Earth Obs. Geoinformation 10, 388–397.
Clevers, J.G.P.W., Kooistra, L., Salas, E.A.L., 2004. Study of heavy metal contamination in river floodplains using the red-edge position in spectroscopic data. Int. J. Remote Sens. 25, 3883–3895.
Cochrane, M.A., 2000. Using vegetation reflectance variability for species level classification of hyperspectral data. Int. J. Remote Sens. 21, 2075–2087.
Cole, B., McMorrow, J., Evans, M., 2014. Empirical Modelling of Vegetation Abundance from Airborne Hyperspectral Data for Upland Peatland Restoration Monitoring. Remote Sens. 6, 716–739.
Corbane, C., Lang, S., Pipkins, K., Alleaume, S., Deshayes, M., Millán, V.E.G., Strasser, T., Borre, J.V., Toon, S., Foerster, M., 2015. Remote sensing for mapping natural habitats and their conservation status–New opportunities and challenges. Int. J. Appl. Earth Obs. Geoinformation 37, 7–16.
Crawley, M.J., 1996. Life History and Environment, in: Crawley, M.J. (Ed.), Plant Ecology. Blackwell Publishing Ltd., Oxford, UK, pp. 73–131.
Curran, P.J., 1989. Remote sensing of foliar chemistry. Remote Sens. Environ. 30, 271–278.
Curran, P.J., Dungan, J.L., Peterson, D.L., 2001. Estimating the foliar biochemical concentration of leaves with reflectance spectrometry. Remote Sens. Environ. 76, 349–359.
Cutler, D.R., Edwards, T.C., Beard, K.H., Cutler, A., Hess, K.T., Gibson, J., Lawler, J.J., 2007. Random Forest for Classification in Ecology. Ecology 88, 2783–2792.

Daily, G.C. (Ed.), 1997. Nature's services: societal dependence on natural ecosystems. Island Press, Washington, DC.
Dale, M.R.T., MacIsaac, D.A., 1989. New Methods for the Analysis of Spatial Pattern in Vegetation. J. Ecol. 77, 78.
Danson, F.M., Steven, M.D., Malthus, T.J., Clark, J.A., 1992. High-spectral resolution data for determining leaf water content. Int. J. Remote Sens. 13, 461–470
Dargie, T.C.D., 1984. On the integrated interpretation of indirect site ordinations: a case study using semi-arid vegetation in southeastern Spain. Vegetatio 55, 37–55.
Darvishzadeh, R., Atzberger, C., Skidmore, A., Schlerf, M., 2011. Mapping grassland leaf area index with airborne hyperspectral imagery: A comparison study of statistical approaches and inversion of radiative transfer models. ISPRS J. Photogramm. Remote Sens. 66, 894–906.
Dash, J., Curran, P.J., 2004. The MERIS terrestrial chlorophyll index. Inter. J. Remote Sens. 25, 5403–5413.
Datt, B., 1999. A New Reflectance Index for Remote Sensing of Chlorophyll Content in Higher Plants: Tests using Eucalyptus Leaves. J. Plant Physiol. 154, 30–36.
Daughtry, C.S.T., Nagler, P.L., Kim, M.S., McMurtrey III, J.E., Chappelle, E.W., 1996. Spectral reflectance of soils and crop residues. Near Infrared Spectroscopy: The FutureWaves. NIR Publications, Chichester, UK, pp. 505–510.
Day, M.B., Taylor, G.R., Roff, A.M., Mitchell, A.L., 2006. Hyperspectral discrimination of halophytic vegetation as an indicator of stressed arable land. J. Spat. Sci. 51, 115–128.
De'ath, G., 1999. Principal curves: a new technique for indirect and direct gradient analysis. Ecology 80, 2237–53.
Deb, K., Pratap, A., Agarwal, S., Meyarivan, T., 2002. A fast and elitist multiobjective genetic algorithm: NSGA-II. IEEE Trans. Evol. Comput. 6, 182–197.
DeFries, R., 2008. Terrestrial Vegetation in the Coupled Human-Earth System: Contributions of Remote Sensing. Annu. Rev. Environ. Resour. 33, 369–390.
Delalieux, S., Somers, B., Haest, B., Spanhove, T., Vanden Borre, J., Mücher, C.A., 2012. Heathland conservation status mapping through integration of hyperspectral mixture analysis and decision tree classifiers. Remote Sens. Environ. 126, 222–231.
Delcourt, H.R., Delcourt, P.A., Webb, T., 1982. Dynamic plant ecology: the spectrum of vegetational change in space and time. Quat. Sci. Rev. 1, 153–175.
Dietz, M.S., Belote, R.T., Aplet, G.H., Aycrigg, J.L., 2015. The world's largest wilderness protection network after 50years: An assessment of ecological system representation in the U.S. National Wilderness Preservation System. Biol. Conserv. 184, 431–438.
Dowd, P.A., 1984. The Variogram and Kriging: Robust and Resistant Estimators, in: Verly, G., David, M., Journel, A.G., Marechal, A. (Eds.), Geostatistics for Natural Resources Characterization. Springer Netherlands, Dordrecht, pp. 91–106.
Dudley, K.L., Dennison, P.E., Roth, K.L., Roberts, D.A., Coates, A.R., 2015. A multi-temporal spectral library approach for mapping vegetation species across spatial and temporal phenological gradients. Remote Sens. Environ. 167, 121–134.
Efron, B., Tibshirani, R.J., 1993. An introduction to the bootstrap, volume 57 of Monographs on Statistics and Applied Probability. Chapmann Hall.
EjrnÆs, R., Aude, E., Nygaard, B., Münier, B., 2002. Prediction of habitat quality using ordination and neural networks. Ecol. Appl. 12, 1180–1187.
Ellenberg, H., 1988. Vegetation ecology of central Europe, 4th ed. Cambridge University Press.
Ellenberg, H., Weber, H., Dull, R., Wirth, V., Werner, W., Paulissen, D., 1991. Zeigerwerte von Pflanzen in Mitteleuropa. Scripta Geobotanica, 18, 1–248. Hill MO Preston CD

Roy DB 2004 Plantatt Attrib. Br. Ir. Plants Status Size Life Hist. Geogr. Habitats Cent. Ecol. Hydrol. Monks Wood Cambs.
Ellis, E.C., Klein Goldewijk, K., Siebert, S., Lightman, D., Ramankutty, N., 2010. Anthropogenic transformation of the biomes, 1700 to 2000. Glob. Ecol. Biogeogr. 19 (5), 589-606.
Elvidge, C.D., 1990. Visible and near infrared reflectance characteristics of dry plant materials. Int. J. Remote Sens. 11, 1775–1795.
Epstein, Y., 2016. Favourable Conservation Status for Species: Examining the Habitats Directive's Key Concept through a Case Study of the Swedish Wolf. J. Environ. Law 28, 221–244.
EU, 1992. Council Directive 92/43/EEC of 21 May 1992 on the Conservation of Natural Habitats and of Wild Fauna and Flora.
Evans, D., Arvela, M., 2011. Assessment and Reporting under Article 17 of the Habitats Directive. Explanatory Notes and Guidelines for the Period 2007–2012. Eur. Top. Cent. Biol. Divers. Final Draft, Paris, France.
Evans, J.S., Cushman, S.A., 2009. Gradient modeling of conifer species using random forests. Landsc. Ecol. 24, 673–683.
Ewen, J.G., Armstrong, D.P., 2007. Strategic monitoring of reintroductions in ecological restoration programmes. Ecoscience 14, 401–409.
Faith, D.P., Minchin, P.R., Belbin, L., 1987. Compositional dissimilarity as a robust measure of ecological distance. Vegetatio 69, 57–68.
Fancy, S.G., Gross, J.E., Carter, S.L., 2009. Monitoring the condition of natural resources in US national parks. Environ. Monit. Assess. 151, 161–174.
Farrar, D.E., Glauber, R.R., 1967. Multicollinearity in Regression Analysis: The Problem Revisited. Rev. Econ. Stat. 49, 92.
Fassnacht, F.E., Neumann, C., Forster, M., Buddenbaum, H., Ghosh, A., Clasen, A., Joshi, K.P., Koch, B., 2014. Comparison of feature reduction algorithms for classifying tree species with hyperspectral data on three central European test sites. Sel. Top. Appl. Earth Obs. Remote Sens. IEEE J. Of 7, 2547–2561.
Feilhauer, H., Dahlke, C., Doktor, D., Lausch, A., Schmidtlein, S., Schulz, G., Stenzel, S., 2014. Mapping the local variability of Natura 2000 habitats with remote sensing. Appl. Veg. Sci. 17, 765–779.
Feilhauer, H., Faude, U., Schmidtlein, S., 2011. Combining Isomap ordination and imaging spectroscopy to map continuous floristic gradients in a heterogeneous landscape. Remote Sens. Environ. 115, 2513–2524.
Feilhauer, H., Oerke, E.-C., Schmidtlein, S., 2010. Quantifying empirical relations between planted species mixtures and canopy reflectance with PROTEST. Remote Sens. Environ. 114, 1513–1521.
Feilhauer, H., Schmidtlein, S., 2011. On variable relations between vegetation patterns and canopy reflectance. Ecol. Inform. 6, 83–92.
Feilhauer, H., Thonfeld, F., Faude, U., He, K.S., Rocchini, D., Schmidtlein, S., 2013. Assessing floristic composition with multispectral sensors—A comparison based on monotemporal and multiseasonal field spectra. Int. J. Appl. Earth Obs. Geoinformation 21, 218–229.
Feret, J.-B., Asner, G.P., 2013. Tree Species Discrimination in Tropical Forests Using Airborne Imaging Spectroscopy. IEEE Trans. Geosci. Remote Sens. 51, 73–84.
Fernández, N., Delibes, M., Palomares, F., Mladenoff, D.J., 2003. Identifying breeding habitat for the iberian Lynx: Inferences from a fine-scale spatial analysis. Ecol. Appl. 13, 1310–1324.

Ferrer-Paris, J.R., Rodríguez, J.P., Good, T.C., Sánchez-Mercado, A.Y., Rodríguez-Clark, K.M., Rodríguez, G.A., Solís, A., 2013. Systematic, large-scale national biodiversity surveys: NeoMaps as a model for tropical regions. Divers. Distrib. 19, 215–231.

Ferringer, M.P., Spencer, D.B., 2006. Satellite Constellation Design Tradeoffs Using Multiple-Objective Evolutionary Computation. J. Spacecr. Rockets 43, 1404–1411.

Förster, M., Frick, A., Walentowski, H., Kleinschmit, B., 2008. Approaches to utilising QuickBird data for the monitoring of NATURA 2000 habitats. Community Ecol. 9, 155–168.

Fourty, T., Baret, F., Jacquemoud, S., Schmuck, G., Verdebout, J., 1996. Leaf optical properties with explicit description of its biochemical composition: Direct and inverse problems. Remote Sens. Environ. 56, 104–117.

Franklin, J., 1995. Predictive vegetation mapping: geographic modelling of biospatial patterns in relation to environmental gradients. Prog. Phys. Geogr. 19, 474–499.

Galvão, L.S., Formaggio, A.R., Tisot, D.A., 2005. Discrimination of sugarcane varieties in Southeastern Brazil with EO 1 Hyperion data. Remote Sens. Environ. 94, 523–534.

Gamon, J.A., Surfus, J.S., 1999. Assessing leaf pigment content and activity with a reflectometer. New Phytol. 143 (1), 105–117.

Gao, B.C., 1996. NDWI—A normalized difference water index for remote sensing of vegetation liquid water from space. Remote Sens. Environ. 58, 257–266

Gao, T., Qiu, L., Hammer, M., Gunnarsson, A., 2012. The Importance of Temporal and Spatial Vegetation Structure Information in Biotope Mapping Schemes: A Case Study in Helsingborg, Sweden. Environ. Manage. 49, 459–472.

Gates, D.M., Keegan, H.J., Schleter, J.C., Weidner, V.R., 1965. Spectral properties of plants. Appl. Opt. 4, 11–20.

Gauch, H.G., 1982. Multivariate analysis in community ecology, Cambridge studies in ecology. Cambridge University Press, Cambridge [Cambridgeshire] ; New York.

Gausman, H.W., Allen, W.A., Cardenas, R., Richardson, A.J., 1970. Relation of Light Reflectance to Histological and Physical Evaluations of Cotton Leaf Maturity. Appl. Opt. 9, 545.

Geldmann, J., Barnes, M., Coad, L., Craigie, I.D., Hockings, M., Burgess, N.D., 2013. Effectiveness of terrestrial protected areas in reducing habitat loss and population declines. Biol. Conserv. 161, 230–238.

Gitelson, A.A., Merzlyak, M.N., 1994. Spectral Reflectance Changes Associated with Autumn Senescence of Aesculus hippocastanum L. and Acer platanoides L. Leaves. Spectral Features and Relation to Chlorophyll Estimation. J. Plant Physiol. 143, 286–292.

Gitelson, A.A., Merzlyak,M.N., Chivkunova, O.B., 2001. Optical Properties and Nondestructive Estimation of Anthocyanin Content in Plant Leaves. Photochem. Photobiol. 74, 38–45.

Gitelson, A.A., Gritz †, Y., Merzlyak, M.N., 2003. Relationships between leaf chlorophyll content and spectral reflectance and algorithms for non-destructive chlorophyll assessment in higher plant leaves. J. Plant Physiol. 160, 271–282.

Gleason, H.A., 1926. The Individualistic Concept of the Plant Association. Bull. Torrey Bot. Club 53, 7.

Gong, P., 1997. Conifer species recognition: An exploratory analysis of in situ hyperspectral data. Remote Sens. Environ. 62, 189–200.

Goodall, D.W., 1963. The continuum and the individualistic association. Vegetatio 11, 297–316.

Gorsich, D.J., Genton, M.G., 2000. Variogram model selection via nonparametric derivative estimation. Math. Geol. 32, 249–270.
Gosz, J.R., 1991. Fundamental Ecological Characteristics of Landscape Boundaries, in: Holland, M.M., Risser, P.G., Naiman, R.J. (Eds.), Ecotones. Springer US, Boston, MA, pp. 8–30.
Gould, W., 2000. Remote sensing of vegetation, species richness and regional biodiversity hotspots. Ecol. Appl. 10, 1861–1870.
Graham, M.H., 2003. Confronting multicollinearity in ecological multiple Regression. Ecology 84, 2809–2815.
Grime, J.P., 2006. Plant strategies, vegetation processes, and ecosystem properties, 2. ed. ed. Wiley, Chichester.
Guanter, L., Kaufmann, H., Segl, K., Foerster, S., Rogass, C., Chabrillat, S., Kuester, T., Hollstein, A., Rossner, G., Chlebek, C., Straif, C., Fischer, S., Schrader, S., Storch, T., Heiden, U., Mueller, A., Bachmann, M., Mühle, H., Müller, R., Habermeyer, M., Ohndorf, A., Hill, J., Buddenbaum, H., Hostert, P., van der Linden, S., Leitão, P., Rabe, A., Doerffer, R., Krasemann, H., Xi, H., Mauser, W., Hank, T., Locherer, M., Rast, M., Staenz, K., Sang, B., 2015. The EnMAP Spaceborne Imaging Spectroscopy Mission for Earth Observation. Remote Sens. 7, 8830–8857.
Guisan, A., Zimmermann, N.E., 2000. Predictive habitat distribution models in ecology. Ecol. Model. 135, 147–186.
Haboudane, D., Miller, J.R., Tremblay, N., Zarco Tejada, P.J., Dextraze, L., 2002. Integrated narrow band vegetation indices for prediction of crop chlorophyll content for application to precision agriculture. Remote Sens. Environ. 81, 416–426.
Haest, B., Thoonen, G., Borre, J.V., Spanhove, T., Delalieux, S., Bertels, L., Kooistra, L., Mücher, C.A., Scheunders, P., 2010. An object-based approach to quantity and quality assessment of heathland habitats in the framework of NATURA 2000 using hyperspectral airborne AHS images. Proc. Third Int. Conf. Asp. Geogr. Object-Based Image Anal. Gent, Belgium.
Ham, J., Chen, Y., Crawford, M.M., Ghosh, J., 2005. Investigation of the random forest framework for classification of hyperspectral data. IEEE Trans. Geosci. Remote Sens. 43, 492–501.
Hamada, Y., Stow, D.A., Coulter, L.L., Jafolla, J.C., Hendricks, L.W., 2007. Detecting Tamarisk species (Tamarix spp.) in riparian habitats of Southern California using high spatial resolution hyperspectral imagery. Remote Sens. Environ. 109, 237–248.
Hansen, P.M., Schjoerring, J.K., 2003. Reflectance measurement of canopy biomass and nitrogen status in wheat crops using normalized difference vegetation indices and partial least squares regression. Remote Sens. Environ. 86, 542–553.
Hauser, M., Mucina, L., 1991. Spatial Interpolation Methods for Interpretation of Ordination Diagrams, in: Feoli, E., Orlóci, L. (Eds.), Computer Assisted Vegetation Analysis. Springer Netherlands, Dordrecht, pp. 299–316.
Hautier, Y., Tilman, D., Isbell, F., Seabloom, E.W., Borer, E.T., Reich, P.B., 2015. Anthropogenic environmental changes affect ecosystem stability via biodiversity. Science 348, 336–340.
He, K.S., Bradley, B.A., Cord, A.F., Rocchini, D., Tuanmu, M.-N., Schmidtlein, S., Turner, W., Wegmann, M., Pettorelli, N., 2015a. Will remote sensing shape the next generation of species distribution models? Remote Sens. Ecol. Conserv. 1, 4–18.
He, K.S., Bradley, B.A., Cord, A.F., Rocchini, D., Tuanmu, M.-N., Schmidtlein, S., Turner, W., Wegmann, M., Pettorelli, N., 2015b. Will remote sensing shape the next generation of species distribution models? Remote Sens. Ecol. Conserv. 1, 4–18.

Hengl, T., Heuvelink, G.B.M., Rossiter, D.G., 2007a. About regression-kriging: From equations to case studies. Comput. Geosci. 33, 1301–1315.
Hengl, T., Toomanian, N., Reuter, H.I., Malakouti, M.J., 2007b. Methods to interpolate soil categorical variables from profile observations: Lessons from Iran. Geoderma 140, 417–427.
Herben, T., Krahulec, F., Hadincová, V., Skálová, H., 1993. Small-scale variability as a mechanism for large-scale stability in mountain grasslands. J. Veg. Sci. 4, 163–170.
Herrick, J.E., Schuman, G.E., Rango, A., 2006. Monitoring ecological processes for restoration projects. J. Nat. Conserv. 14, 161–171.
Herrmann, I., Karnieli, A., Bonfil, D.J., Cohen, Y., Alchanatis, V., 2010. SWIR based spectral indices for assessing nitrogen content in potato fields. Inter. J. Remote Sens. 31, 5127–5143.
Hiemstra, P.H., Pebesma, E.J., Twenhöfel, C.J.W., Heuvelink, G.B.M., 2009. Real-time automatic interpolation of ambient gamma dose rates from the Dutch radioactivity monitoring network. Comput. Geosci. 35, 1711–1721.
Hill, M.O., 1973. Reciprocal averaging: an eigenvector method of ordination. J. Ecol. 61, 237–249.
Hill, M.O., Gauch, H.G., 1980. Detrended correspondence analysis: An improved ordination technique. Vegetatio 42, 47–58.
Hill, M.O., Roy, D.B., Thompson, K., 2002. Hemeroby, urbanity and ruderality: bioindicators of disturbance and human impact. J. Appl. Ecol. 39, 708–720.
HilleRisLambers, R., Rietkerk, M., van den Bosch, F., Prins, H.H.T., de Kroon, H., 2001. Vegetation Pattern Formation in Semi-Arid Grazing Systems. Ecology 82, 50.
Himmelsbach, D.S., 1989. Use of Modern NMR Spectroscopy in Plant Cell Wall Research, in: Chesson, A., Ørskov, E.R. (Eds.), Physico-Chemical Characterisation of Plant Residues for Industrial and Feed Use. Springer Netherlands, Dordrecht, pp. 3–12.
Hockings, M., 2003. Systems for Assessing the Effectiveness of Management in Protected Areas. BioScience 53, 823.
Hodgson, J.A., Moilanen, A., Wintle, B.A., Thomas, C.D., 2011. Habitat area, quality and connectivity: striking the balance for efficient conservation: Area, quality and connectivity. J. Appl. Ecol. 48, 148–152.
Hooper, D.U., Chapin, F.S., Ewel, J.J., Hector, A., Inchausti, P., Lavorel, S., Lawton, J.H., Lodge, D.M., Loreau, M., Naeem, S., Schmid, B., Setälä, H., Symstad, A.J., Vandermeer, J., Wardle, D.A., 2005. Effects of Biodiversity on Ecosystem Functioning: A Consensus of Current Knowledge. Ecol. Monogr. 75, 3–35.
Höskuldsson, A., 1988. PLS regression methods. J. Chemom. 2, 211–228.
Hotelling, H., 1933. Analysis of a complex of statistical variables into principal components. J. Educ. Psychol. 24, 417–441.
Huang, Z., Turner, B.J., Dury, S.J., Wallis, I.R., Foley, W.J., 2004. Estimating foliage nitrogen concentration from HYMAP data using continuum removal analysis. Remote Sens. Environ. 93, 18–29.
Hudson, L.N., Newbold, T., Contu, S., Hill, S.L.L., Lysenko, I., De Palma, A., Phillips, H.R.P., Senior, R.A., Bennett, D.J., Booth, H., Choimes, A., Correia, D.L.P., Day, J., Echeverría-Londoño, S., Garon, M., Harrison, M.L.K., Ingram, D.J., Jung, M., Kemp, V., Kirkpatrick, L., Martin, C.D., Pan, Y., White, H.J., Aben, J., Abrahamczyk, S., Adum, G.B., Aguilar-Barquero, V., Aizen, M.A., Ancrenaz, M., Arbeláez-Cortés, E., Armbrecht, I., Azhar, B., Azpiroz, A.B., Baeten, L., Báldi, A., Banks, J.E., Barlow, J., Batáry, P., Bates, A.J., Bayne, E.M., Beja, P., Berg, Å., Berry, N.J., Bicknell, J.E., Bihn, J.H., Böhning-Gaese, K., Boekhout, T., Boutin, C., Bouyer, J., Brearley, F.Q.,

Brito, I., Brunet, J., Buczkowski, G., Buscardo, E., Cabra-García, J., Calviño-Cancela, M., Cameron, S.A., Cancello, E.M., Carrijo, T.F., Carvalho, A.L., Castro, H., Castro-Luna, A.A., Cerda, R., Cerezo, A., Chauvat, M., Clarke, F.M., Cleary, D.F.R., Connop, S.P., D'Aniello, B., da Silva, P.G., Darvill, B., Dauber, J., Dejean, A., Diekötter, T., Dominguez-Haydar, Y., Dormann, C.F., Dumont, B., Dures, S.G., Dynesius, M., Edenius, L., Elek, Z., Entling, M.H., Farwig, N., Fayle, T.M., Felicioli, A., Felton, A.M., Ficetola, G.F., Filgueiras, B.K.C., Fonte, S.J., Fraser, L.H., Fukuda, D., Furlani, D., Ganzhorn, J.U., Garden, J.G., Gheler-Costa, C., Giordani, P., Giordano, S., Gottschalk, M.S., Goulson, D., Gove, A.D., Grogan, J., Hanley, M.E., Hanson, T., Hashim, N.R., Hawes, J.E., Hébert, C., Helden, A.J., Henden, J.-A., Hernández, L., Herzog, F., Higuera-Diaz, D., Hilje, B., Horgan, F.G., Horváth, R., Hylander, K., Isaacs-Cubides, P., Ishitani, M., Jacobs, C.T., Jaramillo, V.J., Jauker, B., Jonsell, M., Jung, T.S., Kapoor, V., Kati, V., Katovai, E., Kessler, M., Knop, E., Kolb, A., Kőrösi, Á., Lachat, T., Lantschner, V., Le Féon, V., LeBuhn, G., Légaré, J.-P., Letcher, S.G., Littlewood, N.A., López-Quintero, C.A., Louhaichi, M., Lövei, G.L., Lucas-Borja, M.E., Luja, V.H., Maeto, K., Magura, T., Mallari, N.A., Marin-Spiotta, E., Marshall, E.J.P., Martínez, E., Mayfield, M.M., Mikusinski, G., Milder, J.C., Miller, J.R., Morales, C.L., Muchane, M.N., Muchane, M., Naidoo, R., Nakamura, A., Naoe, S., Nates-Parra, G., Navarrete Gutierrez, D.A., Neuschulz, E.L., Noreika, N., Norfolk, O., Noriega, J.A., Nöske, N.M., O'Dea, N., Oduro, W., Ofori-Boateng, C., Oke, C.O., Osgathorpe, L.M., Paritsis, J., Parra-H, A., Pelegrin, N., Peres, C.A., Persson, A.S., Petanidou, T., Phalan, B., Philips, T.K., Poveda, K., Power, E.F., Presley, S.J., Proença, V., Quaranta, M., Quintero, C., Redpath-Downing, N.A., Reid, J.L., Reis, Y.T., Ribeiro, D.B., Richardson, B.A., Richardson, M.J., Robles, C.A., Römbke, J., Romero-Duque, L.P., Rosselli, L., Rossiter, S.J., Roulston, T.H., Rousseau, L., Sadler, J.P., Sáfián, S., Saldaña-Vázquez, R.A., Samnegård, U., Schüepp, C., Schweiger, O., Sedlock, J.L., Shahabuddin, G., Sheil, D., Silva, F.A.B., Slade, E.M., Smith-Pardo, A.H., Sodhi, N.S., Somarriba, E.J., Sosa, R.A., Stout, J.C., Struebig, M.J., Sung, Y.-H., Threlfall, C.G., Tonietto, R., Tóthmérész, B., Tscharntke, T., Turner, E.C., Tylianakis, J.M., Vanbergen, A.J., Vassilev, K., Verboven, H.A.F., Vergara, C.H., Vergara, P.M., Verhulst, J., Walker, T.R., Wang, Y., Watling, J.I., Wells, K., Williams, C.D., Willig, M.R., Woinarski, J.C.Z., Wolf, J.H.D., Woodcock, B.A., Yu, D.W., Zaitsev, A.S., Collen, B., Ewers, R.M., Mace, G.M., Purves, D.W., Scharlemann, J.P.W., Purvis, A., 2014. The PREDICTS database: a global database of how local terrestrial biodiversity responds to human impacts. Ecol. Evol. 4, 4701–4735.

Hughes, G., 1968. On the mean accuracy of statistical pattern recognizers. IEEE Trans. Inf. Theory 14, 55–63.

Huntjr, E., Rock, B., 1989. Detection of changes in leaf water content using Near- and Middle-Infrared reflectances. Remote Sens. Environ. 30, 43–54.

Hunt, E.R., Daughtry, C.S.T., Eitel, J.U., Long, D.S., 2011. Remote sensing leaf chlorophyll content using a visible band index. Agron. J. 103, 1090–1099.

Hunt Jr., E.R., Rock, B.N., 1989. Detection of changes in leaf water content using near and middle infrared reflectances. Remote Sens. Environ. 30, 43–54.

Hunt Jr., R., Rock, B.N., Nobel, P.S., 1987. Measurement of leaf relative water content by infrared reflectance. Remote Sens. Environ. 22, 429–435.

Huston, M., Smith, T., 1987. Plant Succession: Life History and Competition. Am. Nat. 130, 168–198.

Irisarri, J.G.N., Oesterheld, M., Verón, S.R., Paruelo, J.M., 2009. Grass species differentiation through canopy hyperspectral reflectance. Int. J. Remote Sens. 30, 5959–5975.
Jackson, R.D., 1986. Remote Sensing of Biotic and Abiotic Plant Stress. Ann Rev Phytopathol 24, 265–287.
Jago, R.A., Cutler, M.E., Curran, P.J., 1999. Estimating canopy chlorophyll concentration from field and airborne spectra. Remote Sens. Environ. 68, 217–224.
Jalas, J., 1955. Hemerobe und hemerochore Pflanzenarten. Ein terminologischer Reformversuch. Acta Soc. Fauna Flora Fenn. 72, 1–15.
Jeltsch, F., Bonte, D., Pe'er, G., Reineking, B., Leimgruber, P., Balkenhol, N., Schröder, B., Buchmann, C.M., Mueller, T., Blaum, N., Zurell, D., Böhning-Gaese, K., Wiegand, T., Eccard, J.A., Hofer, H., Reeg, J., Eggers, U., Bauer, S., 2013. Integrating movement ecology with biodiversity research - exploring new avenues to address spatiotemporal biodiversity dynamics. Mov. Ecol. 1, 6.
Jentsch, A., Kreyling, J., Boettcher-Treschkow, J., Beierkuhnlein, C., 2009. Beyond gradual warming: extreme weather events alter flower phenology of European grassland and heath species. Glob. Change Biol. 15, 837–849.
Johnson, A.R., Milne, B.T., Wiens, J.A., 1992. Diffusion in Fractcal Landscapes: Simulations and Experimental Studies of Tenebrionid Beetle Movements. Ecology 73, 1968–1983.
Jongman, R.H., Kristiansen, I., Council of Europe, Committee for the Activities of the Council of Europe in the field of Biological and Landscape Diversity, 2001. National and regional approaches for ecological networks in Europe. Council of Europe Pub., Strasbourg.
Jordan, W.R. (Ed.), 1996. Restoration ecology: a synthetic approach to ecological research, Repr. ed. Cambridge Univ. Press, Cambridge.
Juffe-Bignoli, D., Burgess, N.D., Bingham, H., Belle, E., de Lima, M., Deguignet, M., Bertzky, B., Milam, A., Martinez-Lopez, J., Lewis, E., others, 2014. Protected planet report 2014. Camb. UK UNEP-WCMC.
Kahmen, A., Perner, J., Audorff, V., Weisser, W., Buchmann, N., 2005. Effects of plant diversity, community composition and environmental parameters on productivity in montane European grasslands. Oecologia 142, 606–615.
Kaufmann, H., Segl, K., Guanter, L., Hofer, S., Foerster, K.-P., Stuffler, T., Mueller, A., Richter, R., Bach, H., Hostert, P., Chlebek, C., 2008. Environmental Mapping and Analysis Program (EnMAP) - Recent Advances and Status. IEEE, p. IV-109-IV-112.
Keddy, P.A., 2007. Plants and vegetation: origins, processes, consequences. Cambridge University Press, Cambridge ; New York.
Kelly, E.F., Loescher, H.W., 2016. NEON Reboot. BioScience 66, 711–711.
Kerr, J.T., Ostrovsky, M., 2003. From space to species: ecological applications for remote sensing. Trends Ecol. Evol. 18, 299–305.
Khare, V., Yao, X., Deb, K., 2003. Performance Scaling of Multi-objective Evolutionary Algorithms, in: Fonseca, C.M., Fleming, P.J., Zitzler, E., Thiele, L., Deb, K. (Eds.), Evolutionary Multi-Criterion Optimization. Springer Berlin Heidelberg, Berlin, Heidelberg, pp. 376–390.
Knipling, E.B., 1970. Physical and physiological basis for the reflectance of visible and near-infrared radiation from vegetation. Remote Sens. Environ. 1, 155–159.
Knox, R.G., Peet, R.K., 1989. Bootstrapped ordination: a method for estimating sampling effects in indirect gradient analysis. Vegetatio 80, 153–165.
Kokaly, R.F., 2001. Investigating a Physical Basis for Spectroscopic Estimates of Leaf Nitrogen Concentration. Remote Sens. Environ. 75, 153–161.

Kokaly, R.F., Clark, R.N., 1999. Spectroscopic determination of leaf biochemistry using band-depth analysis of absorption features and stepwise multiple linear regression. Remote Sens. Environ. 67, 267–287.

Kooistra, L., Salas, E.A.L., Clevers, J.G.P.W., Wehrens, R., Leuven, R.S.E.W., Nienhuis, P.H., Buydens, L.M.C., 2004. Exploring field vegetation reflectance as an indicator of soil contamination in river floodplains. Environ. Pollut. 127, 281–290.

Krahulec, F., Skálová, H., Herben, T., Hadincová, V., Wildová, R., Pecháčková, S., 2001. Vegetation changes following sheep grazing in abandoned mountain meadows. Appl. Veg. Sci. 4, 97–102.

Kruskal, J.B., 1964. Multidimensional scaling by optimizing goodness of fit to a nonmetric hypothesis. Psychometrika 29, 1–27.

Kubinyi, H., 1996. Evolutionary variable selection in regression and PLS analyses. J. Chemom. 10, 119–133.

Küchler, A.W., Zonneveld, I.S. (Eds.), 1988. Vegetation mapping. Springer Netherlands, Dordrecht.

Kumar, L., Schmidt, K., Dury, S., Skidmore, A., 2002. Imaging Spectrometry and Vegetation Science, in: Meer, F.D. van der, Jong, S.M.D. (Eds.), Imaging Spectrometry. Springer Netherlands, Dordrecht, pp. 111–155.

Laba, M., Tsai, F., Ogurcak, D., Smith, S., Richmond, M.E., 2005. Field Determination of Optimal Dates for the Discrimination of Invasive Wetland Plant Species Using Derivative Spectral Analysis. Photogramm. Eng. Remote Sens. 71, 603–611.

Lake, P.S., 2001. On the maturing of restoration: Linking ecological research and restoration. Ecol. Manag. Restor. 2, 110–115.

LANA, 2015. Beschlüsse der Arbeitsgemeinschaft “Naturschutz” der Landesumweltministerien. http://www.bfn.de/fileadmin/MDB/documents/030306_lana.pdf (accessed on 14 November 2016

Lausch, A., Bannehr, L., Beckmann, M., Boehm, C., Feilhauer, H., Hacker, J.M., Heurich, M., Jung, A., Klenke, R., Neumann, C., Pause, M., Rocchini, D., Schaepman, M.E., Schmidtlein, S., Schulz, K., Selsam, P., Settele, J., Skidmore, A.K., Cord, A.F., 2016. Linking Earth Observation and taxonomic, structural and functional biodiversity: Local to ecosystem perspectives. Ecol. Indic. 70, 317–339.

Lausch, A., Pause, M., Merbach, I., Zacharias, S., Doktor, D., Volk, M., Seppelt, R., 2013. A new multiscale approach for monitoring vegetation using remote sensing-based indicators in laboratory, field, and landscape. Environ. Monit. Assess. 185, 1215–1235.

Law, R., Illian, J., Burslem, D.F.R.P., Gratzer, G., Gunatilleke, C.V.S., Gunatilleke, I.A.U.N., 2009. Ecological information from spatial patterns of plants: insights from point process theory. J. Ecol. 97, 616–628.

Lawler, J.J., Olden, J.D., 2011. Reframing the debate over assisted colonization. Front. Ecol. Environ. 9, 569–574.

Lawrence, M.J., Stemberger, H.L.J., Zolderdo, A.J., Struthers, D.P., Cooke, S.J., 2015. The effects of modern war and military activities on biodiversity and the environment. Environ. Rev. 23, 443–460.

Lawrence, R.L., Wood, S.D., Sheley, R.L., 2006. Mapping invasive plants using hyperspectral imagery and Breiman Cutler classifications (RandomForest). Remote Sens. Environ. 100, 356–362.

Legendre, P., Fortin, M.J., 1989. Spatial pattern and ecological analysis. Vegetatio 80, 107–138.

Levin, S.A., 1987. Scale and Predictability in Ecological Modeling, in: Vincent, T.L., Cohen, Y., Grantham, W.J., Kirkwood, G.P., Skowronski, J.M. (Eds.), Modeling and Management of Resources under Uncertainty. Springer Berlin Heidelberg, Berlin, Heidelberg, pp. 2–10.

Loreau, M., 2001. Biodiversity and Ecosystem Functioning: Current Knowledge and Future Challenges. Science 294, 804–808.

Loss, S.R., Terwilliger, L.A., Peterson, A.C., 2011. Assisted colonization: Integrating conservation strategies in the face of climate change. Biol. Conserv. 144, 92–100.

Louette, G., Adriaens, D., Paelinckx, D., Hoffmann, M., 2015. Implementing the Habitats Directive: How science can support decision making. J. Nat. Conserv. 23, 27–34.

Lowe, D.G., 2004. Distinctive image features from scale-invariant keypoints. Int. J. Comput. Vis. 60, 91–110.

Lu, S., Shimizu, Y., Ishii, J., Funakoshi, S., Washitani, I., Omasa, K., 2009. Estimation of abundance and distribution of two moist tall grasses in the Watarase wetland, Japan, using hyperspectral imagery. ISPRS J. Photogramm. Remote Sens. 64, 674–682.

Łuczaj, Ł., Sadowska, B., 1997. Edge effect in different groups of organisms: vascular plant, bryophyte and fungi species richness across a forest-grassland border. Folia Geobot. Phytotaxon. 32, 343–353.

Luft, L., Neumann, C., Freude, M., Blaum, N., Jeltsch, F., 2014. Hyperspectral modeling of ecological indicators – A new approach for monitoring former military training areas. Ecol. Indic. 46, 264–285.

Luft, L., Neumann, C., Itzerott, S., Lausch, A., Doktor, D., Freude, M., Blaum, N., Jeltsch, F., 2016. Digital and real-habitat modeling of Hipparchia statilinus based on hyper spectral remote sensing data. Int. J. Environ. Sci. Technol. 13, 187–200.

Maarel, E. van der (Ed.), 2005. Vegetation ecology. Blackwell Pub, Malden, MA.

Maccioni, A., Agati, G., Mazzinghi, P., 2001. New vegetation indices for remote measurement of chlorophylls based on leaf directional reflectance spectra. J. Photochem. Photobiol. B Biol. 61, 52–61.

Maestre, F.T., Quero, J.L., Gotelli, N.J., Escudero, A., Ochoa, V., Delgado-Baquerizo, M., Garcia-Gomez, M., Bowker, M.A., Soliveres, S., Escolar, C., Garcia-Palacios, P., Berdugo, M., Valencia, E., Gozalo, B., Gallardo, A., Aguilera, L., Arredondo, T., Blones, J., Boeken, B., Bran, D., Conceicao, A.A., Cabrera, O., Chaieb, M., Derak, M., Eldridge, D.J., Espinosa, C.I., Florentino, A., Gaitan, J., Gatica, M.G., Ghiloufi, W., Gomez-Gonzalez, S., Gutierrez, J.R., Hernandez, R.M., Huang, X., Huber-Sannwald, E., Jankju, M., Miriti, M., Monerris, J., Mau, R.L., Morici, E., Naseri, K., Ospina, A., Polo, V., Prina, A., Pucheta, E., Ramirez-Collantes, D.A., Romao, R., Tighe, M., Torres-Diaz, C., Val, J., Veiga, J.P., Wang, D., Zaady, E., 2012. Plant Species Richness and Ecosystem Multifunctionality in Global Drylands. Science 335, 214–218.

Makisara, K., Meinander, M., Rantasuo, M., Okkonen, J., Aikio, M., Sipola, K., 1993. Airborne imaging spectrometer for applications (AISA). IEEE, pp. 479–481.

Manevski, K., Manakos, I., Petropoulos, G.P., Kalaitzidis, C., 2011. Discrimination of common Mediterranean plant species using field spectroradiometry. Int. J. Appl. Earth Obs. Geoinformation 13, 922–933.

ManjarréS-MartíNez, L.M., GutiéRrez-Estrada, J.C., Hernando, J.A., Soriguer, M.C., 2012. The performance of three ordination methods applied to demersal fish data sets: stability and interpretability: PERFORMANCE OF ORDINATION METHODS ON DEMERSAL DATA. Fish. Manag. Ecol. 19, 200–213.

Marrs, R., 1986. The role of catastrophic death of Calluna in heathland dynamics. Vegetatio 66, 109–115.
Marvin, D.C., Asner, G.P., Schnitzer, S.A., 2016. Liana canopy cover mapped throughout a tropical forest with high-fidelity imaging spectroscopy. Remote Sens. Environ. 176, 98–106.
Matheron, G., 1971. The theory of regionalized variables and its applications. École national supérieure des mines.
Matheron, G., 1970. Random Functions and their Application in Geology, in: Merriam, D.F. (Ed.), Geostatistics. Springer US, Boston, MA, pp. 79–87.
Matheron, G., 1963. Principles of geostatistics. Econ. Geol. 58, 1246–1266.
Mattoni, R., Longcore, T., Novotny, V., 2000. ENVIRONMENTAL AUDITING: Arthropod Monitoring for Fine-Scale Habitat Analysis: A Case Study of the El Segundo Sand Dunes. Environ. Manage. 25, 445–452.
McGwire, K., 2000. Hyperspectral Mixture Modeling for Quantifying Sparse Vegetation Cover in Arid Environments. Remote Sens. Environ. 72, 360–374.
McIntosh, R.P., 1967. The continuum concept of vegetation. Bot. Rev. 33, 130–187.
Mehmood, T., Liland, K.H., Snipen, L., Sæbø, S., 2012. A review of variable selection methods in partial least squares regression. Chemom. Intell. Lab. Syst. 118, 62–69.
Melgani, F., Bruzzone, L., 2004. Classification of hyperspectral remote sensing images with support vector machines. IEEE Trans. Geosci. Remote Sens. 42, 1778–1790.
Mersmann, O., 2014. mco: Multiple Criteria Optimization Algorithms and Related Functions, R package.
Merzlyak, M.N., Gitelson, A.A., Chivkunova, O.B., Rakitin, V.Y., 1999. Non-destructive optical detection of pigment changes during leaf senescence and fruit ripening. Physiol. Plant. 106, 135–141.
Miao, X., Gong, P., Swope, S., Pu, R., Carruthers, R., Anderson, G.L., Heaton, J.S., Tracy, C.R., 2006. Estimation of yellow starthistle abundance through CASI-2 hyperspectral imagery using linear spectral mixture models. Remote Sens. Environ. 101, 329–341.
Miles, J., Schmidt, W., van der Maarel, E. (Eds.), 1989. Temporal and Spatial Patterns of Vegetation Dynamics. Springer Netherlands, Dordrecht.
Möckel, T., Löfgren, O., Prentice, H.C., Eklundh, L., Hall, K., 2016. Airborne hyperspectral data predict Ellenberg indicator values for nutrient and moisture availability in dry grazed grasslands within a local agricultural landscape. Ecol. Indic. 66, 503–516.
Moravec, J., 1989. Influences of the individualistic concept of vegetation on syntaxonomy. Vegetatio 81, 29–39.
Mücher, C.A., Hennekens, S.M., Bunce, R.G.H., Schaminée, J.H.J., Schaepman, M.E., 2009. Modelling the spatial distribution of Natura 2000 habitats across Europe. Landsc. Urban Plan. 92, 148–159.
Mücher, C.A., Kooistra, L., Vermeulen, M., Borre, J.V., Haest, B., Haveman, R., 2013. Quantifying structure of Natura 2000 heathland habitats using spectral mixture analysis and segmentation techniques on hyperspectral imagery. Ecol. Indic. 33, 71–81.
Mutanga, O., Skidmore, A.K., 2003. Continuum-removed absorption features estimate tropical savanna grass quality in situ, in: Proceedings. Presented at the 3rd EARSeL Workshop on Imaging spectroscopy, DLR, Herrsching; Germany, pp. 13–16.
Nachtergaele, F.O., Spaargaren, O., Deckers, J.A., Ahrens, B., 2000. New developments in soil classification. Geoderma 96, 345–357.
Nagelkerke, N.J., 1991. A Note on a General Definition of the Coefficient of Determination. Biometrika 78, 691–692.

Nagendra, H., 2001. Using remote sensing to assess biodiversity. Int. J. Remote Sens. 22, 2377–2400.

Nagendra, H., Lucas, R., Honrado, J.P., Jongman, R.H.G., Tarantino, C., Adamo, M., Mairota, P., 2013. Remote sensing for conservation monitoring: Assessing protected areas, habitat extent, habitat condition, species diversity, and threats. Ecol. Indic. 33, 45–59.

Nathan, R., Getz, W.M., Revilla, E., Holyoak, M., Kadmon, R., Saltz, D., Smouse, P.E., 2008. A movement ecology paradigm for unifying organismal movement research. Proc. Natl. Acad. Sci. 105, 19052–19059.

Nekola, J.C., White, P.S., 1999. The distance decay of similarity in biogeography and ecology. J. Biogeogr. 26, 867–878.

Neumann, C., Forster, M., Kleinschmit, B., Itzerott, S., 2016. Utilizing a PLSR-Based Band-Selection Procedure for Spectral Feature Characterization of Floristic Gradients. IEEE J. Sel. Top. Appl. Earth Obs. Remote Sens. 1–15.

Neumann, C., Weiss, G., Itzerott, I., 2015a. Döberitzer Heide 2008/2009 - An EnMAP Preparatory Flight Campaign (Datasets).

Neumann, C., Weiss, G., Itzerott, S., Kuehling, M., Fuerstenow, J., Luft, L., Nitschke, P., 2013. Entwicklung und Erprobung eines innovativen, naturschutzfachlichen Monitoringverfahrens auf der Basis von Fernerkundungsdaten am Beispiel der Doeberitzer Heide, Brandenburg.

Neumann, C., Weiss, G., Schmidtlein, S., Itzerott, S., Lausch, A., Doktor, D., Brell, M., 2015b. Gradient-Based Assessment of Habitat Quality for Spectral Ecosystem Monitoring. Remote Sens. 7, 2871–2898.

O'Connor, B., Secades, C., Penner, J., Sonnenschein, R., Skidmore, A., Burgess, N.D., Hutton, J.M., 2015. Earth observation as a tool for tracking progress towards the Aichi Biodiversity Targets. Remote Sens. Ecol. Conserv. 1, 19–28.

Odeh, I.O.A., McBratney, A.B., Chittleborough, D.J., 1995. Further results on prediction of soil properties from terrain attributes: heterotopic cokriging and regression-kriging. Geoderma 67, 215–226.

Oehlschlaeger, S., Beier, W., van Dorsten, P., Harnisch, R., Hinrichsen, A., Tschöpe, O., Zierke, I., 2004. Das Naturschutzgebiet Döberitzer Heide, in: Anders, K., Mrzljak, J., Wallschläger, D., Wiegleb, G. (Eds.), Handbuch Offenlandmanagement. Springer Berlin Heidelberg, Berlin, Heidelberg, pp. 187–208.

Okin, G.S., Roberts, D.A., Murray, B., Okin, W.J., 2001. Practical limits on hyperspectral vegetation discrimination in arid and semiarid environments. Remote Sens. Environ. 77, 212–225.

Oldeland, J., Dorigo, W., Lieckfeld, L., Lucieer, A., Jürgens, N., 2010a. Combining vegetation indices, constrained ordination and fuzzy classification for mapping semi-natural vegetation units from hyperspectral imagery. Remote Sens. Environ. 114, 1155–1166.

Oldeland, J., Dorigo, W., Wesuls, D., Jürgens, N., 2010b. Mapping bush encroaching species by seasonal differences in hyperspectral imagery. Remote Sens. 2, 1416–1438.

Ollinger, S.V., 2011. Sources of variability in canopy reflectance and the convergent properties of plants. New Phytol. 189, 375–394.

Ostermann, O.P., 2008. The need for management of nature conservation sites designated under Natura 2000. J. Appl. Ecol. 35, 968–973.

Otegui, J., Ariño, A.H., Encinas, M.A., Pando, F., 2013. Assessing the Primary Data Hosted by the Spanish Node of the Global Biodiversity Information Facility (GBIF). PLoS ONE 8, e55144.

Paganini, M., Leidner, A.K., Geller, G., Turner, W., Wegmann, M., 2016. The role of space agencies in remotely sensed essential biodiversity variables. Remote Sens. Ecol. Conserv. 2, 132–140.

Palmer, M.W., 1988. Fractal geometry: a tool for describing spatial patterns of plant communities. Vegetatio 75, 91–102.

Palmer, M.W., White, P.S., 1994. On the existence of ecological communities. J. Veg. Sci. 5, 279–282.

Papeş, M., Tupayachi, R., Martínez, P., Peterson, A.T., Powell, G.V.N., 2010. Using hyperspectral satellite imagery for regional inventories: a test with tropical emergent trees in the Amazon Basin. J. Veg. Sci. 21, 342–354.

Parker Williams, A., Hunt, E.R., 2002. Estimation of leafy spurge cover from hyperspectral imagery using mixture tuned matched filtering. Remote Sens. Environ. 82, 446–456.

Pasari, J.R., Levi, T., Zavaleta, E.S., Tilman, D., 2013. Several scales of biodiversity affect ecosystem multifunctionality. Proc. Natl. Acad. Sci. 110, 10219–10222.

Pebesma, E.J., 2004. Multivariable geostatistics in S: the gstat package. Comput. Geosci. 30, 683–691.

Pengra, B.W., Johnston, C.A., Loveland, T.R., 2007. Mapping an invasive plant, Phragmites australis, in coastal wetlands using the EO-1 Hyperion hyperspectral sensor. Remote Sens. Environ. 108, 74–81.

Penuelas, J., Baret, F., Filella, I., 1995. Semi empirical indices to assess carotenoids/chlorophyll a ratio from leaf spectral reflectance. Photosynthetica 31, 221–230.

Penuelas, J., Pinol, J., Ogaya, R., Filella, I., 1997. Estimation of plant water concentration by the reflectance water index WI (R900/R970). Int. J. Remote Sens. 18, 2869–2875

Pereira, H.M., Ferrier, S., Walters, M., Geller, G.N., Jongman, R.H.G., Scholes, R.J., Bruford, M.W., Brummitt, N., Butchart, S.H.M., Cardoso, A.C., Coops, N.C., Dulloo, E., Faith, D.P., Freyhof, J., Gregory, R.D., Heip, C., Hoft, R., Hurtt, G., Jetz, W., Karp, D.S., McGeoch, M.A., Obura, D., Onoda, Y., Pettorelli, N., Reyers, B., Sayre, R., Scharlemann, J.P.W., Stuart, S.N., Turak, E., Walpole, M., Wegmann, M., 2013. Essential Biodiversity Variables. Science 339, 277–278.

Pettorelli, N., Laurance, W.F., O'Brien, T.G., Wegmann, M., Nagendra, H., Turner, W., 2014. Satellite remote sensing for applied ecologists: opportunities and challenges. J. Appl. Ecol. 51, 839–848.

Pettorelli, N., Safi, K., Turner, W., 2014. Satellite remote sensing, biodiversity research and conservation of the future. Philos. Trans. R. Soc. B Biol. Sci. 369, 20130190–20130190.

Pettorelli, N., Wegmann, M., Skidmore, A., Mücher, S., Dawson, T.P., Fernandez, M., Lucas, R., Schaepman, M.E., Wang, T., O'Connor, B., Jongman, R.H.G., Kempeneers, P., Sonnenschein, R., Leidner, A.K., Böhm, M., He, K.S., Nagendra, H., Dubois, G., Fatoyinbo, T., Hansen, M.C., Paganini, M., de Klerk, H.M., Asner, G.P., Kerr, J.T., Estes, A.B., Schmeller, D.S., Heiden, U., Rocchini, D., Pereira, H.M., Turak, E., Fernandez, N., Lausch, A., Cho, M.A., Alcaraz-Segura, D., McGeoch, M.A., Turner, W., Mueller, A., St-Louis, V., Penner, J., Vihervaara, P., Belward, A., Reyers, B., Geller, G.N., 2016. Framing the concept of satellite remote sensing essential biodiversity variables: challenges and future directions. Remote Sens. Ecol. Conserv. 2, 122–131.

Pickett, S.T.A., Collins, S.L., Armesto, J.J., 1987. Models, mechanisms and pathways of succession. Bot. Rev. 53, 335–371.

Pillar, V.D., 1999. The bootstrapped ordination re-examined. J. Veg. Sci. 10, 895–902.

Plourde, L.C., Ollinger, S.V., Smith, M.-L., Martin, M.E., 2007. Estimating species abundance in a northern temperate forest using spectral mixture analysis. Photogramm. Eng. Remote Sens. 73, 829–840.

Prach, K., Hobbs, R.J., 2008. Spontaneous Succession versus Technical Reclamation in the Restoration of Disturbed Sites. Restor. Ecol. 16, 363–366.

Prach, K., Walker, L.R., 2011. Four opportunities for studies of ecological succession. Trends Ecol. Evol. 26, 119–123.

Pradervand, J.-N., Dubuis, A., Pellissier, L., Guisan, A., Randin, C., 2014. Very high resolution environmental predictors in species distribution models: Moving beyond topography? Prog. Phys. Geogr. 38, 79–96.

Price, J.C., 1994. How unique are spectral signatures? Remote Sens. Environ. 49, 181–186.

Proença, V., Martin, L.J., Pereira, H.M., Fernandez, M., McRae, L., Belnap, J., Böhm, M., Brummitt, N., García-Moreno, J., Gregory, R.D., Honrado, J.P., Jürgens, N., Opige, M., Schmeller, D.S., Tiago, P., van Swaay, C.A.M., 2016. Global biodiversity monitoring: From data sources to Essential Biodiversity Variables. Biol. Conserv.

Prospere, K., McLaren, K., Wilson, B., 2014. Plant Species Discrimination in a Tropical Wetland Using In Situ Hyperspectral Data. Remote Sens. 6, 8494–8523.

Qiu, L., Gao, T., Gunnarsson, A., Hammer, M., von Bothmer, R., 2010. A methodological study of biotope mapping in nature conservation. Urban For. Urban Green. 9, 161–166.

Ramsey III, E., Rangoonwala, A., Nelson, G., Ehrlich, R., Martella, K., 2005. Generation and validation of characteristic spectra from EO1 Hyperion image data for detecting the occurrence of the invasive species, Chinese tallow. Int. J. Remote Sens. 26, 1611–1636.

Rao, N.R., Garg, P.K., Ghosh, S.K., 2007. Development of an agricultural crops spectral library and classification of crops at cultivar level using hyperspectral data. Precis. Agric. 8, 173–185.

Razgour, O., Hanmer, J., Jones, G., 2011. Using multi-scale modelling to predict habitat suitability for species of conservation concern: The grey long-eared bat as a case study. Biol. Conserv. 144, 2922–2930.

Reichelt, G., Wilmanns, O., 1973. Vegetationsgeographie, Das Geographische Seminar : Praktische Arbeitsweisen. Westermann, Braunschweig.

Richter, R., Schläpfer, D., 2002. Geo-atmospheric processing of airborne imaging spectrometry data. Part 2: Atmospheric/topographic correction. Int. J. Remote Sens. 23, 2631–2649.

Risser, P.G., 1995. The Status of the Science Examining Ecotones. BioScience 45, 318–325.

Rocchini, D., Foody, G.M., Nagendra, H., Ricotta, C., Anand, M., He, K.S., Amici, V., Kleinschmit, B., Förster, M., Schmidtlein, S., Feilhauer, H., Ghisla, A., Metz, M., Neteler, M., 2013. Uncertainty in ecosystem mapping by remote sensing. Comput. Geosci. 50, 128–135.

Rogaß, C., Spengler, D., Bochow, M., Segl, K., Lausch, A., Doktor, D., Roessner, S., Behling, R., Wetzel, H.U., Kaufmann, H., 2011. Reduction of radiometric miscalibration—applications to pushbroom sensors. Sensors 11, 6370–6395.

Rondeaux, G., Steven, M., Baret, F., 1996. Optimization of soil adjusted vegetation indices. Remote Sens. Environ. 55, 95–107.

Rose, R.A., Byler, D., Eastman, J.R., Fleishman, E., Geller, G., Goetz, S., Guild, L., Hamilton, H., Hansen, M., Headley, R., Hewson, J., Horning, N., Kaplin, B.A., Laporte, N., Leidner, A., Leimgruber, P., Morisette, J., Musinsky, J., Pintea, L., Prados, A., Radeloff, V.C., Rowen, M., Saatchi, S., Schill, S., Tabor, K., Turner, W.,

Vodacek, A., Vogelmann, J., Wegmann, M., Wilkie, D., Wilson, C., 2015. Ten ways remote sensing can contribute to conservation: Conservation Remote Sensing Questions. Conserv. Biol. 29, 350–359.

Roth, K.L., Roberts, D.A., Dennison, P.E., Alonzo, M., Peterson, S.H., Beland, M., 2015. Differentiating plant species within and across diverse ecosystems with imaging spectroscopy. Remote Sens. Environ. 167, 135–151.

Rothmaler, W., 2005. Exkursionsflora von Deutschland. Band 4, Gefässpflanzen: kritischer Band, 18th ed, Hrsg.: Jäger, EJ & Werner, K. Spektrum Verlag, München.

Rubin, J., 1967. Optimal classification into groups: An approach for solving the taxonomy problem. J. Theor. Biol. 15, 103–144.

Sandbrook, C., 2015. The social implications of using drones for biodiversity conservation. Ambio 44, 636–647.

Savitzky, A., Golay, M.J., 1964. Smoothing and differentiation of data by simplified least squares procedures. Anal. Chem. 36, 1627–1639.

Schaepman, M.E., Jehle, M., Hueni, A., D'Odorico, P., Damm, A., Weyermann, J., Schneider, F.D., Laurent, V., Popp, C., Seidel, F.C., Lenhard, K., Gege, P., Küchler, C., Brazile, J., Kohler, P., De Vos, L., Meuleman, K., Meynart, R., Schläpfer, D., Kneubühler, M., Itten, K.I., 2015. Advanced radiometry measurements and Earth science applications with the Airborne Prism Experiment (APEX). Remote Sens. Environ. 158, 207–219.

Schaepman, M.E., Ustin, S.L., Plaza, A.J., Painter, T.H., Verrelst, J., Liang, S., 2009. Earth system science related imaging spectroscopy—An assessment. Remote Sens. Environ. 113, S123–S137.

Scheuring, I., Riedi, R.H., 1994. Application of multifractals to the analysis of vegetation pattern. J. Veg. Sci. 5, 489–496.

Schlapfer, F., Schmid, B., 1999. Ecosystem Effects of Biodiversity: A Classification of Hypotheses and Exploration of Empirical Results. Ecol. Appl. 9, 893.

Schmidt, K.S., Skidmore, A.K., 2001. Exploring spectral discrimination of grass species in African rangelands. Int. J. Remote Sens. 22, 3421–3434.

Schmidtlein, S., 2005. Imaging spectroscopy as a tool for mapping Ellenberg indicator values: Remote sensing and plant indicator maps. J. Appl. Ecol. 42, 966–974.

Schmidtlein, S., Feilhauer, H., Bruelheide, H., 2012. Mapping plant strategy types using remote sensing. J. Veg. Sci. 23, 395–405.

Schmidtlein, S., Sassin, J., 2004. Mapping of continuous floristic gradients in grasslands using hyperspectral imagery. Remote Sens. Environ. 92, 126–138.

Schmidtlein, S., Zimmermann, P., Schüpferling, R., Weiss, C., 2007. Mapping the floristic continuum: Ordination space position estimated from imaging spectroscopy. J. Veg. Sci. 18, 131–140.

Scholes, R.J., Walters, M., Turak, E., Saarenmaa, H., Heip, C.H., Tuama, É.Ó., Faith, D.P., Mooney, H.A., Ferrier, S., Jongman, R.H., Harrison, I.J., Yahara, T., Pereira, H.M., Larigauderie, A., Geller, G., 2012. Building a global observing system for biodiversity. Curr. Opin. Environ. Sustain. 4, 139–146.

Schönemann, P.H., Carroll, R.M., 1970. Fitting one matrix to another under choice of a central dilation and a rigid motion. Psychometrika 35, 245–255.

Schweiger, A.K., Schütz, M., Risch, A.C., Kneubühler, M., Haller, R., Schaepman, M.E., 2016. How to predict plant functional types using imaging spectroscopy: Linking vegetation community traits, plant functional types and spectral response. Methods Ecol. Evol.

Seddon, P.J., 2010. From Reintroduction to Assisted Colonization: Moving along the Conservation Translocation Spectrum. Restor. Ecol. 18, 796–802.
Serrano, L., Filella, I., Pen˜uelas, J., 2000. Remote Sensing of Biomass and Yield of Winter Wheat under Different Nitrogen Supplies. Crop Sci. 40, 723.
Serrano, L., Penuelas, J., Ustin, S.L., 2002. Remote sensing of nitrogen and lignin in Mediterranean vegetation from AVIRIS data: Decomposing biochemical from structural signals. Remote Sens. Environ. 81, 355–364.
Serrano, L., Ustin, S.L., Roberts, D.A., Gamon, J.A., Penuelas, J., 2000. Deriving water content of chaparral vegetation from AVIRIS data. Remote Sens. Environ. 74, 570–581.
Shi, R.Z., Zhuang, D., Niu, Z., 2003. Effects of spectral transformations in statistical modeling of leaf biochemical concentrations, in: Advances in Techniques for Analysis of Remotely Sensed Data. Presented at the IEEE Workshop, IEEE, Greenbelt, Maryland USA, pp. 263–267.
Siegmann, B., Glässer, C., Itzerott, S., Neumann, C., 2014. An Enhanced Classification Approach using Hyperspectral Image Data in Combination with in situ Spectral Measurements for the Mapping of Vegetation Communities. Photogramm. - Fernerkund. - Geoinformation 2014, 523–533.
Sims, D.A., Gamon, J.A., 2002. Relationships between leaf pigment content and spectral reflectance across a wide range of species, leaf structures and developmental stages. Remote Sens. Environ. 81, 337–354.
Skowronek, S., Ewald, M., Isermann, M., Van De Kerchove, R., Lenoir, J., Aerts, R., Warrie, J., Hattab, T., Honnay, O., Schmidtlein, S., Rocchini, D., Somers, B., Feilhauer, H., 2016. Mapping an invasive bryophyte species using hyperspectral remote sensing data. Biol. Invasions.
Smith, G.M., Milton, E.J., 1999. The use of the empirical line method to calibrate remotely sensed data to reflectance. Int. J. Remote Sens. 20, 2653–2662.
Smith, K.L., Steven, M.D., Colls, J.J., 2004. Use of hyperspectral derivative ratios in the red-edge region to identify plant stress responses to gas leaks. Remote Sens. Environ. 92, 207–217.
Smith, M.-L., Ollinger, S.V., Martin, M.E., Aber, J.D., Hallett, R.A., Goodale, C.L., 2002. Direct Estimation of Aboveground Forest Productivity Through Hyperspectral Remote Sensing of Canopy Nitrogen. Ecol. Appl. 12, 1286–1302.
Somers, B., Asner, G.P., 2013. Multi-temporal hyperspectral mixture analysis and feature selection for invasive species mapping in rainforests. Remote Sens. Environ. 136, 14–27.
Song, S., Gong, W., Zhu, B., Huang, X., 2011. Wavelength selection and spectral discrimination for paddy rice with laboratory measurements of hyperspectral leaf reflectance. ISPRS J. Photogramm. Remote Sens. 66, 672–682.
Spanhove, T., Vanden Borre, J., Delalieux, S., Haest, B., Paelinckx, D., 2012. Can remote sensing estimate fine-scale quality indicators of natural habitats? Ecol. Indic. 18, 403–412.
SPECTATION [WWW Document], 2015. URL http://www.gfz-potsdam.de/spectation
Ståhl, G., Allard, A., Esseen, P.-A., Glimskär, A., Ringvall, A., Svensson, J., Sundquist, S., Christensen, P., Torell, Å.G., Högström, M., Lagerqvist, K., Marklund, L., Nilsson, B., Inghe, O., 2011. National Inventory of Landscapes in Sweden (NILS)—scope, design, and experiences from establishing a multiscale biodiversity monitoring system. Environ. Monit. Assess. 173, 579–595.

Steinhardt, U., Herzog, F., Lausch, A., Müller, E., Lehmann, S., 1999. Hemeroby index for landscape monitoring and evaluation, in: Environmental Indices – System Analysis Approach. EOLSS Publ., Oxford, pp. 237–254.

Stenzel, S., Feilhauer, H., Mack, B., Metz, A., Schmidtlein, S., 2014. Remote sensing of scattered Natura 2000 habitats using a one-class classifier. Int. J. Appl. Earth Obs. Geoinformation 33, 211–217.

Sterling, A., Peco, B., Casado, M.A., Galiano, E.F., Pineda, F.D., 1984. Influence of Microtopography on Floristic Variation in the Ecological Succession in Grassland. Oikos 42, 334.

Sterling, S., Ducharne, A., 2008. Comprehensive data set of global land cover change for land surface model applications: GLOBAL LAND COVER CHANGE DATA SET. Glob. Biogeochem. Cycles 22.

Süβ, K., Storm, C., Zehm, A., Schwabe, A., 2004. Succession in Inland Sand Ecosystems: Which Factors Determine the Occurrence of the Tall Grass Species Calamagrostis epigejos (L.) Roth and Stipa capillata L.? Plant Biol. 6, 465–476.

Tahvanainen, T., 2004. Water chemistry of mires in relation to the poor-rich vegetation gradient and contrasting geochemical zones of the north-eastern Fennoscandian Shield. Folia Geobot. 39, 353–369.

Tenenbaum, J.B., 2000. A Global Geometric Framework for Nonlinear Dimensionality Reduction. Science 290, 2319–2323.

Ter Braak, C.J., Prentice, I.C., 1988. A theory of gradient analysis. Adv. Ecol. Res. 18, 271–317.

Ter Braak, C.J.F., Prentice, I.C., 2004. A Theory of Gradient Analysis, in: Advances in Ecological Research. Elsevier, pp. 235–282.

The Plant List, 2013.

Thenkabail, P.S., Enclona, E.A., Ashton, M.S., Van Der Meer, B., 2004. Accuracy assessments of hyperspectral waveband performance for vegetation analysis applications. Remote Sens. Environ. 91, 354–376.

Thenkabail, P.S., Lyon, J.G., Huete, A. (Eds.), 2012. Hyperspectral remote sensing of vegetation. CRC Press, Boca Raton, FL.

Thenkabail, P.S., Mariotto, I., Gumma, M.K., Middleton, E.M., Landis, D.R., Huemmrich, K.F., 2013. Selection of hyperspectral narrowbands (HNBs) and composition of hyperspectral twoband vegetation indices (HVIs) for biophysical characterization and discrimination of crop types using field reflectance and Hyperion/EO-1 data. IEEE J. Sel. Top. Appl. Earth Obs. Remote Sens. 6, 427–439.

Thessler, S., Ruokolainen, K., Tuomisto, H., Tomppo, E., 2005. Mapping gradual landscape-scale floristic changes in Amazonian primary rain forests by combining ordination and remote sensing. Glob. Ecol. Biogeogr. 14, 315–325.

Thorp, K.R., Dierig, D.A., French, A.N., Hunsaker, D.J., 2011. Analysis of hyperspectral reflectance data for monitoring growth and development of lesquerella. Ind. Crops Prod. 33, 524–531.

Thorp, K.R., French, A.N., Rango, A., 2013. Effect of image spatial and spectral characteristics on mapping semi-arid rangeland vegetation using multiple endmember spectral mixture analysis (MESMA). Remote Sens. Environ. 132, 120–130.

Titeux, N., Dufrene, M., Jacob, J.-P., Paquay, M., Defourny, P., 2004. Multivariate analysis of a fine-scale breeding bird atlas using a geographical information system and partial canonical correspondence analysis: environmental and spatial effects. J. Biogeogr. 31, 1841–1856.

Townsend, P.A., Foster, J.R., Chastain Jr, R.A., Currie, W.S., 2003. Application of imaging spectroscopy to mapping canopy nitrogen in the forests of the central Appalachian Mountains using Hyperion and AVIRIS. IEEE Trans. Geosci. Remote Sens. 41, 1347–1354.

Trodd, N.M., 1996. Analysis and representation of heathland vegetation from near-ground level remotely-sensed data. Glob. Ecol. Biogeogr. Lett. 206–216.

Tucker, C.J., 1980. Remote sensing of leaf water content in the near infrared. Remote Sens. Environ. 10, 23–32.

Turner, W., Rondinini, C., Pettorelli, N., Mora, B., Leidner, A.K., Szantoi, Z., Buchanan, G., Dech, S., Dwyer, J., Herold, M., Koh, L.P., Leimgruber, P., Taubenboeck, H., Wegmann, M., Wikelski, M., Woodcock, C., 2015. Free and open-access satellite data are key to biodiversity conservation. Biol. Conserv. 182, 173–176.

Turner, W., Spector, S., Gardiner, N., Fladeland, M., Sterling, E., Steininger, M., 2003. Remote sensing for biodiversity science and conservation. Trends Ecol. Evol. 18, 306–314.

Underwood, E., 2003. Mapping nonnative plants using hyperspectral imagery. Remote Sens. Environ. 86, 150–161.

Ustin, S.L., DiPietro, D., Olmstead, K., Underwood, E., Scheer, G.J., 2002. Hyperspectral remote sensing for invasive species detection and mapping. IEEE, pp. 1658–1660.

Ustin, S.L., Gamon, J.A., 2010. Remote sensing of plant functional types: Tansley review. New Phytol. 186, 795–816.

Ustin, S.L., Roberts, D.A., Gamon, J.A., Asner, G.P., Green, R.O., 2004. Using Imaging Spectroscopy to Study Ecosystem Processes and Properties. BioScience 54, 523.

Vaiphasa, C., Ongsomwang, S., Vaiphasa, T., Skidmore, A.K., 2005. Tropical mangrove species discrimination using hyperspectral data: A laboratory study. Estuar. Coast. Shelf Sci. 65, 371–379.

van Aardt, J.A.N., Wynne, R.H., 2007. Examining pine spectral separability using hyperspectral data from an airborne sensor: An extension of field-based results. Int. J. Remote Sens. 28, 431–436.

Vanden Borre, J., Paelinckx, D., Mücher, C.A., Kooistra, L., Haest, B., De Blust, G., Schmidt, A.M., 2011. Integrating remote sensing in Natura 2000 habitat monitoring: Prospects on the way forward. J. Nat. Conserv. 19, 116–125.

Velázquez, J., Tejera, R., Hernando, A., Núñez, V., M., 2010. Environmental diagnosis: Integrating biodiversity conservation in management of Natura 2000 forest spaces. J. Nat. Conserv. 18, 309–317.

Vetaas, O.R., 1997. Relationships between floristic gradients in a primary succession. J. Veg. Sci. 8, 665–676.

Vitousek, P.M., 1997. Human Domination of Earth's Ecosystems. Science 277, 494–499.

Vitt, D.H., Chee, W.L., 1990. The relationships of vegetation to surface water chemistry and peat chemistry in fens of Alberta. Can. Veg. 89, 87–106.

Vogelmann, J.E., Rock, B.N., Moss, D.M., 1993. Red edge spectralmeasurements fromsugar maple leaves. Remote Sens. Environ. 14, 1563–1575.

W. C. Bausch, H. R. Duke, 1996. Remote Sensing of Plant Nitrogen Status in Corn. Trans. ASAE 39, 1869–1875.

Wali, M.K., 1999. Ecological succession and the rehabilitation of disturbed terrestrial ecosystems. Plant Soil 213, 195–220.

Walker, L.R., Moral, R. del, 2003. Primary succession and ecosystem rehabilitation. Cambridge University Press, Cambridge, UK ; New York.

Walker, L.R., Walker, J., Hobbs, R.J. (Eds.), 2007. Linking Restoration and Ecological Succession, SPRINGER SERIES ON ENVIRONMENTAL MANAGEMENT. Springer New York, New York, NY.

Wang, K., Franklin, S.E., Guo, X., Cattet, M., 2010. Remote sensing of ecology, biodiversity and conservation: a review from the perspective of remote sensing specialists. Sensors 11, 9647–9667.

Wang, L., Sousa, W.P., 2009. Distinguishing mangrove species with laboratory measurements of hyperspectral leaf reflectance. Int. J. Remote Sens. 30, 1267–1281.

Warren, S.D., Holbrook, S.W., Dale, D.A., Whelan, N.L., Elyn, M., Grimm, W., Jentsch, A., 2007. Biodiversity and the Heterogeneous Disturbance Regime on Military Training Lands. Restor. Ecol. 15, 606–612.

Watson, J.E.M., Dudley, N., Segan, D.B., Hockings, M., 2014. The performance and potential of protected areas. Nature 515, 67–73.

Watt, A.S., 1955. Bracken Versus Heather, A Study in Plant Sociology. J. Ecol. 43, 490.

Weiers, S., Bock, M., Wissen, M., Rossner, G., 2004. Mapping and indicator approaches for the assessment of habitats at different scales using remote sensing and GIS methods. Landsc. Urban Plan. 67, 43–65.

White, P.S., Jentsch, A., 2004. Disturbance, succession, and community assembly in terrestrial plant communities, in: Assembly Rules and Restoration Ecology. Island Press, pp. 342–366.

Whittaker, R.H., 1974. Climax Concepts and Recognition, in: Knapp, R. (Ed.), Vegetation Dynamics. Springer Netherlands, Dordrecht, pp. 137–154.

Whittaker, R.H., 1967. Gradient Analysis of Vegetation. Biol. Rev. 42, 207–264.

Whittaker, R.H., 1962. Classification of natural communities. Bot. Rev. 28, 1–239.

Wiens, J., Sutter, R., Anderson, M., Blanchard, J., Barnett, A., Aguilar-Amuchastegui, N., Avery, C., Laine, S., 2009. Selecting and conserving lands for biodiversity: The role of remote sensing. Remote Sens. Environ. 113, 1370–1381.

Wiens, J.A., 1989. Spatial Scaling in Ecology. Funct. Ecol. 3, 385.

Williamson, M., 1990. Relationship of species number to area, distance and other variables, in: Myers, A.A., Giller, P.S. (Eds.), Analytical Biogeography. Springer Netherlands, Dordrecht, pp. 91–115.

Willis, K.S., 2015. Remote sensing change detection for ecological monitoring in United States protected areas. Biol. Conserv. 182, 233–242.

Wilmanns, O., 1998. Ökologische Pflanzensoziologie: eine Einführung in die Vegetation Mitteleuropas, 6., neu bearb. Aufl. ed, UTB für Wissenschaft Uni-Taschenbücher Botanik/Ökologie. Quelle & Meyer, Wiesbaden.

Wold, H., 1966. Estimation of principal components and related models by iterative least squares. Multivar. Anal. 1, 391–420.

Wold, S., Sjöström, M., Eriksson, L., 2001. PLS-regression: a basic tool of chemometrics. Chemom. Intell. Lab. Syst. 58, 109–130.

Wold, S., Sjöström, M., Eriksson, L., 2002. Partial Least Squares Projections to Latent Structures (PLS) in Chemistry, in: von Rague Schleyer, P., Allinger, N.L., Clark, T., Gasteiger, J., Kollman, P.A., Schaefer, H.F., Schreiner, P.R. (Eds.), Encyclopedia of Computational Chemistry. John Wiley & Sons, Ltd, Chichester, UK.

Woodcock, C.E., Strahler, A.H., 1987. The factor of scale in remote sensing. Remote Sens. Environ. 21, 311–332.

Woodley, S., Bertzky, B., Crawhall, N., Dudley, N., Londoño, J.M., MacKinnon, K., Redford, K., Sandwith, T., 2012. Meeting Aichi Target 11: what does success look like for protected area systems. Parks 18, 23–36.

Xie, Y., Sha, Z., Yu, M., 2008. Remote sensing imagery in vegetation mapping: a review. J. Plant Ecol. 1, 9–23.

Young, T.P., Petersen, D.A., Clary, J.J., 2005. The ecology of restoration: historical links, emerging issues and unexplored realms: Ecology of restoration. Ecol. Lett. 8, 662–673.

Yusoff, Y., Ngadiman, M.S., Zain, A.M., 2011. Overview of NSGA-II for Optimizing Machining Process Parameters. Procedia Eng. 15, 3978–3983.

Zarco-Tejada, P.J., Guillén-Climent, M.L., Hernández-Clemente, R., Catalina, A., González, M.R., Martín, P., 2013. Estimating leaf carotenoid content in vineyards using high resolution hyperspectral imagery acquired from an unmanned aerial vehicle (UAV). Agric. For. Meteorol. 171–172, 281–294.

Zentelis, R., Lindenmayer, D., 2015. Bombing for Biodiversity-Enhancing Conservation Values of Military Training Areas: Bombing for biodiversity. Conserv. Lett. 8, 299–305.

Zentelis, R., Lindenmayer, D., 2014. Conservation: Manage military land for the environment. Nature 516, 170–170.

Zhang, T.-T., Zeng, S.-L., Gao, Y., Ouyang, Z.-T., Li, B., Fang, C.-M., Zhao, B., 2011. Using hyperspectral vegetation indices as a proxy to monitor soil salinity. Ecol. Indic. 11, 1552–1562.

Zimmermann, 2015. Lebensraumtypen nach Anhang I der FFH-Richtlinie/LUGV. http://www.lugv.brandenburg.de/cms/detail.php/bb1.c.315320.de (accessed on 14 November 2016)

Zomer, R.J., Trabucco, A., Ustin, S.L., 2009. Building spectral libraries for wetlands land cover classification and hyperspectral remote sensing. J. Environ. Manage. 90, 2170–2177.

Appendix

A - Publications Related to the Thesis

Peer-reviewed articles

Luft, L., **Neumann, C.**, Freude, M., Blaum, N., Jeltsch, F. (2014): Hyperspectral modeling of ecological indicators – A new approach for monitoring former military training areas. - Ecological Indicators, 46, p. 264-285.

Siegmann, B., Glässer, C., Itzerott, S., **Neumann, C.** (2014): An Enhanced Classification Approach using Hyperspectral Image Data in Combination with in situ Spectral Measurements for the Mapping of Vegetation Communities. - Photogrammetrie - Fernerkundung - Geoinformation - PFG, 2014, 6, p. 523-533.

Fassnacht, F., **Neumann, C.**, Forster, M., Buddenbaum, H., Ghosch, A., Clasen, A., Joshi, P., Koch, B. (2014): Comparison of Feature Reduction Algorithms for Classifying Tree Species With Hyperspectral Data on Three Central European Test Sites. - IEEE Journal of Selected Topics in Applied Earth Observations and Remote Sensing, 7, 6, p. 2547-2561.

Neumann, C., Luft, L. (2014): Digital- und Real-Habitatmodellierung von Hipparchia statilinus in der Döberitzer Heide. - Oedippus, 29, p. 14-20.

Neumann, C., Weiss, G., Schmidtlein, S., Itzerott, S., Lausch, A., Doktor, D., Brell, M. (2015): Gradient-Based Assessment of Habitat Quality for Spectral Ecosystem Monitoring. - Remote Sensing, 7, 3, p. 2871-2898.

Luft, L., **Neumann, C.**, Itzerott, S., Lausch, A., Doktor, D., Freude, M., Blaum, N., Jeltsch, F. (2016): Digital and real-habitat modeling of Hipparchia statilinus based on hyper spectral remote sensing data. - International Journal of Environmental Science and Technology, 13, 1, p. 187-200.

Neumann, C., Itzerott, S., Weiss, G., Kleinschmit, B., Schmidtlein, S. (2016): Mapping multiple plant species abundance patterns - A multiobjective optimization procedure for combining reflectance spectroscopy and species ordination. - Ecological Informatics, 36, p. 61-76.

Neumann, C., Förster, M., Kleinschmit, B., Itzerott, S. (2016): Utilizing a PLSR-Based Band-Selection Procedure for Spectral Feature Characterization of Floristic Gradients. - IEEE Journal of Selected Topics in Applied Earth Observations and Remote Sensing, 9, 9, p. 3982-3996.

Scientific reports

Neumann, C. (2011): Monitoring in der Döberitzer Heide - Vegetation und Fernerkundung. - In: Workshop Monitoring Döberitzer Heide, (Fachbeiträge des Landesamts für Umwelt, Gesundheit und Verbraucherschutz; 123), p. 20-24

Neumann, C., Weiß, G., Itzerott, S., Kühling, M., Fürstenow, J., Luft, L., Nitschke, P. (2013): Entwicklung und Erprobung eines innovativen, naturschutzfachlichen Monitoringverfahrens auf der Basis von Fernerkundungsdaten am Beispiel der Döberitzer Heide, Brandenburg: Abschlussbericht, (Scientific Technical Report ; 13/02), Potsdam : Deutsches GeoForschungsZentrum GFZ

Neumann, C., Weiss, G., Itzerott, S. (2015): Döberitzer Heide 2008/2009 - an EnMAP Preparatory Flight Campaign, (EnMAP Flight Campaigns Technical Report), Potsdam : GFZ Data Services, 19 p.

Conference Paper

Neumann, C., Itzerott, S., Kühling, M., Förster, S., Weiß, G. (2009): Monitoring of Plant Community Changes in a Nature Conservation Heathland Area in Germany with Multi-Temporal HyMap Data, 3rd Workshop of the EARSeL Special Interest Group on Land Use and Land Cover (Bonn 2009)

Neumann, C., Förster, S., Itzerott, S. (2010): From field spectra to an area-wide monitoring – a case study in a dryland nature reserve in germany, Hyperspectral Workshop 2010 (Frascati, Italy 2010) (Noordwijk)

Neumann, C., Förster, S., Itzerott, S. (2011): A Synthesis of Ecological Gradient Analysis and Hyperspectral Remote Sensing for the Monitoring of Heterogeneous Vegetation Structures in a Dryland Nature Reserve in Germany, 7th EARSeL SIG Imaging Spectroscopy workshop (Edinburgh, Scotland 2011)

Neumann, C., Itzerott, S., Weiss, G. (2012): The importance of spatial, spectral and temporal constraints for a hyperspectral modeling of vegetational continuum and habitat assessment parameter, IEEE International Geoscience and Remote Sensing Symposium - IGARSS (Munich 2012)

Neumann, C., Weiss, G., Itzerott, S. (2014): A Natura 2000 Monitoring Framework - Using Plant Species Gradients for Spectral Habitat Assessment - Proceedings, International Workshop on Remote Sensing and GIS for Monitoring of Habitat Quality (Vienna 2014), p. 125-129.

B- Acknowledgment

I would like to give my special thanks to Dr. Sibylle Itzerott. Her infinite patience told me a thousand times that there is reliable trust in what I am doing. Without her support, my thoughts would never bridge the mind to come down on paper. She is the mentor of my scientific career!

It is incredible to witness the pleasant and friendly working climate at the Remote Sensing Section 1.4 of the GFZ Potsdam. All the people are kind and very helpful. There is a lively professional exchange between all colleagues as well as plentiful nonsense talks about the daily life during the coffee breaks. I wish that one day our section will become a standard for other working environments.

Special thanks to my office partner Robert Behling. During our PhD time and the hours outside the office we have become friends!

Thank you Prof. Birgit Kleinschmit for the patient supervision of my thesis. Thank you Charly for your wisdom words about science in general and remote sensing in particular that were very helpful for me as a young scientists. Thank you Prof. Sebastian Schmidtlein for your inspiration. Your research opened my fascination for the ecological continuum.

Great thanks goes to Gabriele Weiß and Dr. Michael Förster. Their profound knowledge crucially contributes to the successful preparation of the published manuscripts.

Thank you Heinz Sielmann Stiftung! Your engagement is important! Important for having places of retreat to study ecological processes and even more important for protecting the nature of our blue planet Earth.

Thanks to my family for keeping my life exciting!

And thanks to all the people I did not mention but that will definitely be kept into my mind for their steady support.